

The acoustics of the violin: a review

Jim Woodhouse

Cambridge University Engineering Department, Trumpington St, Cambridge CB2 1PZ, UK
jw12@cam.ac.uk

Abstract

To understand the design and function of the violin requires investigation of a range of scientific questions. This paper presents a review: the relevant physics covers the non-linear vibration of a bowed string, the vibration of the instrument body, and the consequent sound radiation. Questions of discrimination and preference by listeners and players require additional studies using the techniques of experimental psychology, and these are also touched on in the paper. To address the concerns of players and makers of instruments requires study of the interaction of all these factors, coming together in the concept of “playability” of an instrument.

1. Introduction

A violin is a wooden box that serves as a mechanical amplifier (or more properly, a mechanical transformer), to convert some of the energy from a set of vibrating strings into radiated sound. How does it work, and what distinguishes a good one from a bad one? At first glance this sounds like a rather straightforward physics question; but to set the scene, consider a preliminary example. If one were choosing a loudspeaker to do a somewhat similar job, one might expect to learn quite a lot about quality differences by looking at suitable frequency response plots. Figure 1 shows representative frequency responses of two violins. The details will be explained later, but for now we simply note two things. First, the market values of these two particular violins differ by about four orders of magnitude (a few hundred to a few million dollars). Second, the two curves look remarkably similar in general terms, and it is almost certainly not apparent to the general reader which of the two is a classic Cremonese Guarneri “del Gesu”. Indeed, the two plots are almost as close to each other as frequency response measurements that have been made on successive automobiles from the same production line [1].

Of course, these plots have been carefully selected to make a point: not all violins are quite this similar in frequency response. Nevertheless the comparison suggests immediately that the preferences of violinists, and the pricing policy of dealers, may turn on physical differences that are quite subtle. This in turn challenges the physicist: many of the things that matter most to a violinist turn out to involve fine details. It is rarely sufficient to explain *roughly* how something works, it is usually necessary to dig deep before enough of the detail is laid bare to give sufficient explanatory power to satisfy a musician or an instrument maker. As another preliminary example of the importance of subtle effects, experienced “tone adjusters” routinely delight the owners of instruments by doing no more than removing a

fraction of a gram of wood from the bridge, or by moving the soundpost (described later) by a millimetre or two.

The acoustics of musical instruments occupies a rather odd place in the world of science. The subject is found fascinating by many, both scientists and the general public, but it is not beloved of funding agencies. This makes it a slow-moving subject, but nevertheless one that taps into contemporary science in several disciplines. Musical instruments raise a variety of problems of classical physics, materials science and engineering, and offer applications of many theoretical and experimental techniques, but the distinctive flavour of the subject comes from the fact that the key questions are posed by subjective judgements: what is “good sound”? This survey of violin physics must involve an excursion into perception and psychophysics, the science of giving quantitative form to subjective judgements. A review of violin physics is timely, because interesting developments have occurred since a general account was last published. The most comprehensive discussion is the book by Cremer [2], and other reviews have been written by McIntyre and Woodhouse [3] and Hutchins [4]. A shorter but more recent account has been given by Gough [5].

The pattern of this article will follow the main stages of making sound on a violin. First, the string is set into stick-slip frictional oscillation by the bow. Exploring this will reveal a problem in nonlinear dynamics, containing many features that have become generically familiar in recent decades (for an introduction, see for example Strogatz [6]): multiple alternative oscillation regimes, questions of stability and chaos, questions of transient response and pattern selection. The vibrating string then excites the violin body. Vibration amplitudes are small enough that linear theory seems to apply, at least to a very good first approximation. That gives rise to questions about the vibration modes and their sound radiation efficiency and patterns, and also to questions of how these can be controlled and manipulated by the violin maker by choice of materials and details of construction. In common with other problems involving the vibration response of complex structures over a broad frequency range, fruitful understanding will require both classical deterministic analysis, and also statistical analysis that recognises the importance of variability beyond human ability to control.

Once the sound has been produced and radiated into the room, it enters the ears of the player or a listener, and questions of perception and psychophysics immediately come into play. Some recent work will be reviewed that begins to shed light on the preferences of players and listeners for what constitutes “good” violin sound. But “sound” is not the whole story. An experienced player may be able to make most violins sound “good”, at least when playing single notes or unchallenging passages. However, the player is inside a feedback loop, adjusting the bowing details to achieve the best sound, and he or she will be very well aware that some instruments make that job easier than others. All the threads of this article, physical and psychological, come together in the idea of “playability”. What might a violinist mean when they say that one instrument, or one note or one string on an instrument, is “easier to play” than another? This question involves an interplay between the bowed string and the vibration of the instrument body, and is a topic that has excited a lot of interest in recent years. The article will end with a review of the issue.

One important statement must be made at the outset: throughout this introduction we have spoken of the violin, but it should be understood that much of what will be said in this article can be applied, to some extent at least, to all bowed-string instruments. This includes the viola, cello and double bass of the Western orchestra, but also less familiar instruments like the viol family, and bowed instruments from other cultures such as the Chinese erhu.

2. The bowed string

A familiar feature of the violin is that it is only too easy to make a truly dreadful noise on one. Part of that is simply the difficulty of playing in tune, but there is more to it. A beginner on the guitar may play the wrong note, but the individual note will still be recognisably “musical”. A first attempt to bow a violin string, in contrast, may produce a very un-musical sound. This contrast points to the most fundamental difference in the physics of plucking a string versus bowing one: the plucked string is, to a good approximation, a linear system but a bowed string is strongly non-linear. Plucking a string elicits a mixture of its natural frequencies, which are approximately harmonically spaced. All the player can do is vary the mixture by the method and position of the pluck. Bowing elicits a self-sustained oscillation through the slip-stick action of friction between the bow-hair and the string. As will be seen in some detail shortly, that oscillation may be, at least approximately, periodic, or it may not: the wide range of sounds a player can produce gives rise to the glory and the frustration of violin playing. An expert can learn to control the sound and harness the variety for musical purposes, but only with a lot of native talent reinforced by a lot of practice.

2.1 Early work

The motion of a bowed string has probably fascinated scientists ever since there have been scientists. The first breakthrough was made by Helmholtz [7], who with a very ingenious experiment observed and described the commonest motion, the one violinists are nearly always striving to achieve. This “Helmholtz motion” is illustrated in its most idealised form in Fig. 2. At any given instant the string has a triangular shape, two straight portions being separated by a sharp kink, the “Helmholtz corner”. This corner travels back and forth along the string, reversing its orientation each time it reflects from one end of the string (for an animation, see [8]).

As the Helmholtz corner passes the bow it triggers transitions from slipping to sticking friction between the string and the bow-hair, and back again. The string sticks to the bow for the majority of each period, while the corner travels the long way to the player’s finger and back. During the shorter trip to the bridge and back, the string slips rapidly across the bow-hair. The waveform of velocity of the point of the string in contact with the bow is shown in Fig. 2b: it alternates between two constant values; the bow speed during sticking and a slipping speed determined by the condition that the velocity must integrate to zero over a single period of oscillation. To a first approximation the Helmholtz motion is confined to a single plane, that of the string and the bow-hair. The body of the violin is then excited by the

transverse force exerted by the string at the bridge in this plane, and for the ideal Helmholtz motion this takes the form of a sawtooth wave as shown in Fig. 2c.

The earliest research was mainly concerned with cataloguing and explaining the many other types of periodic motion that a bowed string can produce: a rich array of possibilities was revealed by experiments with mechanically-bowed strings, for example Krigar-Menzel and Raps [9]. Clarification was brought by Raman, who gave a kinematic description of a large family of possible stick-slip motions [10]. He argued that any periodic motion in which the bowed string oscillates at the same frequency as the free string, as was observed, must have a friction force at the bow that remains essentially constant: the modes of a string have very low damping, so any significant variation of the friction force at the frequency of string modes would produce a resonant response to high amplitude. Indeed, the Helmholtz motion is a possible free motion of an undamped string, of the kind found in elementary textbooks: perfectly flexible, and having overtone frequencies at exact integer multiples of the fundamental frequency (see for example [11], [12]).

Based on a simple assumption about the variation of friction force with relative sliding speed, to which we return later (see Fig. 6), Raman then argued that the velocity of the string under the bow must always alternate between just two fixed values. A particular example has already been seen for the Helmholtz motion, but more than one alternation might occur in each period of oscillation, corresponding to more than one “Helmholtz corner” travelling on the string. The number of corners gave Raman the basis for a classification scheme for what he called “higher types” of bowed-string motion, and he was able to use this scheme to bring order to the earlier observations. Raman’s work, of which only a part has been described here, was a very early example of detailed study of a non-linear dynamical system of sufficient complexity to show multiple solutions that are qualitatively different: probably the only such system about which more was known at this early date was the motion of the planets.

Raman later turned his attention to the work on spectroscopy for which he is more famous, and he was not alone in such a shift of attention: for the next few decades the gaze of most physicists was focussed on quantum mechanics and other emerging topics. The bowed string was largely ignored as a subject for research until the advent of electronic means of making detailed observations, around 1970. Two important developments then occurred, from which all modern work in the area has stemmed. Both are concerned with understanding details of the Helmholtz motion: violinists do not in fact make much use of Raman’s “higher types”, except in so far as some of them set limits to the availability of Helmholtz motion in the player’s parameter space through what would now be called bifurcation events.

The first explicit illustration of part of the player’s parameter space, with a hint of such bifurcations, came from Schelleng [13]. He combined and extended earlier results of Raman to produce the now-famous diagram shown in Fig. 3. Ignoring transients and concentrating for the moment on the bowing of steady notes, the violinist has only a rather small number of parameters to control: the speed of the bow, the normal force with which the bow is pressed against the string, the position of the bowed point along the length of the string, and the angle of tilt of the bow-hair ribbon relative to the string. Ignoring tilt at this stage, just three

parameters remain. Schelleng chose to fix the bow speed, and look at the region in the force-position plane within which steady Helmholtz motion is possible.

For a given position of the bowing point, usually described by a parameter β which is the distance from the bridge divided by the total vibrating length of the string, it is a familiar fact to all string players that the normal bow force must lie within a certain range. Press too lightly and the result is a sound that players often describe as “not getting into the string”, or “surface sound”. Press too hard and the result may be a raucous “crunch”. It is easy to describe the essential physics underlying these two force limits. Below the minimum bow force, the string is not able to stick to the bow-hair as long as it is supposed to. Two or more slips occur in every period of oscillation: a bifurcation to one of Raman’s higher types. Above the maximum force the opposite problem arises: the arrival of the Helmholtz corner at the bow is insufficient to guarantee a transition from sticking to slipping. The string continues to stick, the time-keeping role of the circulating Helmholtz corner is lost, and the motion usually ceases to be periodic: hence the non-musical “crunch”.

Approximate analysis by Raman [10] and Schelleng [13] of these two force limits suggested that they both vary with β : based on the simplest theory, the minimum force varies proportional to β^{-2} while the maximum force is proportional to β^{-1} . Plotting these results on log-log axes gives Schelleng’s diagram, Fig. 3. Helmholtz motion is only possible within a triangular region of this parameter space. If the bow is moved nearer to the bridge the force must be increased, and the allowed range gets narrower so the player needs more precise control.

This pattern has a significant effect on the sound of a violin note, by a mechanism that was the second major development of the early 1970s. When the motion of real bowed strings was observed in detail, it probably comes as no great surprise that things were found to be a little more complicated than the idealised Helmholtz motion described so far. Cremer and Lazarus [14] used an electromagnetic sensor to observe the string velocity at the position of bowing, and they saw waveforms like those illustrated in Fig. 4. While both waveforms are recognisably similar to the idealised version of Fig. 2b, no abrupt jumps of velocity are seen. Instead there is smooth variation, and crucially the detailed shape varies with the normal bow force: the lower the bow force, the more rounded the waveform becomes, and this translates into a sound containing less energy in higher harmonics.

Without this variation, Helmholtz motion would pose a kind of paradox. In its idealised form, the sawtooth waveform of force driving the violin body is completely independent of anything the player does, except for changing the amplitude of the motion. But it is well known to every violinist that changes in bowing can influence the tone colour of a steady note on a violin. We will see later that “tone colour” is a somewhat slippery concept: the naïve idea that tone colour is determined purely by the distribution of energy across the harmonics of a periodic note is by no means the whole story, but nevertheless it does have some force. The observation of Cremer and Lazarus shows that a violinist can vary tone colour, while still producing a recognisable Helmholtz motion, by varying the bow force. Schelleng’s diagram then shows the limits on such force variation. In broad terms, these two ideas combine to explain the common experience of violinists: a “brighter” tone containing more high-

frequency content can be produced by bowing closer to the bridge and consequently pressing harder.

Cremer followed up this experimental work by giving an analysis to explain the link between bow force and “roundedness” of the string waveform [15]. He followed the progress of the Helmholtz corner around one cycle of the motion. Starting from the moment when the corner leaves the bow heading towards the player’s finger, the effects of propagation along the string, reflection from the finger, and propagation back again all tend to make an initially sharp corner more rounded. Wave dispersion on the string, mainly due to bending stiffness (see for example [11], [16]), will disrupt the phase coherence necessary to maintain a sharp corner, and the tendency of higher frequency components to be damped more rapidly than lower frequencies (see for example [17], [18]) will also result in a degradation of the sharpness of the corner. Furthermore, the mechanical properties of the player’s fingertip will result in some frequency-dependent energy dissipation during wave reflection [19]. The returning Helmholtz corner next passes the bow, and triggers a transition from sticking to slipping friction. If we ignore for the moment the finite width of the ribbon of bow-hair, this transition must happen at a definite moment: the string sticks to the hair until limiting friction is reached, then releases rather abruptly. That abruptness has the effect of sharpening up the rounded corner. The corner then travels to the bridge and back, becoming somewhat more rounded, then passes the bow again triggering the opposite frictional transition and getting sharpened up.

Competing effects of rounding and sharpening thus happen during each cycle, and the equilibrium periodic waveform is determined by the balance of the two effects. But the rounding effects are independent of what the player does with their bow, whereas the sharpening effect is crucially dependent on bow force: pressing harder makes the effect stronger. Thus higher bow force shifts the balance in favour of sharpening, and the pattern seen in Fig. 4 is explained, at least qualitatively.

2.2 *The first simulation models*

Cremer backed the above description with simple analytical calculations to show the balance of corner-rounding and corner-sharpening in operation, but he was a scientist from the pre-computer age. Reading his paper [15], it became apparent to scientists of the next generation that he had in fact described the essential stages of a time-stepping numerical simulation of the bowed string. Such simulations started to be performed in the late 1970s [20], [21], allowing Cremer’s mechanism for the influence of bow force on tone quality to be investigated in quantitative detail. However, simulations do much more than that because they open the door to the investigation of transient motions of the string: these include initial transients from a given bow gesture, transitions between oscillation regimes when bifurcation events occur, non-periodic motion of the string (for example when the maximum bow force is exceeded), and the curious transient interaction that sometimes occurs between bowed-string vibration and the motion of the violin body, known as a “wolf note”.

The most popular style of simulation can be described quite easily. The general approach is not restricted to studying bowed strings: similar methods have been used to study

self-sustained oscillations in woodwind and brass instruments (e.g. [21], [22]), and indeed have been applied to other engineering problems involving wave propagation and local nonlinear interaction, such as the vibration of oilwell drill-strings [23], [24], [25]. The approach has also been used as a method of real-time synthesis of sound for the purpose of musical performance: in that context it is usually known as “physical modelling synthesis” or the “digital waveguide” method (see for example Smith [22], Valimaki [26]).

It is clearest to introduce the model methodology via the simplest case: assume that the motion of the string is confined to a single plane, the bow-hair is driven at a constant bow-speed v_b , and the bow-string frictional contact occurs at a single point. Just two dynamical variables are then needed: the time-varying string velocity $v(t)$ at the bowed point, and the frictional force $f(t)$ at that point, as sketched in Fig. 5a. These two variables are related in two different ways, indicated in Fig. 5b. On the one hand, the force f is applied to a complicated linear system comprised of the string with its attached violin body, and familiar linear-systems theory can reveal the resulting response v . On the other hand, the two variables are related via a nonlinear constitutive relation characterising dynamic friction at the contact. A closed feedback loop including these two effects results in self-excited vibration.

Taking the linear response first, the string near the bowed point is a one-dimensional waveguide that can support propagating transverse waves. These will behave roughly like the waves on an ideal “textbook” stretched string, but modified in detail by a number of real-world effects including damping, non-zero bending stiffness and interaction with resonances of the violin body and the properties of the player’s finger-tip. If the string were infinitely long, extending away from the bowed point in both directions, the applied force f would simply generate outgoing waves, propagating symmetrically in both directions and never coming back. The string velocity at the bowed point associated with these waves should be well approximated by the ideal-string assumption, giving the simple proportional behaviour

$$v = f / 2Z_0 \quad (1)$$

where $Z_0 = \sqrt{Tm}$ is the characteristic wave impedance of a string with tension T and mass per unit length m [20].

The real string is not, of course, infinite. In due time, reflected waves arrive back at the bowed point from the two ends of the string. These waves will have been modified by the effects of propagation, damping and boundary reflection, but those are all linear effects that can be represented by convolution with suitable impulse response functions $h_1(t), h_2(t)$ for the two segments of the string on either side of the bowed point. For definiteness, suppose that h_1 describes the side towards the bridge of the violin and h_2 the side towards the fingerboard and the player’s left-hand fingers. The most important thing about these impulse responses, from the point of view of a time-stepping simulation, is that they both involve a finite time delay between the outgoing wave being sent, and the reflected wave returning: these time delays will be roughly equal to the propagation times to the relevant terminations of the string and back again, at the ideal-string wave speed $c = \sqrt{T/m}$. If the combined effect of returning waves from both ends of the string arriving at the bowed point at time t is a string velocity contribution $v_h(t)$, then adding to eq. (1) gives

$$v = v_h + f / 2Z_0. \quad (2)$$

The subscript h stands for “history”, because $v_h(t)$ can be calculated from the past history of the motion as a result of the finite time delay.

The nonlinear response of friction is a more difficult thing to characterise. In the early literature on the bowed string, an assumption was made that friction force is a nonlinear function of the instantaneous sliding speed, with a form like that sketched in Fig. 6 (for example Raman [10], McIntyre et al. [21], Cremer [2]). We will use this assumption for the moment, but we will be forced to re-examine it later. When the string’s speed v matches the bow speed v_b , the two are sticking and the force can take any value up to the limit of sticking friction: this gives the vertical portion of the curve. During sliding, experiments based on imposed steady sliding reveal a falling characteristic like that shown in the plot. The sign of the friction force depends on the direction of sliding: a bowed string usually slips backwards relative to the bow motion, but occasionally forward slipping occurs, and this is represented by the mirror-image portion of the curve for $v > v_b$.

Note in passing that the friction curve plotted in Fig. 6 explains the basis of Raman’s argument described earlier. If the friction force is to remain constant throughout a cycle of oscillation, as Raman’s model required, the velocity must jump between two points (one slipping and one sticking) connected by a horizontal line in the diagram [10]. A velocity jump like this corresponds to a Helmholtz corner propagating past the location of the bow.

The steps of a simulation can now be described. At time t , the quantity $v_h(t)$ is calculated by convolution of the outgoing waves sent out in the two directions with the functions $h_1(t), h_2(t)$. Equation (2) now describes a straight line in the f - v plane, and the new values of f and v must lie on this line. But they must also lie on the nonlinear friction curve, so the new values are found as the intersection of the two curves as indicated by three representative examples in Fig. 7: this geometrical construction was first presented by Friedlander [27]. These new values generate the next values of the two outgoing waves, which are stored. Time is advanced by one step, and the process repeated. Notice that the intersection of the two curves is perfectly well defined on the vertical sticking portion of the friction curve (see the point labelled II): one might have anticipated difficulties with the mathematical description of this vertical portion. The case which does require some thought is when there are multiple intersections, as with the example labelled III. The resolution of that question has a physical consequence discussed in section 2.2.2 below.

This simple simulation procedure quickly gave very encouraging qualitative agreement with observations for several aspects of the behaviour of real bowed strings: we will illustrate a few examples briefly, then return to the question of whether the agreement can be made quantitative.

2.2.1. Helmholtz motion, higher types, and variation with bow force

Since this simulation model had its origin in Cremer’s work on corner rounding and sharpening [15], it is reassuring to find that the model can indeed simulate Helmholtz motion and show the influence of bow force on the roundedness of the Helmholtz corner: examples are shown in Fig. 8a,b. The precise details of the particular model used here are not important, since the aim is to show qualitative behaviour. Discussion of such detail is

deferred to section 2.3. One important feature is immediately apparent in Fig. 8a. Each ramp of the sawtooth waveform is not a straight line as in the sketch of Fig. 2c: instead, it shows a rather regular pattern of wiggles called “ripples” by Schelleng [13] and “secondary waves” by Cremer [15]. These ripples are caused by brief peaks in friction force during transitions between slipping and sticking, and their repeat time is associated with the wave travel time from the bow to the bridge and back.

Other waveforms from the same simulation model, simply varying the input parameters of bow force and position, are shown in Fig. 8c,d. Figure 8c shows a typical waveform exhibiting two slips per cycle instead of one, the result of a bow force just below the Schelleng minimum value. The opposite problem is not illustrated: there is no such thing as a “typical” example of non-periodic string motion resulting from bow force above the maximum limit, and a short section would not be very illuminating to show. Such motion is probably chaotic, but that is not a question of great musical significance for the bowed-string problem, so it is not explored further here.

Figure 8d shows a rather different periodic waveform, usually called “double flyback motion” [28]. Like Fig. 8c it involves more than one slip per cycle, but here the two slips occur close together in time and are both shorter than the Helmholtz slip time. This oscillation regime is significant because of an empirical observation. If the motion of a bowed string is monitored during actual musical performance, double flyback motion is found to be the most common error an expert violinist is likely to make, in the sense of a departure from Helmholtz motion (other than during starting and ending transients of notes). Good players learn to control their bowing to keep within the permitted triangle of Schelleng’s diagram, but double-flyback motion can occur in that same region of the diagram so they may occasionally produce it inadvertently. This observation gives a first hint of a “playability” question: in section 6 we will discuss the use of measurements, theory and simulations to explore what kind of bowing gesture a player should use to give Helmholtz motion with an acceptably short initial transient, as opposed to something undesirable like double-flyback motion. To anticipate a little, no easy answers to that question will be found.

2.2.2. *The flattening effect*

The next effect revealed by early simulations is a consequence of resolving the ambiguity implicit in Fig. 7: when the straight line intersects the friction curve in three points rather than one, what should be done? The answer to that question has been shown to be exactly what one might guess: the intersection that should be chosen is the one that maintains continuity as long as possible; until that becomes impossible, when a jump occurs. The result is hysteresis: when $v_h(t)$ increases through the ambiguous range the string continues to slip as long as possible, but when it decreases through the range it continues to stick as long as possible. The middle intersection of any group of three is unstable and is never chosen [20].

By including this hysteresis into Cremer’s argument and tracking a rounded Helmholtz corner through one cycle of vibration, an unexpected effect is discovered. The period of the motion is systematically lengthened relative to the natural period of the free string. In musical terms, hysteresis means that the note plays flat. The extent of hysteresis increases

when bow force increases (because the friction force is proportional to the bow force, but the slope of the straight line in eq. (2) remains the same), and the result is that if bow force is slowly increased after a Helmholtz motion has been established, the note may play progressively flat. This is an effect that can be readily demonstrated on a real bowed instrument. The scope for flattening is determined by how rounded the Helmholtz corner is: each stick-slip transition must occur *somewhere* within the range of the rounded corner, and so the corner width puts a limit on the possible extent of flattening. As a result, the flattening effect occurs most strongly when playing in a high position on a thicker string, when the rounded corner can occupy a substantial proportion of the whole period of the note. (The effect is sometimes masked by a contrary tendency for a note to play *sharp* at high amplitudes because of an increase in mean tension of the string.)

This flattening effect has been further investigated, both theoretically [29] and experimentally [30], [31]. However, the results must be interpreted with some care, because it will be argued in section 2.4 that the friction-curve model does not give a very accurate representation of the true frictional behaviour of violin rosin. Alternative friction models are still likely to include hysteresis effects qualitatively similar to the one described here, and Boutilon's study [29] indicates that any hysteresis mechanism is likely to lead to flattening, but the details may be significantly different.

2.2.3. *The effect of finite bow width*

In the simple form of simulation model introduced so far, the bow-string contact has been assumed to occur at a single point. This is obviously unrealistic: the ribbon of bow hair is several millimetres wide. When a finite contact width is taken into account, another physical phenomenon seen (and heard) with real bowed strings can be explained. The earliest exploration of this effect looked at two discrete points of contact, for computational simplicity [32]; later studies extended this to a set of contact points that approximate a distributed patch [33], [34].

The most important effect can be explained by a simple kinematic argument, illustrated in Fig. 9a. Just after the Helmholtz corner has passed the bow on its way towards the player's finger, the string should be sticking to the bow. If it continued to stick across the entire width of the bow-hair for the full time until the Helmholtz corner returned, the portion of string in this contact region would be transported by the bow motion in a parallel manner (perhaps modified a little by the axial elasticity of the individual bow hairs). This parallel motion would lead to kinks in the string at the edges of the bow, requiring concentrations of friction force to maintain the state of sticking. These may prove impossible without exceeding the limit of sticking friction, and the result is that the string slips over some, but not all, of the bow-hairs near one or both edges to relieve the stress. This "differential slipping" may occur in a regular or an irregular way [33], [34]. Two typical measured examples of the resulting bridge force waveform are shown in Fig. 9b, exhibiting differential slipping with different degrees of severity. To a listener the result is a component of "noise" accompanying the musical note, which grows with the severity of the differential slips.

A skilled player can control this level of noise from differential slipping: it is sometimes used for deliberate musical effect, especially by soloists wanting to cut through the sound of an orchestra. The level of noise is influenced by the bow position and force, and also by the degree of tilt of the bow. Tilting means that the normal force varies across the width of the bow-hair ribbon, and this alters the relative propensity for differential slips at the two sides of the ribbon. Under some circumstances the differential slips can become quite regular, from an effect described by Pitteroff and Woodhouse [33] as a “miniature Helmholtz motion” between the bridge and the far side of the hair ribbon. There have been no systematic perceptual experiments on this, but it seems very likely that altering the periodicity of differential slips would have directly audible effects.

2.2.4. *The wolf note*

So far, the influence of the instrument body has been ignored. The most striking illustration of the rashness of this assumption is given by a phenomenon called the “wolf note”. It is more common in the viola than the violin, and more common still in the cello. When a cellist tries to play a note that coincides with a strong resonance of the instrument body, the response may be a stuttering or warbling sound, rather than the steady note expected. The effect is strongest on the lower, and heavier, strings of the instrument and the wolf note is most troublesome when trying to play with light bow force. The reason the wolf is worse on the larger instruments is that they are under-sized compared to a scaled-up violin, for ergonomic reasons [35]. Since the strings are relatively short, they have to be heavier and hence have higher impedance. On the other hand, since the body is small it has to be made thinner to get the resonance frequencies into the right place in the playing range of the instrument. The combined effect is that the coupling between strings and body is stronger than in the violin, and thus any effect that depends on that coupling strength, like the wolf note, is more marked.

The explanation of the wolf note is connected with the Raman-Schelleng minimum bow force already mentioned. For an ideal string with rigid terminations, the minimum bow force would go to zero: Helmholtz motion is a free solution of the governing equation, and no intervention from friction force at the bow is actually needed to sustain it. In the real world, though, there are always losses, and in a steady-state vibration the bow must somehow replace just the right amount of energy in each cycle to compensate for the losses. Non-zero friction forces are required, and the minimum bow force is calculated from the requirement that it must be possible to supply the required force without exceeding the limit of static friction.

For losses associated with wave reflection at a non-rigid termination, the more the body moves the greater is the energy dissipation rate, and the higher the resulting minimum bow force. Now consider what happens when starting to bow a note matching a strong body resonance. Initially the body is not vibrating, and it may be possible to start the Helmholtz motion with a relatively low bow force. The resonant response of the body will then grow, with a timescale determined by the damping factor of the mode in question. This causes the bridge motion to increase, so the effective minimum bow force rises. If the player maintains the low initial bow force, it may happen that the minimum level overtakes the actual bow

force. Helmholtz motion then gives way to double-slipping motion. But such motion, especially if the two slips are rather symmetrical, produces far less excitation at the fundamental frequency, and this allows the body vibration to die away. The effective minimum bow force may fall below the actual force, and Helmholtz motion may be able to re-establish. The cycle then repeats, and the result is the “warbling wolf”.

An example of a wolf simulated using the simple model described above, with the effect of a single body resonance included via a suitable form of impulse response function $h_1(t)$, is shown in Fig. 10. The bridge force waveform shows alternation between Helmholtz motion and double-slipping motion. The body motion is also shown, and the phase relation between it and the string oscillation regime bears out the description just given: Helmholtz motion breaks down when the body motion becomes too large, and resumes when it becomes sufficiently small.

2.3. The ingredients of a full bowed-string model

The examples just described show that the simple theoretical model allows qualitative explanation of several phenomena that are seen and heard in real bowed strings, and which have direct relevance to musicians. However, as already mentioned, musical judgements often hinge on matters of fine detail. If theoretical/computational models are to make an impact on makers and players of musical instruments, qualitative explanations are not enough. What is needed is a model that can be calibrated by measurements on a particular violin, with particular strings, bow etc, and then be relied upon to predict the transient response of the string to a particular bow gesture in quantitative detail — or at least, in enough detail to match the ability of human perception to discriminate differences. This is a tall order, but if it could be achieved it would open the way to a wide range of computer-based investigations into the “playability” of violins and their relatives, as will be discussed in section 5. In this subsection and the next the requirements of a complete model are reviewed, and the current state of knowledge assessed. This subsection concentrates on effects associated with the “linear system” box of Fig. 5b, while the next subsection examines the more difficult question of characterising the physics of friction. The requirements imposed by human perceptual abilities are discussed later, in section 4.

2.3.1. Details of string physics

There are a number of details of the behaviour of real strings that need to be considered first. The transverse motion has already been discussed: the two impulse response functions $h_1(t), h_2(t)$ are influenced by the mass distribution and the tension of the string, but also by the bending stiffness, and the frequency-dependent damping [16]. It also needs to be kept in mind that transverse vibration of the string can occur in two polarisations: only one is directly excited by the friction force from bowing, but the other can be excited by variations of normal bow force, and in any case the two polarisations are coupled together at the terminations of the string, especially at the bridge, by the three-dimensional nature of the body’s vibration response [36], [37].

Less obviously, the torsional response of the string needs to be considered. The frictional force is, of course, applied to the surface of the string rather than to its centre, and it will automatically excite torsional motion. It seems unlikely that torsion is directly responsible for much of the audible sound of a violin, but such measurements as have been published [38], [39] suggest that torsional modes of typical multi-layer musical strings have much higher damping than the transverse modes, and this may influence the energy balance of the feedback loop that determines the details of the string motion. This may in turn influence the regions in parameter space in which Helmholtz motion, for example, is stable. There are many other contexts of nonlinear dynamical systems theory in which the structure of bifurcation diagrams, for example, is influenced by details of energy dissipation (see for example Kuznetsov [40]). Numerical studies (Serafin et al. [41]) suggest that the influence of torsional dynamics on bowed-string behaviour may in fact be rather small, but this issue should be revisited as more complex and accurate models are developed.

There is one more wavetype on a stretched string that may have to be considered: axial or compressional waves. Such waves could be directly excited by the player if the angle of the bow is not precisely perpendicular to the string, and in any case they can be excited via the motion of the bridge, as was the case with the second polarisation of transverse motion. They will also be excited to some extent by nonlinear effects: transverse vibration of the string changes the length and hence induces tension variations [42], [43].

In total, then, there are four types of wave on the string rather than the single type considered in section 2.2. Provided attention is restricted to linear theory, the same strategy can be adopted for all four types: outgoing waves are generated by interactions at the bow, and returning reflected waves calculated using appropriate impulse response functions. The set of these impulse responses needs to include all the cross terms to represent, for example, reflected transverse waves in one polarisation caused by outgoing waves of the other polarisation. The result is a model that is more elaborate than the earlier one, but one that does not bring in any fundamentally new or controversial concepts. Exploration of extended models of this kind is in its infancy, but some preliminary results have been published [44].

If nonlinear effects (other than those arising from the frictional interaction) need to be incorporated, that would require a more serious reformulation of the model. However, one might hope to get away with a predominantly linear theory, perhaps incorporating weak nonlinear effects via a perturbation approach. This question has so far received only very limited attention in the literature, but the basic equations for coupled transverse and axial vibration of a string are well known [45]. Some direct measurements of axial string forces in a violin have been made by Harris [46], and related effects have been studied in plucked strings: for example the guitar [17] and the Kantele [47].

2.3.2. Dynamics of the violin body

Vibration of the violin body will be discussed in detail in section 3, but for the moment it is sufficient to note that interactions with the strings occur only at the contact points. Presumably the main influence comes via the notches where the strings pass over the bridge, but there may be some interaction at the other ends of the strings, especially if the dynamic

behaviour of a player's fingertip is for this purpose included as part of the "body response". For the case of longitudinal waves in the string, it is far from clear that either the bridge or the fingertip acts as a very strong reflector, and it may be that dynamic interactions with the body also occur at the nut, the pegs, and the tailpiece (the names of these violin components will be explained in section 3.1).

At a string notch on the bridge, the body vibration can be captured (provided linear theory is adequate) by impulse response functions, or their equivalent in the frequency domain, frequency response functions. If full three-dimensional motion is to be taken into account, there will be a 3×3 matrix of frequency response functions at each notch. These have been measured in full detail only rather rarely [36], [37], but there is far more extensive experimental data relating to the direction of excitation by bowing. This will be discussed in some detail later. It is straightforward, at least in principle, to include this information in the bowed-string simulation model. Either by using measured data directly, or by fitting the measurement to a standard modal superposition formula, or indeed by using a theoretical model of the violin body in terms of, for example, Finite Element Analysis, each frequency response function provides an impulse response that could be incorporated into the function $h_l(t)$ or one of its relatives describing other wavetypes.

As was the case with string vibration, there is always the possibility to consider that nonlinear effects might occur in the body vibration, requiring a more careful approach. Of course, things like the detailed micro-scale mechanisms of vibration damping in any complex structure, whether a violin body or an aeroplane, are usually nonlinear when examined closely (see for example Nashif et al. [48], and Chapter III of Cremer et al. [49]). It is generally thought that the macroscopic behaviour of such systems can be adequately approximated using linear theory, via such ideas as effective modal loss factors (see for example Heckl [50]). However, we have already emphasised the occasional importance of subtle physical effects in musical acoustics, so the possibility of nonlinear effects of body vibration should be kept in the back of the mind. There have been suggestions of such effects, but these have been in the context of the perceived sound of instruments rather than of feedback to the string influencing the bowing response, so further discussion will be deferred to section 5.1.

2.3.3. Dynamics of the bow

So far the violin bow has been treated as a rigid object, but of course this is far from being the case, and it has its own dynamic behaviour. There is widespread agreement among musicians that the choice of bow can make a large difference to the sound and playing properties of an instrument. Relatively little research has been published on this subject, but it is possible to distinguish several routes by which influence might occur. One influence undoubtedly comes via such factors as the taper, camber, weight and balance point, which can have a profound influence on a player's ability to control certain bowing gestures; especially techniques like *spiccato* that rely critically on the bouncing behaviour of the bow on the string [51], [52], [53], [54]. Another aspect has already been mentioned, when discussing differential slipping of the string in section 2.2.3: the longitudinal elasticity of the bow-hairs can affect the details

of stress concentration near the edges of the bow-hair ribbon, and thus modify the details of string slipping, possibly with directly audible effect [55], [33], [34].

What is less clear is whether the vibration resonances of the bow-hair and bow stick ([56], [57], [58]) have a direct influence. It is certainly possible. Bow-hair is, after all, somewhat similar to the strings of an instrument: each hair is a tensioned string, capable of transverse vibration in two polarisations, and of longitudinal vibration. These hair motions are in turn mechanically coupled to vibration of the bow stick: in particular, dynamic axial forces in the hair, driven directly by the frictional force at the bow-string contact, act through the cranked tip of the bow to provide a bending moment at the end of the stick and thus couple to bending modes of the stick.

It is straightforward in principle to include this influence in the bow-string simulation model by exactly the same strategy originally used for the string. Outgoing transverse and longitudinal waves are generated on the bow-hair in the contact region with the string. These travel along the hair and, in due time, return as reflected waves after modification by the physical processes of propagation, dissipation, reflection and coupling to other wavetypes. Yet another set of impulse response functions can be introduced to capture this behaviour. Numerical experiments with such a model are currently under way [44], and these should allow the influence of the various factors added to the original simulation model in the last three subsections to be assessed quantitatively.

2.4. *The physics of rosin friction*

The final physical ingredient of a “complete” simulation model for the bowed string poses scientific challenges of a different order. The effects discussed so far, especially when attention is restricted to linear theory, are complicated but well understood. It will be emphasised in Section 3 that fully deterministic analysis may not in fact be the best way to approach violin body acoustics at higher frequencies because of issues of variability and sensitivity, but nevertheless few would doubt that, given enough care and perseverance, any desired degree of fidelity of modelling could in principle be achieved for a given violin body in a given condition. Describing the friction force at the bow-string interface is quite different: the literature on constitutive equations for dynamic friction contains many proposals and measurements, but no consensus. Interest in the issue is by no means restricted to understanding violin strings: friction-excited vibration occurs in many contexts and at many length- and time-scales, and research from fields as disparate as earthquake mechanics, vehicle brake squeal and atomic force microscopy is relevant.

2.4.1 *Overview of friction models*

The simplest and most familiar model for dry friction at an interface is based on the “Amontons/Coulomb laws”: these suggest that friction force is proportional to the normal load, independent of the apparent area of contact, and independent of the sliding speed. The first two of these statements lead to the notion of characterising friction between a given pair

of materials via a “coefficient of friction” which is the ratio of friction force to normal force. If the third statement is assumed, then during sliding the coefficient of friction is a constant. The simplest empirical experiment consists of finding the maximum angle of an inclined plane before sliding of a small block begins, and the minimum angle for which sliding can be sustained once it is started. Such a test often reveals that the coefficient of friction during sticking can exceed the value during sliding, leading to the notion of a static coefficient of friction μ_s and a dynamic coefficient of friction μ_d , with $\mu_s > \mu_d$.

The next stage of sophistication leads to the friction model introduced earlier. Steady sliding can be imposed on the chosen interface, and the friction force measured as the sliding speed is slowly varied. The coefficient of friction would then naturally be plotted against sliding speed, perhaps leading to a curve of the form shown in Fig. 6. As a representation of the results of that particular experimental measurement, such a plot is uncontroversial. What is far more contentious is to jump to the conclusion that friction force is *determined* by sliding speed alone, so that during a dynamic process such as stick-slip vibration of a violin string the friction force simply tracks back and forth along the curve revealed by the steady-sliding tests. That assumption, sometimes called the “friction-curve model” or “Stribeck model”, was ubiquitous in the earlier literature of the bowed string, and in many other fields: the book by Sheng gives a wide-ranging review [59]. The discussion in Section 2.2 was based on precisely this assumption. However, with the power of hindsight, it is hard to see any logical reason why this should ever have seemed convincing (although we have seen that it led to a model which gave qualitative explanations for several observed effects).

As soon as direct measurements were made of the dynamic friction force during stick-slip vibration or unsteady sliding, the friction-curve model was seen to be seriously flawed: see for example Rabinowicz [60], Ko and Brockley [61], Dieterich [62]. Different investigators designed different styles of testing, each revealing a particular pattern of behaviour. Quite naturally, they then proposed friction models tailored to explain their particular observations. The result is a bewildering array of proposed models: Sheng gives a useful review [59]. Rather than trying to cover the whole field here, we will concentrate on results specifically relevant to the bowed-string problem.

The key ingredient here is rosin: all players of bowed-string instruments control the frictional behaviour by coating their bow hair with some variant of this substance, usually obtained by extraction from softwood timber as a by-product of making turpentine. It is the frictional behaviour of rosin that is responsible for the stick-slip vibration: contrary to persistent folklore, bow-hair does not have “barbs” on its surface that catch the string [63]. The main chemical constituent of natural rosin is abietic acid [64], but synthetic rosins have also been made using other chemicals with similar properties. Rosin is a glassy material, showing brittle behaviour at lower temperatures but becoming sticky and eventually becoming a viscous liquid as temperature rises. The transition occurs over a range of temperatures, usually characterised by a glass transition temperature T_G defined to fall in the middle of the range. Typical musical rosins have their glass transition a little above normal room temperature. Commercial products cover a range, from violin rosin with a relatively high transition temperature to some types of bass rosin that are sold in pots because, like brie and other soft cheeses, they have a tendency to flow at warmer room temperatures.

The viscosity of rosin has been directly measured as a function of temperature. The first such viscosity measurements were not made because of interest in rosin as a frictional material, but in order to use it in laboratory studies of plate tectonics to mimic the behaviour of material in the Earth’s mantle [65]. More recent results showing similar values but more detail are shown in Fig. 11. This plot combines measurements made in two different instruments: one measuring a “solid” specimen and the other a “liquid” specimen. This explains the gap in the plot: for an intermediate temperature range, neither instrument could be used. However, the trends of the two measurements can easily be imagined to join up in a smooth way across the gap. Notice that the measured values cover seven orders of magnitude, so it is not surprising that a single measuring instrument could not easily cover the entire temperature range.

2.4.2 The tribology of rosin

The first direct measurements of the properties of rosin relate to steady conditions. Measurements of the friction force under conditions of imposed steady sliding have been published by Cremer [2] and by Smith and Woodhouse [66], both obtaining very similar results: one set of results was illustrated by the set of discrete points included in Fig. 6. Measurements of rosin behaviour under dynamic conditions came later. The first study drew on earlier work by Ko and Brockley [61] in the context of the frictional dynamics of automobile brakes. The essence of the method is to design an oscillator, in the appropriate frequency range, that can reasonably be treated as having a single degree of freedom. Calibration tests can be carried out to give the effective mass, stiffness and damping of this oscillator. It can then be excited into stick-slip oscillation using a rosin-coated rod, and the details of the vibration waveform monitored. The measured displacement, velocity and acceleration can be substituted into the equation of motion using the known parameters of the oscillator, and the dynamic friction force thus obtained.

Typical results are illustrated in Fig. 12 [66]. When the trajectory is plotted in the force-velocity plane, the slipping portion reveals a loop that is traversed in an anticlockwise direction during the oscillation. The sticking portion shows as an approximately vertical line at the right-hand side of the plot: the superimposed loops here are a measurement artefact because the measuring sensor could not be placed exactly at the frictional contact point. The curve fit to the steady-sliding measurements shown in Fig. 6 (which used exactly the same particular violin rosin) is superimposed as the dashed line: no part of the dynamic trajectory falls close to this line. It is clear that something more than the Stribeck model of friction is needed to account for these measurements.

This observation is confirmed by a second set of dynamic measurements using a different principle. Schumacher and Garoff [67] developed a rig in which a violin E string (a steel monofilament) was bowed by a rosin-coated glass rod. Friction force and velocity at the contact point cannot easily be measured directly, but they can be deduced by an inverse calculation based on non-intrusive measurements of the force waveform at the two terminations of the string. The inverse calculation was initially developed in the frequency domain and applied to periodic motion, but was later extended to the time domain and applied to transient motions [68], [69]. The results showed hysteresis loops in the force-velocity trajectory very reminiscent of the one shown in Fig. 12.

This rig also yields another thread of evidence to give a clue about the nature of an improved model of the dynamic friction of rosin. A glass “bow” can be used for a single stroke along a given line on the rod, then examined in a scanning electron microscope. The track left in the rosin surface by the stick-slip motion can be observed directly. Examples are shown in Fig. 13. The first picture shows parts of three tracks on the same rod: each sticking event during the string motion leaves a visible scar in the rosin surface. The second picture shows a close-up view of one of these scars. An area of rough terrain is seen, presumably generated by the string rolling back and forth due to torsional motion during sticking. The left-hand portion of the picture reveals quite different terrain during slipping, showing very clear evidence that the rosin has been partially melted during the slipping event.

Such evidence suggests that rosin friction exhibits melt lubrication, as has been used to explain, for example, the behaviour of ice skates [70]. During sliding, the friction force generates heat at the contact. This causes the rosin to heat up, and so its viscosity decreases: rather rapidly, as shown by Fig. 11. When the kinematics of the stick-slip motion result in the relative sliding speed reducing, the temperature falls and the viscosity increases. This can lead to the re-establishment of a state of sticking, perhaps with some residual creep motion: notice that the top portion of the “sticking” line in Fig. 12 seems to deviate systematically towards the left, away from the vertical dashed line. That is just what would be expected if there was some slow viscous flow during “sticking” at with high tangential force. It is easy to see how such a thermally-driven mechanism could result in the kind of steady-sliding characteristics seen in Fig. 6: for steady sliding, contact temperature naturally rises with sliding speed.

This suggests a frictional constitutive model of the same general kind as the family of “rate-and-state” models initially developed in the context of rock mechanics [62] and later extended to a variety of other materials [71]. The friction force might be influenced directly by sliding speed, but also by one or more internal state variables: in this case, representing the local contact temperature, or perhaps the distribution of temperature near the contact region. Preliminary models of this kind have been developed [66], but a discussion of how well they perform in the context of bowed-string simulations is best deferred until section 5, when issues of playability are discussed. Before we are ready for that, we need to consider in more detail the vibrational behaviour of the violin body.

3. Vibration and sound radiation of a violin body

3.1. Background

The dynamics of the violin body matter in two different ways. As has just been discussed, the body motion influences the bowed string through motion at the bridge, and to a lesser extent at the other points where the string touches the body. This influence can result in “playability” effects: the most striking is the wolf note, already mentioned, but further details will be discussed in section 5. However, there is a more obvious significance of body vibration for the sound of a violin: the resonances of the body produce a filter for the radiated sound, emphasising some frequencies and reducing others. The pattern of resonances thus gives an “acoustic fingerprint” of each particular violin. It is worth noting that at this general level of description, “body resonances” should include the effects of sympathetic vibration of the non-bowed strings, if the player does not damp them with the left hand.

Before starting any detailed discussion, it is useful to summarise the names of the parts of a violin. Many of them are labelled in Fig. 14. The box, or *corpus*, is made up of a *top plate* (usually made of spruce) and a *back plate* (usually made of maple), separated by the garland of *ribs*, thin strips of maple held together by *corner blocks* and *end blocks*. The top plate has a pair of *f-holes*, and on its underside is a reinforcing strut called the *bass bar*

running for about $\frac{3}{4}$ of the length of the plate, passing more or less under the bass foot of the *bridge*. Approximately under the other foot of the bridge is a small wooden rod called the *soundpost*, which is inserted through the treble f-hole and wedged between the top and back plates, held in place by friction. Ordinarily, the top and back plates are carved from solid blocks of wood, quite often made from a pair of adjacent pieces from the same log, joined back-to-back along the centre-line of the instrument. The ribs are the only parts of the violin that are normally made into their curved shape by bending, as opposed to carving. The rib garland divides naturally into three sections: the *upper bout* near the neck, the *centre bout* where the shape narrows to form the waist of the violin, and the wider *lower bout*.

Joined to the corpus, usually by a shallow dovetail joint in the top block, is the *neck*, terminating in the decorative *scroll*. The strings are held and tensioned by means of four tapered *pegs* in the *pegbox*. To resist the wear and tear of playing, the top surface of the neck is covered by a *fingerboard*, usually made of a hard wood such as ebony. The strings are located in place over the fingerboard by grooves in the *nut* at the pegbox end of the fingerboard. At the other end of the playing length, the strings are located in notches in the top curve of the bridge. The strings pass over these notches, and are then held by the *tailpiece* which is in turn anchored to the *endpin*, a tapered pin fitted into the bottom block. The final component is a *chinrest*: most players like to use one pattern or another of chinrest to assist in holding the instrument securely while playing. For more details about violin construction, see for example Gill [72].

The first stage in understanding the acoustics of the violin body is to examine the structural vibration in response to the dynamic force applied by the vibrating strings. This structural response then leads to a certain pattern and strength of sound radiation. Provided linear theory is an adequate approximation, both the structural response and the sound radiation can be written as a linear combination of modal contributions: each mode has a natural frequency, a damping factor, a mode shape and a radiation pattern and strength. In principle, if we knew all these modal parameters for all the modes within the audible frequency range, that information would encapsulate everything there is to know about a particular violin body.

However, this statement, while formally true, is rather misleading. A violin, in common with most other vibrating structures, shows qualitatively different behaviour at high and low frequency. The first few modes are well separated from each other, but as frequency rises the damping bandwidth goes up while the typical modal spacing stays roughly constant. The ratio of these two quantities is called the *modal overlap factor* (see for example Lyon and DeJong [73]), and once it is bigger than unity (which happens around 1–2 kHz in a typical violin [74], [75]) it becomes questionable whether modes are the best way to describe the response since at each particular frequency, more than one mode is contributing significantly. At higher frequencies the modal overlap factor becomes larger still, and the language of modes becomes progressively less useful.

There is a second general phenomenon that also produces a distinction between high and low frequency behaviour. Suppose a violin maker was set the task of making 10 identical instruments. Because of variability of the raw materials combined with the limitations on any human's ability to control fine details of shape, thickness, joint details and so on, the 10

instruments will all behave slightly differently. The mode shapes and natural frequencies will vary across this ensemble of violins. A parameter known as the *statistical overlap factor* can be defined by analogy with the modal overlap factor [76]: it is the spread across the ensemble of the frequency of a given mode, divided by the typical modal spacing. When the statistical overlap factor is small, as it is likely to be at low frequencies, the individual modes will retain their identity across the ensemble in a recognisable way. However, at higher frequency the statistical overlap factor will become of order unity, and it is no longer meaningful to look for the “same” mode in different violins: the sensitivity to small physical differences mixes the shapes beyond recognition.

An essential ingredient of any discussion of violin acoustics is sound radiation by the vibrating violin body, and here again the generic behaviour at high and low frequencies is different. This time the characteristic non-dimensional number is called the *Helmholtz number*, defined as the ratio of the typical linear dimension of the object to the wavelength of sound (strictly, divided by π) [2], [77]. When the Helmholtz number is small, at low frequencies, there is a standard way to describe sound radiation by a series of terms describing source contributions with progressively weaker behaviour: monopole, dipole, quadrupole and so on: see for example Ffowcs Williams and Dowling [77]. In particular, the most efficient sound radiators at low Helmholtz number are monopole sources, with a source strength proportional to the net change of volume associated with the vibration mode shape in question. Modes with no net volume change can be at best dipole sources [77].

Note that when calculating the net volume change for a mode of a violin body it is important to take into account any air flow through the f-holes. This flow can be visualised as “air pistons” moving in and out of the holes, behaving as part of the structural vibration. At the very lowest frequencies, the air flow exhibits the “toothpaste effect” [78]: the internal air behaves approximately incompressibly, so that any volume change in the structural motion is exactly cancelled by the air flow through the holes, leading to zero monopole strength as frequency tends to zero.

Once the frequency rises enough that the Helmholtz number is bigger than unity (around 1 kHz for a violin body), the multipole way of thinking about sound radiation becomes misleading. The calculation of sound radiation now becomes a complicated problem: it is necessary to take account of interference between sound fields generated by different parts of the vibrating body, and also to allow for the shadowing effect of the body (and perhaps the violinist as well). The directional radiation patterns become increasingly complicated: some examples for violins can be seen in Meyer [79], Cremer [2], [80] and Bissinger [81], [82], while corresponding results for guitar bodies have been shown by Hill et al. [83].

Three dimensionless numbers have been introduced, each indicating a qualitative difference of behaviour at high and low frequencies. The combination of these three effects sets the agenda for this section. First, the low-frequency modes of a typical violin are discussed. There are a small number of modes, often called the “signature modes”, with frequencies that fall in the range where all three of the dimensionless numbers are small. This means that similar mode shapes can be recognised in most normal violins, a violin maker can realistically think about controlling these modes deliberately and explicitly, and the sound

radiation behaviour can be understood, to a good first approximation, by considering only the net volume change and the consequent monopole strength.

Many researchers have made measurements relating to these signature modes and discussed aspects of the behaviour revealed. A long series of experiments by Jansson and co-workers laid the groundwork for the modern understanding of these modes: see for example [84], [85], [86]. When the technique of experimental modal analysis arrived, the first study of the violin was by Marshall [87], and the most elaborate subsequent studies have been by Bissinger and co-workers, for example [88], [82], [89]. However, a satisfying explanation of how and why these particular mode shapes arise is only now beginning to appear. This will be summarised in the next subsection.

In the following subsection, studies of the vibration and sound radiation of the violin over the wider audio frequency range are discussed. A different perspective is required in this range, to recognise the modal overlap and the uncertainty of modes. A statistically-based approach is called for, but we will also find some interesting problems requiring a hybrid combination of both points of view. Such hybrid modelling of high-frequency structural vibration has been applied in a wide range of engineering areas in recent years [90], [91]. Some recent results relating to sound radiation in this high-frequency range will also be discussed.

In section 3.4, the scientific approach to violin body behaviour is examined from the point of view of an instrument maker. Makers usually have a pragmatic perspective, wanting to use measurement technology and theoretical understanding to help them make better instruments — although of course the word “better” covers many aspects of behaviour and has no simple definition. One specific concern of makers is the choice of materials: this question includes detailed choice between specimens of the same wood species, comparison of different species, treatment of wood by various means to improve the properties, and also possible alternative materials such as carbon-fibre composites. A short discussion on the question will be given in section 3.5.

3.2. *The low modes of a violin body*

3.1.1 *Measurement methods*

The importance of the low-frequency modes of a violin body has seemed obvious to generations of researchers, and each time a new measurement technology for structural vibration has become available, it has been used to look at violin bodies; often with the hope that if a few good and bad violins were measured, the supposed “secret of Stradivari” would become obvious in some clear difference of mode shapes or frequencies. The earlier measurements were not really of mode shapes but of what would now be called Operating Deflection Shapes (ODSs): the spatial pattern of forced vibration in response to sinusoidal force input. When modal peaks are well separated, then the ODS created by driving at a suitable location with a frequency matching a modal peak gives a reasonable approximation of a mode shape. This idea was applied when electroacoustic measurements first became

possible (e.g. [92], [93]), and again when holographic interferometry was invented: in the latter case, studies of musical instrument bodies were among the earliest publications featuring the method [94], [95], [84].

Holographic methods continue to have their enthusiasts, particularly the real-time versions based on speckle patterns: see for example Jansson [96]. The great attraction of the method is that it gives a full-field visualisation of the body vibration, or at least of as much of it as the experimenter's ingenuity allows to be illuminated simultaneously: tricks can be done with mirrors to combine different views in one image (see for example Fig. 9.9 of Cremer [2]). Developments of the method based on double exposures have also been used to show the evolution of transient wave propagation following impulsive excitation: see Molin et al. [97], [98], [99]. However, in the last 20 years or so most attention has shifted away from holographic methods to measurements based on experimental modal analysis: for a general account of the method, see Ewins [100].

The usual approach is to use a small instrumented impulse hammer to tap the violin and a non-intrusive sensor such as a laser-Doppler vibrometer or a very small accelerometer to measure response. Using standard methods from the more general field of structural vibration measurement, such as averaging results of a number of impacts and computing the coherence function to give an indication of the frequency range over which the data is of sufficiently high quality (see for example McConnell [101]), transfer functions are measured. Examples of such transfer functions have already been shown, in Fig. 1. These particular examples are measurements of what is usually called the *bridge admittance* (or *bridge mobility*): the driving point response at one corner of the bridge, in the direction of bowing on the nearest string. The particular significance of the bridge admittance will be discussed in some detail in section 3.3.1.

There is a standard formula by which any such vibration transfer function can be expressed as a linear combination of modal contributions (see for example Hodges and Woodhouse [102]): the velocity response at a position x to sinusoidal forcing at position y at frequency ω is

$$H(x, y, \omega) = i\omega \sum_n \frac{u_n(x) u_n(y)}{\omega_n^2 + 2i\omega\omega_n\xi_n - \omega^2} \quad (3)$$

where the n th mode has natural frequency ω_n , damping factor ξ_n and mode shape $u_n(x)$. The mode shapes are normalised with respect to the mass distribution of the system, so that

$$\int u_n^2(x) dm = 1 \quad (4)$$

where the integral is taken over the entire structure and dm denotes the element of mass associated with the integration. Note that this “mass normalisation” has the consequence that for a driving-point measurement (with $x=y$), the squared modal amplitude which then appears in eq. (3) is the inverse of the effective mass of that mode when measured at that point.

Signal processing techniques have been developed to invert eq. (3), and estimate the modal parameter values from a measured transfer function (see for example [100], [103]). If

many transfer functions are measured, at a grid of points covering the entire instrument body, the spatial variation of the mode shapes can be deduced and plotted. Note that this approach really does extract mode shapes rather than ODSs: the effect of a degree of overlap between modal peaks in each transfer function is allowed for by the fitting methods. Of course there are issues of accuracy and reliability, progressively more severe as modal overlap increases [75], and care and attention to detail is needed to obtain results that are fully convincing. Because of a general reciprocal theorem for transfer functions of linear vibrating systems [11], obvious from the symmetry of eq. (3) in x and y , the grid of measurements can be performed either by keeping the tapping point fixed and moving the measurement point, or vice versa. Both methods are used: if a scanning laser vibrometer is available it is convenient to keep the hammer fixed and scan the laser beam, but if an accelerometer is used it may be easier to keep that fixed and move the tapping point.

3.2.2 Modal results

What has been revealed by the various measurements of ODS or mode shapes described in the previous subsection is a little surprising. For most structures, it is fairly easy to guess roughly what the lowest vibration modes are likely to look like. This is true, for example, of the modes of a guitar body, but it is not true for the violin body. Some examples of a few of the lower-frequency modes of a guitar are shown in Fig. 15, visualised by time-average holographic interferometry (and discussed further in Chapter 9 of Fletcher and Rossing [12]). Most of the motion in these modes takes place in the top plate of the instrument, with very little motion at the edges, and the sequence of mode shapes shows a general pattern that is familiar from theory or measurements of vibrating plates or membranes (see for example Rayleigh [11] or Waller [104]). There are similar modes mainly confined to the back plate of the guitar. There are also modes mainly involving the neck and fingerboard of the guitar, vibrating in bending or torsion. Finally, not visible by this kind of measurement and plot, there is motion of the air in the cavity, including the possibility of some “breathing” in and out through the soundhole. There is another experimental technique that can make these flows visible: near-field acoustical holography, using measurements by a grid of microphones close to the surface of the plate [105].

As already mentioned, early measurements of the low-frequency “signature modes” of a violin body were based on point measurements or holographic interferometry. The results were often plotted as nodal line patterns, such as the examples shown in Fig. 16. The patterns revealed are not easy to describe or to visualise, and they seem much less intuitive than those of the guitar. This difficulty of description is perhaps a contributory factor in the variety of different labels that researchers have proposed to classify these modes. In particular, the two modes labelled B1- and B1+ in Fig 16 have been described as “baseball modes” (because of the sinuous loop of nodal line that seems to encircle both back and top plates like the seam on a baseball), or given a variety of acronyms: P1 and P2, T1 and C3, and (as here) B1- and B1+ (arising from an early designation of the “main body resonance”, which turned out in fact to consist of these two modes that are usually fairly close in frequency).

It is easy to be misled by a plot like Fig. 16b. Such plots only reveal one component of the motion at each point, whereas the true motion often involves three-dimensional deformations. If the motion is visualised as being purely perpendicular to the plane of the plot, the “baseball” nodal line, disappearing off the edge of the top plate and reappearing at about the same place on the back plate, gives an impression that the ribs must be deforming in in-plane shear across their full height. But this is implausible given the stiffness of the ribs to such in-surface deformation. What is actually happening does indeed involve motion of the ribs, but it consists largely of out-of-plane bending and flexing of the rib garland. The first thorough investigations of this 3D motion were by Bissinger, who developed an elaborate test procedure involving the measurement of vibration at a very large number of points over the body of the instrument, including motion of the ribs perpendicular to their surface: see for example [106], [107], [82], [88]. The most striking examples of Bissinger’s measurements appear in the “Strad 3D” project [89], a collaboration with violin maker Sam Zygmuntowicz to assemble a wide range of technical and constructional information about three classic Italian violins into a single DVD. Bissinger also measured the radiated sound field on a spherical array of microphones: this aspect of his measurements is somewhat similar to measurements by Richardson and co-workers on sound radiation from guitars, see Hill et al. [83].

3.2.3 The origin of the signature modes

Until recently, no very persuasive description had been given of why the low modes of a violin body should take these particular forms, or how an instrument maker might be able to influence the details (and in particular the sound radiation from them). However, an extensive series of explorations by Gough using Finite Element (FE) analysis is now giving answers to these questions. Other researchers have built FE models of the violin (for example Knott [108], Bretos et al. [109]), but their goal has generally been to reproduce the complicated structure of a violin body, and demonstrate agreement with experimental results. Rodgers went beyond this in a series of papers using FE models to explore the effects of selective wood removal in an effort to give useful guidance to instrument makers: for example [110], [111], [112]. But Gough has done something more fundamental: he has explored a series of models starting from very simple assumptions, then gradually adding in the complications of violin design one at a time so that the progressive evolution and emergence of the signature modes can be charted, and the relative influence of various contributory factors assessed [113], [114], [115]. The full picture revealed by Gough’s work is complicated, but an abbreviated caricature will be given here to show some key aspects.

A useful starting point is to consider a violin body with no bass bar, soundpost or neck. Furthermore, the top and back plates will be initially supposed to be identical, with no f-holes in the top. Under those conditions, the box has two planes of mirror symmetry: back-front and left-right. Every mode shape of such a box must be either symmetric or antisymmetric in each of these planes, giving four types of mode by combining the possibilities. Typical examples of the first few such modes are illustrated in Fig. 17. They do

not yet look very much like the modes of the final violin, but they make a useful set of “component modes” or basis functions, which can be used in linear combinations to describe the evolving make-up of actual mode shapes when the two symmetries are successively broken as the model is made progressively more realistic.

A key aspect is that only one of the shapes shown here, the one labelled “breathing”, involves significant net volume change. Most of the others are antisymmetric in one or both symmetry planes, so the volume change is exactly zero. The mode labelled “Longitudinal dipole” is symmetric in both planes, but it has almost equal and opposite volume change in the upper and lower bouts. That means that the low-frequency sound radiation of each mode of the later models will be determined (predominantly) by the amount of this “breathing” shape that goes into its make-up. Familiar patterns of behaviour of coupled oscillators then lead to insights into the frequency dependence of that sound radiation.

Another aspect to notice in these shapes is that some have particularly large motion around the centre bouts (the waist of the box). The origin of this motion lies in the particular three-dimensional form of the typical violin box. British violin maker George Stoppani has produced a striking physical demonstration, by making a “floppy violin” with a normal rib garland, but very thin top and back plates made by hot forming of thin laminate sheet . The result was a structure that could be readily flexed in the fingers. With this, it was easy to discover that there is a particular deformation in which one C-bout area could be flexed and rotated: this is the motion that appears in symmetric form in the “Bending” mode and in anti-symmetric form in the “Centre bout rotation” mode of Fig 17. The fact that the deformation can be done in the hands, with plates that allow bending but are still stiff with respect to stretching deformations, strongly suggests that it is, at least approximately, an *inextensional* motion of the box. As Rayleigh pointed out in his pioneering work on the vibration of thin shells [11], if such an inextensional motion is kinematically possible for a given shell geometry, it is very likely to appear as the whole or a significant part of the low-frequency vibration mode shapes, because such motion represents a strong local minimum of potential energy.

The next step towards a normal violin is to add the f-holes, and allow the top and back plates to be more realistically different in details (but still with no soundpost, bass bar or neck). This breaks the front-back symmetry, but preserves the left-right symmetry. It also has the advantage of being close to a stage that most violin makers go through while building an instrument (although in reality the bass bar will always be present, but this turns out to be a relatively minor perturbation). That means that experimental data can be collected from violin bodies in this state, and compared with the FE model predictions.

Several effects are introduced at this stage. First, the addition of f-holes introduces the possibility of a Helmholtz-like resonance based on the stiffness of the air inside the cavity, and the effective mass of air flowing in and out through the f-holes. This new degree of freedom couples strongly to the breathing shape from Fig. 17, leading to a well-separated pair of modes that lie above and below the frequency of an ideal Helmholtz resonance in a cavity of the same shape but with rigid walls. This adds a useful additional low-frequency mode, usually designated A0, and also pushes the second mode of the pair significantly higher in frequency than the “breathing” mode in Fig. 17.

Depending on the details, this second mode may be pushed quite close to the frequency of the previous “bending” mode, introducing the second major change: since these shapes both have left-right symmetry they can couple together to give a pair of modes involving elements of both breathing and bending. The coupling process involves a phenomenon often called “curve veering” (see for example Perkins and Mote [116], Pierre [117]), whereby the two frequencies never become equal. Instead, the mode shapes change character through a frequency range around where one might have anticipated two equal mode frequencies, and emerge at higher frequencies having swapped characters entirely.

Now recall that of the two “coupled oscillators” being considered here, the modified “breathing” shape and the “bending” shape, only one is responsible for significant sound radiation. That means that the coupled modes of the system can display a range of sound radiation behaviour, depending upon whereabouts in the veering process a particular instrument finds itself. One mode might radiate sound much more strongly than the other, or both may have comparable sound radiation. This balance of radiation between the two modes can be quite sensitive to details of the violin structure, and it may point to a significant source of variability between instruments, and also to a significant way that a maker might exercise control over the sound. Variations in sound radiation behaviour in line with this description have been observed in real violins.

To preserve mode orthogonality, the two modes always combine the two characters, bending and breathing in this case, with opposite phases. This “sum and difference” combination is the first stage of the formation of the modes B1- and B1+ seen in Fig. 16. Examples of the modes, compared to experimental measurements on a normal violin at this stage of construction, are shown in Fig. 18. The FE model still has many simplifications that have not been described in detail here, but nevertheless the agreement is very encouraging.

At this stage, the proto-violin has three low-frequency modes exhibiting significant volume change, and hence able to radiate sound effectively: A0, and the embryonic B1- and B1+. However, there is a crucial snag. When a violin body is driven by the bowed strings, the excitation force at the bridge is predominantly side-to-side: in other words, it is antisymmetric with respect to the left-right symmetry plane. That means that the strings will be unable to excite any of the three strongly radiating modes, which are all symmetric in that plane. The remaining symmetry needs to be broken. The main way this is done in a normal violin is by introducing the soundpost, although the bass bar also contributes some asymmetry.

The effect of the soundpost on these low-frequency modes is to couple a certain amount of the shapes “Centre bout rotation” and “Transverse dipole” from Fig. 17 into the modes A0, B1- and B1+, so that the nodal line on the top plate is shifted away from the centre-line to pass approximately through the soundpost position. This achieves the effect of giving those modes a significant component of rotation in the plane of the bridge, and thus allows them to be driven effectively by the bowed strings. Adding the soundpost, and adjusting its exact position, also makes further changes to the mode frequencies. These effects can still be interpreted in terms of “coupled oscillators” representing the original component motions, undergoing various veering interactions as the soundpost is adjusted. This goes some way towards explaining the sensitivity to soundpost adjustment that is found

in practice: in the completed violin, the soundpost (and to a lesser extent the bridge) are the only components that remain adjustable in order to give the violin maker some fine-tuning control over the low-frequency modes, and their associated pattern of sound radiation which varies according to how the original “breathing” component shape is distributed among the modes A0, B1- and B1+.

Many details have been omitted in this account, including the role of plate curvature and the influence of anisotropy of the elastic properties of wood. One of the more surprising findings of the FE studies is that the effects of plate arching are so dominant that once fairly realistic arching is included in the model, the anisotropy of the material properties has a relatively minor effect on the frequencies and mode shapes of the signature modes. This is true despite the fact that typical spruce used for violin top plates may show a cross-grain stiffness (measured by Young’s modulus) about 10–20 times lower than the long-grain stiffness.

Two other aspects of low-frequency vibration of a violin body omitted so far deserve a brief description: the effect of the neck, fingerboard and tailpiece, and the effect of resonances of the internal air beyond the Helmholtz resonance. Both have important effects within the signature mode frequency range, and can play a significant role in the acoustic performance of a violin in that range. The neck and fingerboard of the violin is a rather complicated beam system. It can show bending and torsional modes, which do not in themselves radiate sound efficiently at low frequencies, but which can influence the sound and “feel” of the instrument by coupling to the modes already discussed when the frequencies are sufficiently close. The tailpiece, similarly, has its own modes that can couple to more obviously important body modes.

Violin makers and adjusters sometimes make deliberate use of such couplings. One mode of the tailpiece can sometimes be adjusted, by judicious choice of the mass distribution and the length of the tailcord by which it is attached to the end button, to fall close in frequency to a wolf note (discussed earlier), and thus help to tame the wolf (see for example White [118]). In a similar vein, a bending mode of the fingerboard consisting mainly of cantilever vibration of the projecting portion often falls close in frequency to the Helmholtz-like mode A0. Coupling between these two probably does not have much direct effect on the sound of the instrument, but it can increase the amount of vibration felt in the neck of the instrument by the player’s left hand. Some players like this effect of a “lively” instrument, and so such tuning is sometimes deliberately induced [119].

In a somewhat similar way, acoustic resonances of the air inside the body cavity can sometimes have a significant effect. The first such mode, after the mode A0 already discussed, has the character of a lengthwise standing wave with approximately one half-wavelength in the length of the body: this mode is usually denoted A1, and in a violin it usually appears at a frequency similar to B1- and B1+. There are, of course, many higher standing-wave modes as well [120], [121], [122]. Claims were put forward by Hutchins [123] that the frequency relation between A1 and the B1 modes was a critical determinant of violin quality. More recent work has not lent any clear support to this idea, but Bissinger has argued that an idealised version of A1 provides another “component mode” that needs to be taken into account for a full description of behaviour in the signature mode frequency range, to

allow for the asymmetry between the upper and lower bouts of the violin [124], [125], [126]. Bissinger has also shown that in larger instruments of the violin family the A1 mode can contribute directly to significant sound radiation, because of this same asymmetry [88].

Space does not allow a fuller description of these low-frequency details, because there are more pressing questions to address concerning the behaviour of the violin over the rest of the audible frequency range, to which we now turn.

3.3. Higher frequencies, statistical and hybrid methods

3.3.1 Frequency responses and bridge admittance

The starting point for a discussion of violin behaviour over the full audio range is to examine the various kinds of frequency response function of interest. These fall into two main types, depending on whether the output variable is a structural response such as velocity or acceleration measured at a point on the body, or an acoustical response measured with a microphone. The input will usually be a force, applied at the violin bridge or in some other position. There are several important issues concerning the measurement and interpretation of such frequency responses.

The most obvious frequency response to characterise a violin, one might imagine, would be some measure of the radiated sound in the far field, in response to a force applied at a string notch on the bridge in the direction of the transverse force exerted by that string when bowed. However, there are complications. Each string requires a slightly different position and direction of the applied force. More challengingly, what exactly should be measured to represent far-field sound radiation? The sound field will be highly directional at higher frequencies, and no single microphone position could entirely be regarded as “typical”. Perhaps it would be better to measure an average response over a number of microphones in different positions? But then, should that be a magnitude average, giving some idea of the total sound power radiated, or should it be a linear average representing the spherically-symmetric radiated sound, the component of the sound field which was dominated by the monopole component at low frequencies? In either case the measurement becomes quite elaborate, and unless an anechoic chamber is available, room acoustics will complicate the interpretation of results. Furthermore, to be truly in the far field over the entire frequency range, the measurement distance cannot be too short otherwise non-radiating near-field pressure components will be included.

There is an ingenious way to circumvent these objections, at least for low-frequency measurements [127], [128]. In the monopole frequency range, the *internal* sound pressure inside the body mirrors the far-field monopole radiation. A small internal microphone, positioned on the nodal lines of A1 and the first transverse standing-wave mode, can be used to make the measurement, a trick which is especially valuable for the larger instruments where the problem of getting far enough away to be in the external far field becomes acute. However, this method loses accuracy once the Helmholtz number ceases to be small.

By contrast with microphone measurements, a structural response measurement makes no direct claim to represent aspects of the sound that a listener might hear, but it can have

some compensating advantages. The most important is one that we have already taken advantage of in the previous section. Equation (3), and its relatives for other output variables, expresses any (linear) structural frequency response function in terms of mode shapes, frequencies and damping factors. This means that the functional form of the frequency response is well understood, and allows data-fitting exercises such as experimental modal analysis. There no equivalent general formula for a radiated-sound response function.

There can be more specific advantages to particular structural response functions, especially those relating to interface positions between different components of the violin. As has already been seen in the discussion of low-frequency modes, understanding the details of coupling between parts of the violin can be important and illuminating. Frequency response functions of subsystems at a coupling point, or set of points, can be used to predict how the coupled system will behave (see for example Woodhouse [129]), and thus give a route to improved understanding.

The most important such interfaces in the violin are between the strings and the body at the bridge notches. A lot can be learnt from a structural measurement at such a point, and many researchers have measured this “bridge admittance” or “bridge mobility” on a range of instruments, so that a large body of data exists. The usual strategy for making a single measurement (pioneered by Jansson, see for example [130]) involves measuring from one bridge corner to the other, by hitting with a miniature impulse hammer on one corner, in the direction of bowing of the nearest string, and measuring with a laser vibrometer or a very small accelerometer or other sensor at the other corner, again in the direction of bowing of its nearest string. If the top part of the bridge were to move approximately following round the curve of the bridge top, the input admittance would be the same for all strings. That will not be exactly true, of course, but still this measurement gives an approximation to the input admittance for all four strings.

For some of the earlier published measurements, it is not entirely clear what the direction of the applied force was, but in more recent years awareness has grown that this is an important issue if measurements made in different laboratories or workshops are to be compared. Some researchers now routinely make separate measurements with force applied parallel and perpendicular to the top plate, while others are careful to specify the bowing direction as described above. The issue has also been raised of the extent to which artificially applied force at the bridge produces the same result as excitation by the vibrating string [131]. For an instrument equipped with a bridge-force sensor, as discussed in section 2, it is possible to measure a bridge admittance using actual playing as the input signal. If a glissando covering at least an octave is played on the lowest string, some input is guaranteed at all frequencies: the Helmholtz sawtooth waveform is rich in harmonics, and during the glissando each harmonic covers a frequency range that overlaps with those of its neighbours. Systematic comparisons of different excitation methods can then be made, and these show that there are indeed small differences, but they suggest that the main source of deviation between different measurements on the same instrument comes from the question of forcing direction rather than from any fundamental difference between forcing by a bowed string or an impulse hammer [132].

Admittance is defined as the velocity response per unit applied force, so if an accelerometer is used for the measurement, the result is integrated in the computer. The admittance governs the energy flow into the body from the string, and also determines the strength of feedback from body motion to the string and so is the single most important body measurement when considering “playability” issues, as will be discussed in detail later. For some purposes it is useful to have a non-dimensionalised version of the admittance, obtained by dividing by the wave admittance of the string of interest: the result is then the admittance ratio of body to strings, or more familiarly the impedance ratio of string to body.

Examples of this impedance ratio are shown in Fig. 19, for five typical violins, and also for five typical classical and flamenco guitars: in both cases, the properties of the lowest string of the instrument are used for the normalising. To make the comparison more direct, the frequency scale in each case is logarithmic, starting from the lowest note of the instrument. Successive octaves of that lowest note are indicated on the axis. It is immediately striking that the violins are quite similar to each other, as are the guitars, but that the two families are very different from each other. So the similarity between violins is not something universal to any “wooden box with strings attached”: different design criteria have led makers of violins and guitars to adopt quite different solutions to the problem of making a “mechanical amplifier”. Understanding the mechanism and significance of some of the characteristic features of violin response will be the main goal of this section.

3.3.2 Statistical and hybrid theories of structural vibration

Before looking at details, it is necessary to introduce some background material on structural vibration analysis at high frequencies. For reasons explained earlier, once the modal overlap and statistical overlap factors cease to be small, theoretical modelling needs to adopt a methodology that recognises the futility of trying to predict every detail of response. The most well-known theoretical framework is called Statistical Energy Analysis (SEA), first developed in the 1960s in the context of such problems as noise and vibration prediction for space vehicles during launch. In classical SEA, the system under study is divided into coupled subsystems. For each subsystem, there is no attempt to analyse details of the spatial variation of vibration within the subsystem: the response is described by a single variable representing the total energy of that subsystem.

If the dissipation rate of energy in each subsystem is known, and if the energy flow across boundaries between subsystems can be modelled, then a simple energy balance calculation gives a way to predict the pattern of subsystem energies in response to known driving. The key result underlying SEA concerns subsystem coupling. Under certain conditions (see Lyon and DeJong [73] for details), it can be shown that the *mean energy per mode* plays a role analogous to temperature in a heat flow calculation: the rate of energy flow across a boundary is proportional to the difference of this quantity between the two subsystems concerned. The proportionality constant is known as the “coupling loss factor”. Coupling loss factors have been calculated for a wide range of different kinds of junction: point or line couplings between structures, structure/acoustic interfaces and so on. The

commonest approach is to calculate the reflection and transmission coefficients of waves incident on the junction, then perform a suitable average over angles of incidence. The use of the SEA “energy per mode” variable introduces another important parameter into any theory of this kind: the *modal density* (the average number of modes per unit frequency interval in a given subsystem, or equivalently the inverse of the average frequency spacing between modes). Again, modal densities have been calculated and tabulated for many kinds of component system.

In recent years, an important extension has been made to SEA that opens up a much wider range of potential applications. A feature of many complex structures is a range of intermediate frequencies where some parts of the structure need to be treated by a statistical method like SEA, while others retain fairly low modal and statistical overlap factors, so that deterministic methods are needed. A consistent hybrid theory has been developed to apply to such problems, and a number of example studies have shown that the method can be very effective: see for example Coton et al. [133]. It will be suggested in the next subsection that the violin exhibits features that are best understood in the context of a hybrid theory of this kind: features that allow the violin maker to exert deterministic control over certain aspects of the sound at high frequencies where the instrument as a whole has a high statistical overlap factor.

3.3.3 The “bridge hill” and other hybrid features of violin response

It is useful to look again at Fig. 19. The response pattern of the guitars shows large individual peaks and dips at low frequency, while at high frequency the average trend becomes approximately constant at a level well below the highest peaks. The violins show more complicated behaviour. At low frequency they show individual peaks corresponding to the signature modes discussed earlier. After that they show more structured behaviour than the guitars, with a cluster of modes forming a “hump” around 1 kHz, then another broader hump around 2–3 kHz. The peak levels in this second hump are comparable to the high peaks of B1- and B1+. These humps, with many individual peaks being somehow modulated to form a larger-scale feature, immediately look like typical “hybrid” effects. They are also reminiscent of the vocal-tract formants that are known to be so important in the perception of vowel sounds (see for example Moore [134]).

By far the most well-studied of these features is the broad hump around 2–3 kHz: see particularly Jansson and co-workers [130], [135], [136], [137], Beldie [138], Woodhouse [139]. The hump was originally called the “bridge hill” by Jansson, because its frequency is generally in the same region as the first in-plane bending vibration mode of a typical modern violin bridge, first explained by Reinicke and Cremer [140], [2] and illustrated in Fig. 20a. As will be explained, the bridge is indeed implicated in the formation of this feature, but the full explanation is somewhat complicated and nuanced.

The basic mechanism leading to a feature like the bridge hill in a driving-point response is not controversial. For any structure, the response to driving at a single point can be considered to have two components: a direct field and a reverberant field [141], [139], [75]. The direct field corresponds to the outgoing wave response that would be produced by

forcing an *infinitely extended* system: explicit visualisation of the direct field in a violin has been provided by the transient holographic studies of Molin et al. [98], [99]. The reverberant field corresponds to the combined effect of all reflections of the direct field from discontinuities such as joints or edges. Thus we can write

$$Y(\omega) = Y_{dir}(\omega) + Y_{rev}(\omega). \quad (5)$$

where Y_{dir} and Y_{rev} denote the direct and reverberant contributions to the bridge admittance Y . The phase of the reverberant response will vary in an irregular way with frequency, as the interference effects between different wave paths change, and it may therefore be reasonable to expect that Y_{rev} will average to zero over a frequency band of sufficient width so that

$$Y_{dir}(\omega) \approx \langle Y(\omega) \rangle_{\Delta} \quad (6)$$

where $\langle \dots \rangle_{\Delta}$ represents an average taken over a frequency band of width Δ , centred on ω . It can be expected that Δ will need to contain several modes of the system to average out the reverberant component of the response. In practice it is useful to compute this average using a Hanning window to minimise distracting artefacts as strong features enter or leave the averaging band.

For a simple system, $Y_{dir}(\omega)$ is rather featureless: in the extreme case of bending vibration of a flat plate, the corresponding infinitely-extended plate behaves like a mechanical resistance (or “dashpot”) [49] so the driving-point admittance is independent of frequency. However, if the same plate is driven through a substructure with a resonance, as sketched in Fig. 21, the response becomes more interesting. A simulated example is shown, in amplitude and phase, in Fig. 22a (for more detail, see Woodhouse [139]). Corresponding results for the bridge hill of a typical violin are shown in Fig. 22b. These plots show the full response with all the detailed resonances, and also, as dashed lines, the computed $Y_{dir}(\omega)$. The qualitative similarity is immediately striking, and leads us to look for something in the structure of the violin that might play the role of the simple mass-spring oscillator on the flat plate.

What is needed is a resonance local to the driving point. The bridge bending resonance sketched in Fig. 20a does indeed look like an obvious candidate, but measurements by Jansson and Niewczyk [136] showed clearly that such “bending at the waist” is not necessary: a solid plate bridge without the cutouts showed a similar bridge hill feature. But perhaps this is not really surprising: the top plate of a violin has other local features close to the bridge that can be expected to play a significant role in $Y_{dir}(\omega)$. There is the bass bar and soundpost, and, probably more significant, there is the effect of the nearby f-holes. These slot-like holes create an area of the top plate, called by Cremer the “island” [2], that is able to twist relatively freely in response to transverse forcing by the strings at the top of the bridge: we have already seen some consequences of such movement in the low-frequency modes of the violin body.

It appears that the local resonance responsible for the bridge hill is determined by the combined series stiffness of bridge bending and island local twisting (usually dominated by

the latter), and by the combined inertia of the same two motions (with the bridge probably the more significant contributor). Experiments with bridges of different mass and stiffness on the same violin show clear physical effects on the hill feature, and also show clear perceptual differences for players of the violin. This is no surprise, and it links with two familiar aspects of violin sound adjustment. First, all instrument makers are aware of the importance of bridge choice and adjustment in fine-tuning the sound of an instrument. Second, and more obvious, all violinists make regular use of a “mute” to modify the sound, at the behest of composers. A mute is simply an additional mass that is temporarily attached to the top of the bridge, and its main action is to shift the bridge hill downwards, and thus to reduce the amount of high frequency sound since above the hill the response falls rapidly.

The bridge hill is an important ingredient of violin sound even if no strong “hill” as such is visible in the response. Look again at the comparison of violins and guitars in Fig. 19. All the violins show higher levels of response than all the guitars in the “hill” frequency range, but when the violin responses are considered separately the “hill” is more obvious in some than others. Figure 23 shows plots of $Y_{dir}(\omega)$ for four violins, now including one with significantly different behaviour, and for four typical guitars. The contrast between the violins and guitars is very clear (noting the difference of vertical scale between the two sets of plots). The guitars show results rather similar to what would be expected for a simple flat plate: approximately constant level with a small magnitude. However, all the violins show much higher response, with one or more conspicuous peaks.

The explanation lies largely in the difference of bridge design in the two types of instrument: classical guitars have low, flat bridges while violins have tall bridges. Excitation of the soundboard by string motion in a guitar comes largely from the component of motion normal to the soundboard: a guitarist has control over the initial polarisation of string motion through the finger gesture, via playing techniques such as *apoyando* versus *tirando* playing, see for example Noad [142]. In the bowed instruments, as seen earlier, the main orientation of string motion is determined by the line of bowing and is always predominantly parallel to the top plate. The tall bridge is needed to allow such string motion to feed significant energy into body vibration, and it also leads to the possibility of a bridge hill.

This contrast between the guitar and violin is no mere accident, forced on instrument designers by ergonomic needs. In both cases the musical needs of the respective instruments and their players are met. Many musicians, other things being equal, would opt for a louder instrument if they had the choice. But a guitar maker has a problem with making an instrument louder. Once the choice of strings has been made, a given pluck gesture makes a fixed amount of energy available in the string vibration. This can be taken quickly from the string to the body, giving a loud sound but a fast decay, or it can be taken more slowly, giving a more sustained “singing” sound, but inevitably at the cost of being quieter. By contrast, a violinist feeds energy continuously into the string via the bow, so there is no conflict between sustained sound and loudness. So a violin can afford to have a closer impedance match between strings and body, and the bridge hill achieves that, even in cases where the hill is so broad that it is not immediately apparent in an admittance measurement. Interestingly, measurements on instruments of the viol family show behaviour intermediate between the violin and the guitar [75].

Although the bridge hill is the most-studied “hybrid” feature of the violin, it is almost certainly not the only one. One of the violins shown in Fig. 23, an experimental ultra-light instrument by American violin maker Joseph Curtin, shows a very clear double peak, suggesting the presence of a second similar feature. There is an intriguing hint in the detailed results of Bissinger (for example [106]) that in this frequency range the soundpost appears to show significant extensional deformation, so perhaps a soundpost resonance (modified by added inertia of the top and back plates) is producing a “soundpost hill”? In addition, several researchers such as Jansson and Curtin have recently been looking at the bridge admittance in the perpendicular direction and have commented on another “hill” feature seen in the 5-6 kHz range (an example is shown by Maestre et al. [143]). This “vertical hill” is almost certainly the symmetrical cousin of the regular bridge hill, which is based on antisymmetric motion of bridge and island. It would involve the second in-plane mode of the bridge, shown in Fig. 20b, together with local island deformation.

This area of violin acoustics is ripe for further research. It is surely no coincidence that the candidates discussed here, involving as they do details of bridge and soundpost, suggest that the very components most commonly associated with tonal adjustment might be intimately associated with “hills” having the character of formants: frequency bands with enhanced response much like those created by resonances of the human vocal tract, which are responsible for our ability to produce and discriminate different vowel sounds [134]. In the violin, the details of central arching, bass bar and f-holes will also influence these local resonances, and that also chimes with the general perception of the importance for “sound” of those features.

Before leaving the subject of high-frequency violin acoustics, it is worth noting an intriguing recent observation in the area of sound radiation. The general understanding of sound radiation by vibrating structures at higher frequencies has been dominated by the structure that lends itself most readily to analytical investigation: a flat plate embedded in an infinite rigid baffle. The key concept emerging from this flat plate problem is the *critical frequency*, the frequency at which bending waves in the plate have the same wavelength as sound waves in air. The dispersive nature of bending waves has the consequence that sound radiation is weak below the critical frequency, rising to peak in the vicinity of the critical frequency and then settling to a plateau of strong radiation above the critical frequency (see for example Fahy and Gardonio [144]).

The only other structure amenable to analytical calculation is the complete spherical shell, and when this was studied it was found that the idea of a critical frequency becomes more complicated [145]. Curvature of the shell stiffens the structure and changes the wave dispersion characteristics in such a way that a sphere can exhibit either two “critical frequencies”, or none. To progress further requires numerical investigations, and a recent study has looked at families of shells in the form of oblate spheroids and closed circular cylinders [146]. By keeping the material properties, total area and shell thickness all fixed, it is possible to make fair comparisons of total radiated sound power from the various structures in response to point driving at a “typical” position (see caption for details).

An example of the results is reproduced in Fig. 24. The flat-plate critical frequency is indicated by a vertical dashed line. The result for the baffled flat plate shows the behaviour

described earlier. The complete sphere shows, in this case, a strong peak close to the critical frequency. It has very weak sound radiation at lower frequencies, mainly because the shell has very few resonances: the fundamental frequency is indicated by the short vertical marker. The spheroidal shells (with different degrees of eccentricity) now show something quite surprising. Over a range of frequencies below the flat-plate critical frequency they show significantly stronger sound radiation than either the plate or the sphere, although above that frequency all the structures studied show rather similar behaviour. Perhaps the arching shape of a violin body, as well as affecting the structural vibration as already discussed, might have a direct effect on sound radiation efficiency?

There is one final high-frequency effect on sound radiation that should be mentioned. It has already been noted that all vibrating structures show directional patterns of sound radiation that become increasing complicated as frequency rises, once the Helmholtz number becomes large. More than that, the patterns change rapidly with frequency. When a violinist plays, especially if they use vibrato, the result will be a very complex time-varying pattern of sound radiation. A listener in a reverberant space such as a concert hall will be exposed to this complexity, receiving a rich, “scintillating” sound field. Weinreich has suggested [147], very plausibly, that this richness will contribute to the perception of “tone quality” of the violin: he calls the effect “directional tone colour”. It is one reason that it is very difficult to fool a listener who hears a recorded violin, played back through loudspeakers, into thinking that they hear a live instrument.

3.4. Acoustical measurement and violin making

In the last few decades there has been a significant shift in the pattern of research into violin acoustics: there are probably fewer professional scientists involved than there were, but the gap has been more than filled by a growth in activity by instrument makers. Technically-minded violin makers give papers at conferences, take part in lively internet discussion forums, write software for acoustical analysis, use CT scanners to give geometric and material information about old instruments, and produce web sites with a lot of scientific information — some examples have already been mentioned. However, these makers tend not to publish in traditional scientific journals, so in a review like this concentrating mainly on such journal publications the work of these techno-makers will inevitably be under-represented. This section will give a short review of scientific endeavour centred around the maker’s workshop, and the reader must excuse a certain paucity of citations. Many of the makers mentioned here and earlier have web sites that can provide additional detail: some of this material does not have the status of “accepted scientific fact”, but it is important in providing the inspiration for future research.

One idea that has been influential among makers for a long time is that there is useful information contained in the natural frequencies of the free top and back plates, before they are assembled into the complete box. With care, certain of these free-plate frequencies can be determined by ear, as “tap tones”. The name most strongly associated with deliberate manipulation of free-plate modes in an effort to control the quality of the complete violin is

that of the late American instrument maker Carleen Hutchins: in a string of publications and demonstrations spanning many years, she developed a system of free plate tuning that was influential among many makers (see for example Hutchins [148]).

The approach still has its adherents, but it has generally fallen out of favour since a study by German violin maker Martin Schleske in which experimental modal testing was done at many stages during the construction of a violin to chart the influence of each operation on both free plate frequencies and whole-body frequencies [149]. Schleske's conclusion was that the correlation between the two is not strong. While it is obviously true that the vibration behaviour of the components of a violin must somehow govern the behaviour of the whole, the change in boundary conditions when the box is assembled is so strong that it is hard to follow the details in a way that is useful in the workshop.

Subtle influences on free plate frequencies will not in general have consistent effects on whole-body modes, and detailed free-plate tuning probably only has a useful role in the context of quality control for a single maker, using consistent material, arching shape, outline and so on. A confirmatory line of evidence comes from a set of violins commissioned from maker David Rubio specifically for the purposes of scientific research [150]. These had free-plate tunings that varied over the widest range that is compatible with normal violin-making practice, but other details were very similar across the whole set. The reaction of players was generally that while the instruments are different from each other, they have a strong family resemblance: they all "sound like Rubios".

One area where free-plate frequencies have a continuing interest for makers is as a way to give a simple estimate of wood properties: approximate formulae have been proposed by which long-grain and cross-grain stiffnesses of wood can be quantified using certain free-plate frequencies (see for example Davis [151]). Wood, like any natural material, exhibits considerable variability of properties, and makers use a number of ways to estimate the density and stiffnesses for the purposes of selection and control.

Some authors have developed the idea of characterising stiffness further by proposing models for whole-body behaviour that take free-plate data as input [126], [151]. There have also been correlation studies, in which a variety of data was gathered and the correlation matrix computed. An early example was the study of wood properties by Dettloff [152], and in recent times the Norwegian maker and acoustician Anders Buen has been very active in correlation studies of measured structural and acoustical parameters of violins. Such studies can lead to some suggestive links, but as in many other areas of science one has to beware of confusing correlation with causality.

Violin makers have long been interested in details of the geometrical configuration of instruments, such as outline shape, thickness distribution and, probably most important for acoustical behaviour, arching shape. A number of schemes have been published for generating shapes by geometrical constructions (for example Playfair [153]), which may have historical and practical interest but which do not have any obvious acoustical significance. More interesting for the present purpose, British violin maker Nigel Harris has reported an intriguing experiment in which rather subtle variations in arching shape were tested by players, leading to a proposal by Harris that a parameter which he calls "end arch ratio" or EAR is a critical quantity for makers to control [46].

But the vast majority of involvement of instrument makers with “science” has come through measurement rather than theory. One application of science to violin making combines the measurement of material and geometrical information. In a pioneering study, Sirr and Waddle [154] showed that a wealth of information can be gained, with no risk of damage to the instrument, by putting a violin through a medical CT scanner. This idea has since been applied in a large number of studies relating to the violin and other musical instruments. For example, it is now possible to purchase accurate replicas of plates of famous Cremonese instruments made by combining CT-scan data with 3D printing technology.

With the ubiquity of the personal computer has come the possibility for makers to record their own data in the workshop, for example from tap tests on instruments, and perform FFT analysis. A growing number of makers, including some high-profile ones like Curtin and Schleske, make use of such testing on a regular basis: the PC is becoming another workshop tool, alongside the knife and the thickness calliper. Some use it as a more reliable way to find tap tones, but the language of modal analysis is spreading through the world of violin makers, and some surprisingly sophisticated studies have been carried out, especially using the software developed by Stoppani [155]. Over-arching all these details is a gradual change in attitudes to “science”. Thirty years ago, a common reaction of established figures in the violin world was that the only makers who dabbled with science were amateurs trying to short-cut the proper training in the craft, but this is no longer a position that could reasonably be defended.

3.5. Material choices

One topic close to the hearts of instrument makers has generated its own literature: questions of material choice, possible alternatives to traditional timbers, and the effects on the properties of wood of various physical and chemical treatments and of the varnishing process. A standard analysis sheds light on the question of material choice. If a violin-shaped instrument were to be invented today, would wood be the obvious choice of material, given the huge range of artificial materials now available? A very simple criterion can be used to derive a crude index of merit for the top plate of a violin: seek the material that allows the loudest sound to be made from an instrument of more-or-less conventional design.

The major purpose of the soundboard of any stringed instrument is to take a proportion of the energy from the vibrating string and convert it into radiated sound. The radiated sound pressure will be governed by the amplitude of vibration of the plate, for a given frequency and mode shape. A string of given tension, vibrating at given amplitude and passing over a bridge of given geometry will exert certain forces on the top plate (at the bridge feet). So the criterion amounts to maximising the vibrational response of the plate to a given applied force. We can suppose that the length and width of the instrument body are fixed (being governed by the ergonomics of playing), but that the plate thickness might need to be varied depending on the material. This thickness will be governed by a requirement that the vibration resonances occur at roughly the usual frequencies — any big deviation from the norm in this respect is likely to produce an instrument that doesn’t “sound like a violin”.

Taking the simplest possible model of the soundboard, as a flat plate vibrating in bending, this argument leads to the requirement to maximise the quantity, sometimes called the “radiation ratio”,

$$M = \frac{(E_1 E_2)^{1/4}}{\rho^{3/2}} \quad (7)$$

where E_1 and E_2 are the Young’s moduli along and across the grain, and ρ is the density (see for example, Schelleng [35], Barlow [156]). The relative ranking of materials in terms of this merit index can be visualised using a design chart of a kind pioneered by Ashby [157]. The upper plot of Fig. 25 summarises data for Young’s modulus and density for “all” materials. Broad classes of materials, such as metals or ceramics, are grouped in “islands”. Both axes use logarithmic scales, both because the range of values is very large and also to facilitate the visualisation of a power-law relation like eq. (7).

Wood appears in Fig. 25 as two separate islands, showing results based on E_1 and E_2 separately. The lower plot isolates this wood data, and shows an intermediate island based on the geometric mean $E_{mean} = \sqrt{E_1 E_2}$, in terms of which eq. (7) becomes

$$M = \frac{E_{mean}^{1/2}}{\rho^{3/2}} \quad (8)$$

Any two materials lying along a straight line with slope 3 in Fig. 25 will have equal values of M , and to maximise this quantity we need to push a line of that slope as far to the top left as possible. Bearing in mind that the relevant view of the wood data is the intermediate island shown in the lower plot, the very best material based on this criterion is the leftmost of the woods: balsa wood, with the traditional softwoods like spruce not very far behind. The only other materials that appear to perform as well lie in the “foams” island: but these have very low density, and are impractical for other reasons as a material to construct violin bodies. Otherwise, the next best material is found at the extreme of carbon-fibre reinforced composites, which indeed are the only man-made materials sometimes used in high-class musical instruments: see for example Besnainou [158].

The case of balsa is interesting. Musical instruments are not usually made of lightweight balsa, presumably because it is so fragile. However, there have been some recent experiments with balsa violins (see for example Martin [159], Curtin [160], Waltham [161]); not aiming at the professional musician but perhaps at students. Informal feedback is in line with the prediction of this analysis: players report that the experimental instruments are loud, and satisfying to play in at least some respects. In a similar spirit of pushing the envelope of instrument design, some instrument makers have experimented with other ways to achieve ultra-lightweight construction: one example, by Joseph Curtin, gave the extreme response in Fig. 23. The guitar makers probably lead the way here, with such innovations as sandwich construction top plates with honeycomb cores, sometimes called “double tops”, but the violin makers are not far behind, and further developments in this kind of “extreme construction” can be expected.

There have also been experiments with treating wood to improve its properties, including reducing the density without compromising stiffness too much. Methods have been described involving treatment with chemicals, heat, humidity cycling, bacteria and fungi: for

some examples, see [162], [163], [164], [165], [166]. In many cases the details are somewhat mysterious, since the processes are treated as trade secrets by particular makers or wood suppliers. There is nothing fundamentally new about such ideas: for example “ponding” of softwood to allow bacterial attack of selected portions of the cell structure, and thus increase the porosity of the wood to preservative treatments, goes back many centuries. A useful review is given by Rossell et al. [167].

Finally, some mention must be made of varnish. There is persistent folklore, in the genre of “secrets of Stradivari”, that there is something acoustically magical about the varnish used on classical Italian violins. “Varnish” here is taken to include all components of the finishing system applied to the bare wood to produce the final instrument. It is hard to know where the rumour originated: one candidate is the Hill book on the life of Stradivari [168], where they certainly assert this conjecture but without offering any supporting evidence. There is no doubt that the visual appearance of the varnish is very important to instrument makers and owners, but from the perspective of a scientist there is no compelling evidence for any beneficial effects of a physical nature.

Any influence of varnish on the vibration and sound of a violin can only come from modifying the effective material properties: mass, stiffness and damping. We have already seen that the wood traditionally used for violin soundboards is a very extreme material. This is because of its very efficient cellular structure consisting mainly of aligned thin-walled cylindrical cells called *tracheids* (see for example Bodig and Jayne [169]). Micromechanical models have been used to explain in some detail how the macroscopic properties of wood derive from this microstructure (for example Kahle and Woodhouse [170]). Any layer of solid material applied to the surface of the wood as varnish will inevitably tend to reduce this extreme performance. Furthermore, varnish may add additional damping, and this may be detrimental: many makers choose wood with a “good ring”, presumably aiming to minimise damping. This all suggests that a varnish system should achieve its visual effect with minimal mechanical consequences: this is consistent with the traditional advice offered to violin makers: “not too hard, not too soft, not too thick” [171]. Some kind of initial barrier layer to prevent varnish material penetrating too deeply into the wood may be desirable, since it is the empty space in the wood structure that gives it the extreme properties.

4. Perceptual studies of the violin

Ultimately, the quality of a musical instrument is never determined by measurements alone: judgements by people are necessary. This statement is not unique to musical acoustics, of course, but the challenge of making such subjective judgements reliably quantitative is particularly severe for musical questions. Experimental psychology, and psychoacoustics in particular, has an established body of procedures for testing and analysis. In virtually all cases these rely on carrying out a sufficient number of tests, so that the results become statistically significant. However, a judgement of musical nuance, of the kind that musicians make all the time when deciding on details of performance, does not lend itself to repeating several hundreds of times: all vestiges of musicality tend to be lost. A consequence is that

one might expect subjects in a scientific test to discriminate less acutely than they would in a real musical setting. This suggests that the detailed design of tests should emphasise the very best performances, provided they are convincingly and repeatably demonstrated, since they are likely to relate most closely to the musical world.

With all this in mind, it is no surprise that the subject of violin perception and psychoacoustics is still in its infancy. There is a long history of informal testing, since instrument makers have always sought feedback from players. There is also a long history of public “tests” in which a Stradivari and something else are played behind a curtain, and the audience asked to vote on which is better. Virtually none of this would pass the tests of good experiment design: double-blind testing, sufficient test subjects and repeat tests, results verified by independent researchers. Only in recent years have reliable results begun to be published. This is not to say that less formal tests are without value: but the results can only be treated as anecdotal pointers, not as established scientific fact. The claims by Hutchins about the supposed importance of the frequency of the mode A1 in relation to the B1 modes [123], the work by Dünnwald associating verbal descriptions with particular frequency bands of a violin’s response [172], the quality-rating process used by Bissinger [173] and the EAR tests by Harris all fall into this category of “informal” tests.

There are several types of perceptual question that can be posed, and some are much easier than others to test. The simplest type of question is to vary a single parameter influencing a sound, and determine the threshold of perception for changing that parameter, often called the just-noticeable difference (JND). Standard audiology tests for the assessment of hearing loss are of this kind. The methodology is well established, and there are many published results relating to JNDs for pitch perception, loudness perception, masking and so on (see for example Moore [134]). By exploring JNDs for many different parameters relating to violin construction, one might hope to map out the “sensitivity landscape” for an instrument maker: which aspects of body adjustment give the strongest perceptual effects?

A more challenging type of perceptual question is to associate physical changes with verbal descriptions: what exactly is meant by a sound that is “bright”, or “nasal”? Do different people use these words in the same way? Then come questions of preference: can one meaningfully ask “which of these two violins is better?”, or is it necessary to break the question down into sub-categories, of being “better” in different ways? In this category comes the most famous of all violin-related questions: are certain old Italian violins really better than modern ones? Can listeners reliably tell? Can players reliably tell? The first scientifically-reputable studies of these questions have recently been published. On the general question of whether players are reliable at making comparative judgements, Saitis et al. [174] show that violinists show a good degree of self-consistency, but that there is very little consistency between players when it comes to ranking a given set of instruments, either on overall preference or according to more specific criteria such as “richness” or “dynamic range”.

There is a related field of investigation, which has also led to recent publications. This involves monitoring players as they perform, using various sensors and/or motion-capture systems, and finding what real people actually do, as opposed to what the playing manuals say they are supposed to do [175], [176], [177], [178]. This work is partly driven by

pedagogical needs, to help string teachers direct pupils into good habits. However, it also provides information that links to acoustics: for example it is possible to use the information from measured bowing gestures to drive simulations in a more realistic way [179].

Returning to psychoacoustics, to carry out a JND study it is necessary to have tight control over the parameter to be varied and to have confidence that nothing else is also being varied. This more or less rules out the possibility of doing tests of this kind using physical changes to a violin body. Only in very unusual circumstances is it possible to make such a controlled and limited change. One example might be to find the weight of the lightest mute that has a perceptible effect; but most questions of interest to violin makers are too difficult to approach in this way. The opposite extreme would be to dispense with physical instruments entirely, and conduct tests entirely using computer-synthesised sounds. This method has been applied with success to investigations of guitar acoustics [180], but for the violin no-one has yet produced a synthesised sound that is sufficiently realistic for the purpose. Test subjects tend to find the shortcomings of the synthetic “performance” more obtrusive than variations in the particular parameter under investigation, seriously undermining the “ecological validity” of such tests. This is one reason that it may prove helpful in the future to integrate measured bowing gestures into simulations, to improve realism [179].

The most successful JND tests have used a hybrid methodology based on “virtual violins”, first pioneered in analogue form by Mathews and Kohut [181] and Gorrill [182], then in digital form by Farina et al. [183]. A player performs on a violin fitted with force-measuring sensors at the bridge, so that the input signal to the violin body is measured. That signal is then fed through an electronic realisation of the relevant frequency response function, and the resulting sound is used as the raw material for listening tests. This way, real performance is used but the identical input signal can be used for every test sound. In its modern form, a digital filter realisation of the violin frequency response makes it easy to make controlled changes, for example shifting one or more body resonance frequencies, or changing their amplitudes or their damping factors. If a real-time digital filter system is used (e.g. [184]), this kind of test can be carried out with the players themselves as test subjects: they play a mute electric violin and hear the filtered sound, and the experimenter then makes changes in the filter behaviour to fit the test protocol.

Some initial experiments of this kind have been reported by Fritz et al. [185]. The full picture revealed is quite complicated, but as a broad summary listeners are more acute to changes in modal frequency than in amplitude or damping, and musically-trained listeners typically need the frequencies of the individual low body modes, as discussed in section 3.2, to be shifted by about a semitone (6%) in order to be perceptible. JNDs were lowest for test stimuli consisting of single played notes: using a short fragment of music gave slightly higher JNDs, probably because of “informational masking” [186], [187]. The authors reported reasonable agreement of the measured JNDs with the predictions obtained by mapping the output sound spectra into an excitation pattern on the ear’s basilar membrane [188], and then applying results of earlier (non-musical) psychoacoustic studies of perceptual thresholds [189].

Curiously, a parallel study on guitar sounds gave a somewhat different result [180]. When all the body resonances were moved simultaneously, the most acute test subjects could

perceive a 1% shift, a much lower value than was found in any of the violin tests. The best subject of all could reliably detect a shift of 0.3%. Furthermore, these same acute listeners did best with relatively rich input stimuli, rather than with single notes: apparently they were not fooled by informational masking in the same way as seemed to happen in the violin tests. These results are very promising, but it seems clear that these initial investigations have only scratched the surface of a complicated problem.

That conclusion is even more true of work relating to verbal descriptions. Studies have been published on timbre descriptors used by violinists [190], and of whether there is a quantitative link between sensitivity to vibrato and the sense of “liveliness” in violin sound [191]. The rationale of this second study is that the frequency response of any violin always features strong peaks and dips associated with the body resonances (recall Figs. 1 and 19). When a note is played with vibrato, each harmonic of the sound will encounter a different region of the frequency response. The resulting sound will be very complex, involving modulation of amplitudes with different magnitudes and phases for the different harmonics. There is no doubt that variations in such modulation have audible consequences, and several authors have thought it was likely to contribute to the desirable tone quality of violin vibrato notes [192], [193], [194].

However, attempts to demonstrate this phenomenon conclusively and explore it quantitatively were bedevilled by the general issues raised earlier: it is hard to design a test that is simultaneously statistically reputable and musically valid, and any experiment involving synthesised violin-like sounds runs into the problem that listeners find the results mechanical and unnatural, and this often overwhelms the effects of the variable supposedly being studied. We will return to this question in the next section, when transients and playability will be discussed and the importance will be reinforced of rather subtle physical effects.

Before that, the interesting results of the “new versus old” experiments should be reported. The popular perception of a “secret of Stradivari” is very widespread, and the pattern of market values of violins supports the idea that there is something special about certain old violins, mainly Italian ones. Only very recently have first efforts been made to conduct serious scientific tests to probe this idea [195], [196]. The authors took the very reasonable view that the most acute discrimination between instruments is likely to come from players, rather than from external listeners, however expert. As mentioned earlier, there is a simple reason for this: the player is inside a feedback loop, able to adjust details of bowing to try to create the sound they want, but the listener only hears the end result. It may be that a skilled player can coax a good sound, at least on certain notes, from more or less any violin, but the player will still be well aware that they have to work a lot harder on some violins than others to get this effect. There is another hazard to be considered: it seems likely that a player, if they know they are holding a million-dollar instrument, will go the extra mile and manage to find something good to say about it. If their initial reaction is negative they are more likely to blame themselves, whereas with a lower-value instrument they may blame the violin.

The experiment needed to allow players to handle the different instruments under test in a reasonably natural way, but without being able to see which was which and thus bring in

additional information and bias. This was achieved by making the players work in dim lighting, wearing welding goggles: enough vision to handle valuable instruments safely, but no useful visual cues. Two versions of the experiment have been conducted: the first experiment involved 21 players in a dry acoustic (a hotel room) [195], while the second version involved 10 first-rate soloists in a rehearsal room and then in a concert hall with an option on piano accompaniment [196]. The players were given several different tasks, to choose their favourite and to rate the instruments against one another based on various different criteria.

For both experiments a group of Stradivari and Guarneri violins was pitted against an equal number of modern instruments (presumably very carefully selected, but the authors have kept the details of makers secret). The cautious conclusion of the authors after the first experiment was that no statistically significant difference between the two groups was found in terms of preference, but the message of the raw data is that certain of the modern instruments were if anything slightly preferred. This experiment raised a lot of controversy in some quarters of the violin world, but the authors had good reasons for designing the tests as they did, and they have tried to respond to the criticisms in the second experiment. The results of this second experiment were more clear. When asked to choose a violin that might plausibly replace their own violin for an upcoming tour, six soloists chose new violins and four chose Stradivaris. A single new violin was easily the most-preferred of the 12. On average, soloists rated their favorite new violins more highly than their favorite old for playability, articulation, and projection, and at least equal to old in terms of timbre. Finally, the 10 soloists failed to distinguish new from old at better than chance levels. So, provisionally, there seems to be no secret of Stradivari. The best of the classic Italian instruments are still very good, of course, but the message is that the best of contemporary instruments can hold their own when given a level playing field on which to compete.

5. Playability

5.1. *Playability and minimum bow force*

The choice by Fritz et al. to rely mainly on judgements by players in their new-versus-old trials is an example of a trend in violin research in recent years, to focus attention on “playability”. This word is not easy to define tightly, but it encompasses all aspects of violin quality assessment that can only be made by the player, not by an independent listener. When a player says that one instrument is “easier to play” than another, they presumably mean “easier to achieve the particular musical effect I want”. This suggests an interplay of the response of the string to the bow, the acoustical behaviour of the particular violin body, and the perception of the resulting sound: it combines all the threads of this article.

Players and instrument makers use a variety of terms when talking about playability issues. Some seem to be quite general, others refer to specific bowings. Some seem to refer mainly to quality of sound: terms like “good ring”, “projection” or “core”. Others seem to involve, at least in part, the response to bowing: “support”, “playing through/running out”,

“range of tone”, “resistance”, “cushion”. To engage players and makers in useful dialogue, it is essential to make the attempt to understand what quantifiable meaning, if any, can be attributed to terms like these.

But these are difficult questions to start from. It is useful to look first at the science that is already understood, in search of aspects of behaviour that might make good candidates for being described in playability terms. In particular, it is useful ask which aspects of bowed-string behaviour are likely to be influenced by the vibration response of the particular violin body. The first such candidate is Schelleng’s diagram, shown in Fig. 3. The analysis by Raman and Schelleng suggests that the maximum bow force to sustain Helmholtz motion should not be influenced by body behaviour in any obvious way, but that the minimum bow force is directly determined by body response (and other sources of energy loss).

The original formula for the minimum bow force is couched in terms of representing the body by a simple mechanical resistance. This is not a silly approximation, bearing in mind the result from section 3.3 that this is the correct result for an infinite plate, and so represents an average response of any plate structure. However, it is not obvious what quantitative value should be applied for a given instrument, and in any case a fixed value fails to capture the note-by-note variation. Fortunately, there is a straightforward way to extend Schelleng’s analysis and incorporate a measured bridge admittance into the calculation of the minimum bow force, leading to a quantitative prediction for each played note on a given instrument [197].

An example is shown in Fig. 26. The frequency scale indicates the fundamental frequency of the played note, starting from G3 (196 Hz), the lowest note of the violin. Vertical lines show semitones, and coloured lines denote octaves. There are four curves, one for each string of the instrument. They all have the same shape, but the wave impedance of the string appears as a factor in the formula so the absolute value of the minimum bow force is larger for the lower strings with higher impedance. Plots like this should indicate “wolfiness propensity” from note to note and string to string on a particular instrument: high peaks indicate notes likely to be wolfy. The measurement and necessary calculation to give such a plot is quite simple, so it is possible that such plots will give makers a useful tool for the rapid identification of problem notes, and assessment of the effect of any countermeasure they may use to reduce the effect of the wolf.

Whether the same curve captures other aspects of playability problems is as yet an open question, but there are grounds for optimism. One aspect of playability that is often commented on is “range of tone”. As already seen in section 2.1, if a steady Helmholtz motion is produced by the player the most obvious way they can influence the tone quality is by changing the bow force, to make the Helmholtz corner more or less sharp and hence to vary the high-frequency content in the sound: this has been made explicit in measurements by Schoonderwaldt et al. [198], [199]. Schelleng’s diagram sets the limit on this process. At least within this simple view of “tone quality”, an instrument that has a large range of tone must be one that allows the player to press hardest, by moving the bow close to the bridge and working at the apex of the Schelleng triangle. Since the maximum bow force line is insensitive to the body behaviour, the apex position is governed by the minimum bow force. Slightly paradoxically, reducing the minimum bow force pushes the apex upwards and to the

left, and so it results in an *increase* in the maximum possible bow force. So the variation revealed in a plot like Fig. 26 may also say something about tonal range available to the player.

There are many other possible aspects of perceived differences of “range of tone”. Most of them concern transients, discussed in the next subsection, but there is one that should be mentioned first. More than one technically-minded violin maker has suggested that violin body vibration can exhibit nonlinear behaviour of some kind. Were that to be the case, one would expect amplitude-dependent response and sound. Such dependence could well lead to a perception of tonal variation, and if instruments differ in the strength or details of this nonlinear response then it would influence “range of tone”. At present there is no compelling direct evidence for such nonlinear response, although suggestive hints have been shown by Martin Schleske and Ted White, among others. This could be a worthwhile topic for future investigation.

5.2. *Playability and transients*

Violin sound is famously flexible and versatile: it is often said that of all instruments the violin comes closest to the flexibility of the human voice. But we have seen that the basic Helmholtz motion can only be altered in a rather subtle way, by varying the bow force to change the corner sharpness, or by moving the bowing point to vary the pattern of Schelleng ripples. It is time to stop pretending that violinists mainly produce steady tones: nothing could be further from the truth. Players are constantly “shaping” each note as they play it: some examples will be shown shortly. Most tonal and playability issues probably concern transients of one kind or another, or other departures from periodicity such as irregular differential slips as discussed in section 2.2.3 (see for example Schumacher [200] for explicit analysis of non-periodicity in musical sounds). There is persuasive evidence, albeit somewhat anecdotal, from the worlds of sound engineering and musical synthesis that such effects are often described by listeners using the language of “tone quality”. It would be a mistake to assume that all aspects of tone quality are well captured by frequency-domain analysis such as sonograms. Details of how the human auditory system processes sounds are still very much a matter of active research, and it is very likely that features extracted by direct temporal processing also play an important part.

As soon as the growth in computer power became equal to the task, the early bowed-string simulation models were harnessed to explore transient effects systematically. Relatively clear-cut questions were chosen for these early studies: how quickly, if at all, is the Helmholtz motion established after a given bow gesture? What does the terrain of transient length look like in parameter spaces relevant to a player? For the purposes of graphical presentation, it made sense to choose two-dimensional parameter subspaces to scan using multiple simulations: this work was being done during the heyday of popularity of nonlinear dynamical systems, and the analogy with the Mandelbrot set and its relatives is clear.

This early work established some useful methodology, but the detailed results are not worth discussing here because the studies suffered from two major flaws. The first has

already been discussed in section 2.4: they were based on the friction-curve model, and later studies have revealed serious shortcomings with this friction model, as will be illustrated shortly. The second problem relates to the particular choices of parameter subspaces of transient bowing gestures. The early work (e.g. [201]) considered transients which are perfectly possible in the computer, but which cannot be executed in reality, as was pointed out by Guettler [202]. Any physical transient must start with either the normal force or the speed (or both) equal to zero. If the bow is already in contact with the string with non-zero normal force, the speed must start from zero. On the other hand, if the bow is already moving when the bow makes contact with the string, as in a string-crossing gesture, then the normal force must build up from zero.

This realisation led Guettler to study a particular two-dimensional family of transient gestures, leading to what has become known as a Guettler diagram. The bow force is held constant throughout the gesture, its value being one of the two parameters. The second parameter is the acceleration with which the bow is accelerated from rest. Based on analysis of transients of this kind in a simplified model of the bowed string, Guettler produced a prediction that “perfect transients”, in which Helmholtz-like motion is established from the very first slip of the string over the bow, can only occur in a wedge-shaped region in the force-acceleration plane [202], the wedge being larger when bowing far from the bridge and narrower closer to the bridge.

This prediction has formed a useful target for simulation studies [203], and also for experimental measurements using a mechanical bowing machine [204]. It is convenient to start with measurements: Fig. 27 shows an example, measured on the open D3 string of a cello (147 Hz). Each pixel corresponds to a single constant-acceleration bow gesture. Each bridge force waveform has been captured and automatically processed to give the length of transient before Helmholtz motion was established, indicated by the gray scale: white for perfect transients, through to black for cases that still had not produced Helmholtz motion after 20 nominal period lengths.

To illustrate the kind of transients being discussed, Fig. 28 shows the block of four outlined by a square in Fig. 27. The time range of each plot starts just before the first slip event. Figure 28a shows obviously irregular motion throughout the time frame plotted, and clearly deserves its black pixel in Fig. 27. Figure 28b, by contrast, shows a perfect start. Figure 28d shows a few period-lengths of slightly irregular behaviour before Helmholtz motion is established, much as one would guess from the grey-scale shading of the corresponding pixel, but Fig. 28c is rather different. There is a single marked “glitch” after about 7 period-lengths, determining the nominal transient length, but apart from this the transient looks very close to a perfect start. One would guess that, although this transient is almost as long as Fig. 28d as judged by the automated analysis method used to generate Fig. 27, it probably sounds very similar to the perfect start of the first case.

Figure 27 shows that all occurrences of Helmholtz motion within the allowed time frame fall in a wedge-shaped region, as predicted by Guettler. However, the wedge does not contain smoothly-varying shades of gray, it is conspicuously speckly. Furthermore, when the data was re-measured, the details of the speckles move around unpredictably, although always conforming to the underlying wedge shape. This is familiar behaviour from nonlinear

systems of many kinds: the transient details are sufficiently sensitive to small details of initial conditions and small variations in the bow gesture that precise repeatability is not seen. It should be emphasised that the computer-controlled bowing machine used in these tests has a specification that exceeds the capabilities of a human player [204].

Figure 27 makes a good target for comparisons with the predictions of simulation models. Parameter values can be matched to the cello string used in the measurements, leaving the friction model as the main source of uncertainty (see [203] for details). If the friction-curve model is used, based on measured steady-sliding behaviour of rosin as plotted in Fig. 6, results are obtained as shown in Fig. 29a. If instead a simple thermal-driven friction model is used (as introduced in section 2.4.2), calibrated against the same steady-sliding friction data, the result is as shown in Fig. 29b. It is immediately clear that neither prediction matches the measurements very accurately, but that the thermal model comes a lot closer than the friction-curve model. Figure 29a shows sloping lines only vaguely reminiscent of the Guettler wedge, in the wrong part of the diagram and with far fewer successful gestures leading to Helmholtz motion: a cellist would not like “friction-curve rosin” on their bow, one would guess, because it would make the instrument far harder to play. The thermal model shows a wedge in roughly the right place, and with a speckly terrain quite reminiscent of the measured results, bearing in mind that individual speckles should not be trusted because they are not repeatable. However, it does not appear sufficiently speckly in comparison to the measured results: this particular example of a thermally-driven model seems to be a bit too benign and smooth in its response.

In order for simulations like this to be a useful guide to explore playability issues, the agreement with experiment needs to be convincing. It is crucial to have a model that reproduces transient details reliably. This evidence, together with other similar comparisons, suggests that the friction-curve model is inadequate, and that the thermal model is a step in the right direction. However, more work is needed in this area: certain details of simulated waveforms are qualitatively wrong when compared with measurements, and in the presence of a nonlinear system showing sensitive dependence it is impossible to guess how significant such deviations may turn out to be.

To give a glimpse of the magnitude of the problem of making sufficiently reliable simulations, it is useful to end with some examples of actual musical performance. Figure 30 shows a few seconds of music, played by violinist Keir GoGwilt on the G string of a violin and recorded using a bridge-force sensor. A sound file of this extract is included in the Supplementary Material. Immediately from this plot it can be seen that the string motion is never steady: the envelope of the motion is constantly modulating. Four particular note transitions are highlighted in the plot, and shown in more detail in Fig. 31. Case (a) shows a transition between two notes without a reversal of bow direction (as can be seen from the slope of the sawtooth ramps). But the player has not just put a finger down on the string to produce a “seamless” transition: he has slowed the bow down to produce the falling amplitude before the transition, and has allowed a few period-lengths of differential slipping (see section 2.2.3). The combined effect of these two things produces a subtle articulation of the transition.

Case (b) shows that these features were no accident: this violinist is perfectly capable of playing clean transitions. A bow change is seen here, with the bow slowing down, stopping and holding the string in a sticking state for a few period-lengths, and then starting again in the opposite direction with a perfect transient, immediately into Helmholtz motion. Case (c) shows a similar bow change, but this time the new note has been started in a slightly different place in the Guettler diagram, and there are a few period-lengths of “scratchy” transient before the Helmholtz motion is established. Finally, case (d) shows the opposite kind of note start, in which there is double slipping for a while before Helmholtz motion is established. Cases (c) and (d) illustrate a contrast explored experimentally by Askenfelt and Guettler to establish the limits on acceptable starting transients for violin playing.

A different view of this same musical extract is given by Fig. 32, where the first half of the passage is shown as a time-frequency sonogram: the horizontal axis shows frequency and the vertical axis shows time, running upwards in the plot. The harmonics of each note show as a set of roughly vertical lines. Reading upwards from the bottom, the first note shows a frequency slide, progressively more obvious in the higher harmonics. The slide ends on a higher note, which is faded out, to be followed by a fresh transient on the same pitch. This next note, extending over the range 2.4–4 s in the plot, shows modulated vibrato. It also shows, especially in its earlier part, harmonics reaching up to roughly double the frequency of the previous notes: presumably, the player has pressed harder and sharpened the Helmholtz corner. The remainder of the plot shows four short notes and ends on a longer one. The frequency content is being varied, and the pitch is continually being modulated in various subtle ways. The final note shows fairly steady vibrato from the very start, in contrast to the earlier long note.

In just a few seconds of music, the violinist has made use of most of the aspects of bowed-string motion discussed in section 2. Nothing is ever steady. Different note transitions and initial transients are used, while bow speed, force and position are being modulated to vary the waveform details. Meanwhile the player’s left hand is modulating the pitch in various subtle ways. The player will not be consciously aware of all these details of the underlying physics, but he *will* be aware of the audible consequences and may spend a long time practicing details of the bowing and phrasing to get this passage to sound right. If he is then asked to play the passage on two different violins, and to comment on whether one is “easier to play” than the other, which of these details will he be most aware of? There are no easy answers to that question. The challenge to the scientist, to try to understand enough about this kind of complex interaction between physics and perception to be able to make useful predictions and to give advice to instrument makers, is formidable. It becomes less surprising, having seen this example, that listening tests for the perceptual effects of vibrato based on synthesised notes ran into difficulties of sounding “unnatural” and “mechanical” [191].

6. Concluding remarks

This article has surveyed various aspects of the physics of the violin and of violin playing. It is a quintessentially cross-disciplinary subject. This survey has involved scientific topics

ranging from linear and nonlinear mechanics, tribology and materials science, through to experimental psychology and psychoacoustics. The subject also involves interaction with makers and players of instruments, and raises the rather different problems associated with making quantitative the kind of “expert know-how” that such people have.

Violin makers can, with some justification, still ask “what has science ever done for us?” The sceptics among them see very little of use, and they continue to make and adjust instruments based on traditional methods and training. However, a growing number of scientifically-minded makers are finding benefits from understanding underlying phenomena, and from the use of measurement methods of a variety of types. Some of these positive benefits are clear-cut. For example, simple mechanical and acoustical test methods can give a way of making consistency and quality assurance checks when choosing wood to buy, or to use for a particular instrument. Furthermore, many musical instruments traditionally use timbers and other raw materials that are becoming hard to obtain for various reasons, including export restrictions arising from CITES. How should one set about looking systematically for replacement materials with equivalent or even superior properties? The discussion around Fig. 25 gives an illustration of an approach to that question: see for example [35], [205], [206]. Other benefits to makers from engaging with science are more vague and general: it provides new tools, and exactly what use can be made of those is still being actively explored.

Equally, there can be benefits to players and teachers from understanding the underlying science of what they are trying to do. Schelleng’s diagram and Guettler’s diagram, for example, can have direct pedagogical applications: Guettler was a player and teacher, and much of his bowed-string research was motivated by trying to make his teaching more precise and focussed. Similarly, the ability to visualise the detailed results of bowing a string, as in Figs. 30–32, could provide rapid feedback for training purposes, as is done in other areas such as teaching the deaf to speak naturally, or in a range of sports training.

For the scientist, the subject is inexhaustibly fascinating. Because virtuoso musical performance is, by definition, at the outer limits of human ability, it ought to provide a route for investigating those outer limits of perceptual, learning and motor skills. Even within the tighter confines of physical understanding of how the violin works, unsolved problems have been encountered in nonlinear dynamics, constitutive mechanics of rosin, hybrid deterministic/statistical understanding of body vibration and sound radiation, and many other areas. Some useful progress has been made with all this, but it is in the nature of the subject that each answer leads to ten more questions so there is absolutely no sense of “approaching closure” in the subject.

Acknowledgements

The author expresses gratitude to Keir GoGwilt for the musical performance analysed in Figs. 30–32, to George Stoppani, Colin Gough, Bernard Richardson, Malcolm Mackley, Simon Butler, Michael Ashby, David Cebon, Hugh Shercliff, Chris Lynch, Bob Schumacher, Paul

Galluzzo, Claire Barlow and Alan Heaver for contributions to figures, and to them and many other colleagues for helpful comments on the manuscript.

References

- [1] Kompella M S, Bernhard, R.J. 1993 Variation of structural-acoustic characteristics of automotive vehicles *Noise Control Engineering Journal* **44** 93-9
- [2] Cremer L 1984 *The physics of the violin* (Cambridge, Mass.: MIT Press)
- [3] McIntyre M E and Woodhouse J 1978 Acoustics of Stringed Musical-Instruments *Interdiscipl Sci Rev* **3** 157-73
- [4] Hutchins C M 1983 A History of Violin Research *J Acoust Soc Am* **73** 1421-40
- [5] Gough C 2000 Science and the Stradivarius *Phys World* **13** 27-33
- [6] Strogatz S H 1994 *Nonlinear dynamics and Chaos : with applications to physics, biology, chemistry, and engineering* (Reading, Mass.: Addison-Wesley Pub.)
- [7] Helmholtz H v and Ellis A J 1954 *On the sensations of tone as a physiological basis for the theory of music* (New York: Dover Publications)
- [8] Woodhouse J and Galluzzo P M 2004 Why is the violin so hard to play? In: *Plus Magazine*,
- [9] Krigar-Menzel O and Raps A 1891 Über Saitenschwingungen *Annalen der Physik* **280** 623-41
- [10] Raman C V 1918 On the mechanical theory of vibrations of bowed strings *Bulletin of the Indian Association for the Cultivation of Science* **15** 1-158
- [11] Rayleigh J W S and Lindsay R B 1945 *The theory of sound* (New York,: Dover publications)
- [12] Fletcher N H and Rossing T D 1998 *The physics of musical instruments* (New York: Springer)
- [13] Schelleng J C 1973 Bowed String and Player *J Acoust Soc Am* **53** 26-41
- [14] Cremer L and Lazarus H 1968 Der Einfluss des Bogendruckes beim Anstreichen einer Saite. In: *ICA*, (Tokyo pp N-2-3
- [15] Cremer L 1974 Influence of Bow Pressure on Self-Excited Vibrations of Stringed Instruments *Acustica* **30** 119-36
- [16] Woodhouse J 1993 On the Playability of Violins .1. Reflection Functions *Acustica* **78** 125-36
- [17] Woodhouse J 2004 Plucked guitar transients: Comparison of measurements and synthesis *Acta Acust United Ac* **90** 945-65
- [18] Valette C 1995 *Mechanics of Musical Instruments*, ed A Hirschberg, et al. (New York: Springer-Verlag) pp 116-83
- [19] Saw S-M 2010 Influence of finger forces on string vibration. In: *Department of Engineering*: University of Cambridge) pp 1-43
- [20] McIntyre M E and Woodhouse J 1979 Fundamentals of Bowed-String Dynamics *Acustica* **43** 93-108
- [21] McIntyre M E, Schumacher R T and Woodhouse J 1983 On the Oscillations of Musical-Instruments *J Acoust Soc Am* **74** 1325-45
- [22] Smith J O 1992 Physical Modeling Using Digital Wave-Guides *Comput Music J* **16** 74-98
- [23] Clough R W and Wilson E L 1979 Dynamic Analysis of Large Structural Systems with Local Nonlinearities *Comput Method Appl M* **17-8** 107-29

- [24] Hagedorn P and Schramm W 1988 On the Dynamics of Large Systems with Localized Nonlinearities *J Appl Mech-T Asme* **55** 946-51
- [25] Butlin T and Langley R S 2011 An efficient model of drill-string dynamics with localised non-linearities *Iutam Bookser* **27** 389-402
- [26] Valimaki V 2004 Physics-based modeling of musical instruments *Acta Acust United Ac* **90** 611-7
- [27] Friedlander F G 1953 On the oscillations of the bowed string *Proceedings of the Cambridge Philosophical Society* **49** 516-30
- [28] McIntyre M E and Woodhouse J 1984 A parametric study of the bowed string: the violinist's menagerie *Catgut Acoustical Society Newsletter* **42** 18-21
- [29] Boutillon X 1991 Analytical Investigation of the Flattening Effect - the Reactive Power Balance Rule *J Acoust Soc Am* **90** 754-63
- [30] Faure C A and Boutillon X 1993 The Frequency of a Bowed String - Determination and Measurements *Cr Acad Sci Ii* **317** 1377-82
- [31] Schumacher R T 1994 Measurements of Some Parameters of Bowing *J Acoust Soc Am* **96** 1985-98
- [32] McIntyre M E, Schumacher R T and Woodhouse J 1981 Aperiodicity in Bowed-String Motion *Acustica* **49** 13-32
- [33] Pitteroff R and Woodhouse J 1998 Mechanics of the contact area between a violin bow and a string. Part II: Simulating the bowed string *Acustica* **84** 744-57
- [34] Pitteroff R and Woodhouse J 1998 Mechanics of the contact area between a violin bow and a string. Part III: Parameter dependence *Acustica* **84** 929-46
- [35] Schelleng J C 1963 Violin as a Circuit *J Acoust Soc Am* **35** 326-&
- [36] Boutillon X and Weinreich G 1999 Three-dimensional mechanical admittance: Theory and new measurement method applied to the violin bridge *J Acoust Soc Am* **105** 3524-33
- [37] Woodhouse J and Courtney P E 2003 The admittance matrix of a cello. In: *SMAC03*, (Stockholm pp 107-10)
- [38] Gillan F S and Elliott S J 1989 Measurement of the torsional modes of vibration of strings on instruments of the violin family *J Sound Vib* **130** 347-51
- [39] Woodhouse J and Loach A R 1999 Torsional behaviour of cello strings *Acustica* **85** 734-40
- [40] Kuznetsov Y 2004 *Elements of Applied Bifurcation Theory* (New York: Springer)
- [41] Serafin S, Smith J O and Woodhouse J 1999 An investigation of the impact of torsion waves and friction characteristics on the playability of virtual bowed strings. In: *IEEE Workshop on Applications of Signal Processing to Audio and Acoustics*, (New Paltz, New York pp W99-1-4)
- [42] Gough C 1984 The Nonlinear Free-Vibration of a Damped Elastic String *J Acoust Soc Am* **75** 1770-6
- [43] Hanson R J, Anderson J M and Macomber H K 1994 Measurements of Nonlinear Effects in a Driven Vibrating-Wire *J Acoust Soc Am* **96** 1549-56
- [44] Mansour H, Woodhouse J and Scavone G 2013 Enhanced simulation of the bowed cello string. In: *SMAC13*, (Stockholm pp 94-100)
- [45] Morse P M and Ingard K U 1986 *Theoretical acoustics* (Princeton, N.J.: Princeton University Press)
- [46] Harris N 2003 On the role of longitudinal string vibrations in the generation of violin sound. Southampton
- [47] Erkut C, Karjalainen M, Huang P and Valimaki V 2002 Acoustical analysis and model-based sound synthesis of the kantele *J Acoust Soc Am* **112** 1681-91

- [48] Nashif A D, Jones D I G and Henderson J P 1985 *Vibration damping* (New York: Wiley)
- [49] Cremer L, Heckl M and Petersson B A T 2005 *Structure-borne sound : structural vibrations and sound radiation at audio frequencies* (Berlin ; New York: Springer)
- [50] Heckl M 1962 Measurements of Absorption Coefficients on Plates *J Acoust Soc Am* **34** 803-&
- [51] Guettler K 2010 *The Science of String Instruments*, ed T D Rossing (New York: Springer) pp 279-99
- [52] Gough C 2011 The violin bow: Taper, camber and flexibility *J Acoust Soc Am* **130** 4105-16
- [53] Ablitzer F, Dalmont J P and Dauchez N 2012 Static model of a violin bow: Influence of camber and hair tension on mechanical behavior *J Acoust Soc Am* **131** 773-82
- [54] Guettler K and Askenfelt A 1998 On the kinematics of spiccato and ricochet bowing *Journal of the Catgut Acoustical Society* **3** 9-15
- [55] Pitteroff R and Woodhouse J 1998 Mechanics of the contact area between a violin bow and a string. Part I: Reflection and transmission behaviour *Acustica* **84** 543-62
- [56] Schumacher R T 1975 Some aspects of the bow *Catgut Acoustical Society Newsletter* **24** 5-8
- [57] Gough C E 2012 Violin bow vibrations *J Acoust Soc Am* **131** 4152-63
- [58] Bissinger G 1995 Bounce tests, modal analysis, and the playing qualities of the violin bow *Journal of the Catgut Acoustical Society* **2** 17-22
- [59] Sheng G 2008 *Friction-induced vibrations and sound : principles and applications* (Boca Raton: CRC Press/Taylor & Francis Group)
- [60] Rabinowicz E 1951 The Nature of the Static and Kinetic Coefficients of Friction *J Appl Phys* **22** 1373-9
- [61] Ko P L and Brockley C A 1970 Measurement of Friction and Friction-Induced Vibration *J Lubr Technol* **92** 543-9
- [62] Dieterich J H 1979 Modeling of Rock Friction .1. Experimental Results and Constitutive Equations *J Geophys Res* **84** 2161-8
- [63] James J, Jongeblo W I and Molenaar I 1973 Role of Hair Structure in Sound Production of Bowed Instruments - Study with Light and Scanning Electron-Microscope *Mikroskopie* **28** 298-304
- [64] Fiebach K and Grims D 2000 Resins, natural. In: *Ullmann's Encyclopaedia of Industrial Chemistry*, (New York: Wiley)
- [65] Cobbold P R and Jackson M P A 1992 Gum Rosin (Colophony) - a Suitable Material for Thermomechanical Modeling of the Lithosphere *Tectonophysics* **210** 255-71
- [66] Smith J H and Woodhouse J 2000 The tribology of rosin *J Mech Phys Solids* **48** 1633-81
- [67] Schumacher R T and Garoff S 1996 Bowing with a glass bow *Journal of the Catgut Acoustical Society* **3** 9-17
- [68] Woodhouse J, Schumacher R T and Garoff S 2000 Reconstruction of bowing point friction force in a bowed string *J Acoust Soc Am* **108** 357-68
- [69] Schumacher R T, Garoff S and Woodhouse J 2005 Probing the physics of slip-stick friction using a bowed string *J Adhesion* **81** 723-50
- [70] Evans D C B, Nye J F and Cheeseman K J 1976 Kinetic Friction of Ice *P Roy Soc Lond a Mat* **347** 493-&
- [71] Heslot F, Baumberger T, Perrin B, Caroli B and Caroli C 1994 Creep, Stick-Slip, and Dry-Friction Dynamics - Experiments and a Heuristic Model *Phys Rev E* **49** 4973-88
- [72] Gill D 1984 *The Book of the violin* (New York: Rizzoli)

- [73] Lyon R H, DeJong R G and Lyon R H 1995 *Theory and application of statistical energy analysis* (Boston: Butterworth-Heinemann)
- [74] Woodhouse J 2002 Body vibration of the violin - what can a maker expect to control? *Journal of the Catgut Acoustical Society* **4** 43-9
- [75] Woodhouse J and Langley R S 2012 Interpreting the Input Admittance of Violins and Guitars *Acta Acust United Ac* **98** 611-28
- [76] Manohar C S and Keane A J 1994 Statistics of Energy Flows in Spring-Coupled One-Dimensional Subsystems *Philos T R Soc A* **346** 525-42
- [77] Dowling A P and Ffowcs Williams J E 1983 *Sound and sources of sound* (Chichester: Ellis Horwood)
- [78] Weinreich G 1985 Sound Hole Sum-Rule and the Dipole-Moment of the Violin *J Acoust Soc Am* **77** 710-8
- [79] Meyer J 1972 Directivity of Bowed Stringed Instruments and Its Effect on Orchestral Sound in Concert Halls *J Acoust Soc Am* **51** 1994-2009
- [80] Cremer V L and Lehringe.F 1973 Radiation of Closed Body Surfaces *Acustica* **29** 137-47
- [81] Bissinger G and Keiffer J 2003 Radiation damping, efficiency, and directivity for violin normal modes below 4 kHz *Acoust Res Lett Onl* **4** 7-12
- [82] Bissinger G 2004 Contemporary generalized normal mode violin acoustics *Acta Acust United Ac* **90** 590-9
- [83] Hill T J W, Richardson B E and Richardson S J 2004 Acoustical parameters for the characterisation of the classical guitar *Acta Acust United Ac* **90** 335-48
- [84] Jansson E V, Molin N E and Sundin H 1970 Resonances of a violin studied by hologram interferometry and acoustical methods *Physica Scripta* **2** 243-56
- [85] Moral J A and Jansson E V 1982 Eigenmodes, Input Admittance, and the Function of the Violin *Acustica* **50** 329-37
- [86] Saldner H O, Molin N E and Jansson E V 1996 Vibration modes of the violin forced via the bridge and action of the soundpost *J Acoust Soc Am* **100** 1168-77
- [87] Marshall K D 1985 Modal-Analysis of a Violin *J Acoust Soc Am* **77** 695-709
- [88] Bissinger G 2003 Modal analysis of a violin octet *J Acoust Soc Am* **113** 2105-13
- [89] Zygmuntowicz S and Bissinger G 2009 Strad 3D - a unified enquiry.
- [90] Shorter P J and Langley R S 2005 Vibro-acoustic analysis of complex systems *J Sound Vib* **288** 669-99
- [91] Langley R S and Coton V 2007 Response variance prediction for uncertain vibro-acoustic systems using a hybrid deterministic-statistical method *J Acoust Soc Am* **122** 3445-63
- [92] Backhaus H 1930 Regarding the vibration modes of violin bodies *Z Phys* **62** 143-66
- [93] Eggers F 1959 Untersuchung von Corpus-Schwingungen am Violoncello *Acustica* **9** 463-5
- [94] Agren C H and Stetson K A 1969 Measuring Wood Resonances of Treble Viol Plates by Hologram Interferometry *J Acoust Soc Am* **46** 120-&
- [95] Reinicke W and Cremer L 1970 Application of Holographic Interferometry to Vibrations of Bodies of String Instruments *J Acoust Soc Am* **48** 988-&
- [96] Jansson E V 1973 Investigation of a Violin by Laser Speckle Interferometry and Acoustical Measurements *Acustica* **29** 21-8
- [97] Molin N E and Jansson E V 1989 Transient Wave-Propagation in Wooden Plates for Musical-Instruments *J Acoust Soc Am* **85** 2179-84
- [98] Molin N E, Wahlin A O and Jansson E V 1990 Transient Wave Response of the Violin Body *J Acoust Soc Am* **88** 2479-81

- [99] Molin N E, Wahlin A O and Jansson E V 1991 Transient Wave Response of the Violin Body Revisited *J Acoust Soc Am* **90** 2192-5
- [100] Ewins D J 2000 *Modal testing : theory, practice, and application* (Baldock: Research Studies Press)
- [101] McConnell K G and Varoto P S r 2008 *Vibration testing : theory and practice* (Hoboken, N.J.: John Wiley & Sons)
- [102] Hodges C H and Woodhouse J 1986 Theories of Noise and Vibration Transmission in Complex Structures *Rep Prog Phys* **49** 107-70
- [103] Maia N M N and Silva J M 1997 *Theoretical and experimental modal analysis* (Taunton: Research Studies Press)
- [104] Waller M D 1961 *Chladni figures: a study in symmetry* (London: Bell)
- [105] Williams E 1999 *Fourier Acoustics* (London: Academic Press)
- [106] Bissinger G 1994 The Influence of the Soundpost on the Mechanical Motions of the Violin *Proceedings of the 12th International Modal Analysis Conference, Vols 1 and 2* **2251** 294-300
- [107] French M and Bissinger G 2001 Mechanics of stringed instruments *Exp Techniques* **25** 34-7
- [108] Knott G A 1987 A modal analysis of the violin using MSC/Nastran and Patran. Naval Postgraduate School, Monterey CA)
- [109] Bretos J, Santamaria C and Moral J A 1999 Vibrational patterns and frequency responses of the free plates and box of a violin obtained by finite element analysis *J Acoust Soc Am* **105** 1942-50
- [110] Rodgers O E 1991 Influence of local thickness changes on violin top plate frequencies *Journal of the Catgut Acoustical Society* **1** 6-10
- [111] Roberts G W 1997 *Research Papers in Violin Acoustics 1975-1993*, ed C M Hutchins and V Benade (Woodbury, NY: Acoustical Society of America) pp 575-90
- [112] Rodgers O E 1993 Influence of local thickness changes on violin top plate frequencies:Part 2 *Journal of the Catgut Acoustical Society* **2** 14-6
- [113] Gough C E 2013 Vibrational modes of the violin family. In: *SMAC2013*, (Stockholm pp 66-74
- [114] Gough C E 2014 Violin plate modes *J Acoust Soc Am* In press
- [115] Gough C E 2014 A violin shell model: vibrational modes and acoustics *J Acoust Soc Am* In press
- [116] Perkins N C and Mote C D 1986 Comments on Curve Veering in Eigenvalue Problems *J Sound Vib* **106** 451-63
- [117] Pierre C 1988 Mode Localization and Eigenvalue Loci Veering Phenomena in Disordered Structures *J Sound Vib* **126** 485-502
- [118] White T B 2012 Telling tails *The Strad*
- [119] Woodhouse J 1998 The acoustics of "A0-B0 mode matching" in the violin *Acustica* **84** 947-56
- [120] Jansson E V 1977 Acoustical Properties of Complex Cavities - Prediction and Measurements of Resonance Properties of Violin-Shaped and Guitar-Shaped Cavities *Acustica* **37** 211-21
- [121] Bissinger G 1996 Acoustic normal modes below 4 kHz for a rigid, closed violin-shaped cavity *J Acoust Soc Am* **100** 1835-40
- [122] Bretos J, Santamarfa C and Moral J A 1999 Vibrational patterns of a violin-shaped air cavity obtained by finite element modeling *Acustica* **85** 584-6
- [123] Hutchins C M 1989 A measurable controlling factor in the tone and playing quality of violins *Journal of the Catgut Acoustical Society* **1** 10-5

- [124] Bissinger G 1998 A0 and A1 coupling, arching, rib height, and f-hole geometry dependence in the 2 degree-of-freedom network model of violin cavity modes *J Acoust Soc Am* **104** 3608-15
- [125] Bissinger G 2008 Structural acoustics model of the violin radiativity profile *J Acoust Soc Am* **124** 4013-23
- [126] Bissinger G 2012 Parametric plate-bridge dynamic filter model of violin radiativity *J Acoust Soc Am* **132** 465-76
- [127] Jansson E V, Morset L A and Guettler K 2001 Prediction of violin radiation properties in the 200-700 Hz range. In: *ISMA2001*, (Perugia pp 123-6
- [128] Gough C E 2013 Acoustic characterization of violin family signature modes by internal cavity measurements. In: *SMAC2013*, (Stockholm pp 75-81
- [129] Woodhouse J 2004 On the synthesis of guitar plucks *Acta Acust United Ac* **90** 928-44
- [130] Jansson E V 1997 Admittance measurements of 25 high quality violins *Acustica* **83** 337-41
- [131] Harris N and Fahy F J 2009 A comparative study of the hammered bridge response and the bowed string response of the violin *J Violin Soc Am* **22** 1-14
- [132] Zhang A and Woodhouse J 2013 The influence of different driving conditions on the frequency response of bowed-string instruments. In: *SMAC2013*, (Stockholm pp 147-50
- [133] Cotoni V, Langley R S and Kidner M R F 2005 Numerical and experimental validation of variance prediction in the statistical energy analysis of built-up systems *J Sound Vib* **288** 701-28
- [134] Moore B C J 2003 *An introduction to the psychology of hearing* (Amsterdam ; Boston: Academic Press)
- [135] Jansson E V and Niewczyk B K 1997 Admittance measurements of violins with high arching *Acustica* **83** 571-4
- [136] Jansson E V and Niewczyk B K 1999 On the acoustics of the violin: bridge hill or body hill? *Journal of the Catgut Acoustical Society* **3** 23-7
- [137] Durup E and Jansson E V 2005 The quest of the violin Bridge-Hill *Acta Acust United Ac* **91** 206-13
- [138] Beldie I P 2003 About the bridge hill mystery *Journal of the Catgut Acoustical Society* **4** 9-13
- [139] Woodhouse J 2005 On the "bridge hill" of the violin *Acta Acust United Ac* **91** 155-65
- [140] Reinicke W 1973 Übertragungseigenschaften des Streichinstrumentenstegs *Catgut Acoustical Society Newsletter* **19** 26-32
- [141] Skudrzyk E 1980 The Mean-Value Method of Predicting the Dynamic-Response of Complex Vibrators *J Acoust Soc Am* **67** 1105-35
- [142] Noad F M 1976 *The Classical guitar* (New York,: Ariel Music Publications)
- [143] Maestre E, Scavone G P and Smith J O 2013 Digital modeling of bridge driving-point admittances from measurements on violin-family instruments. In: *SMAC2013*, (Stockholm
- [144] Fahy F and Gardonio P 2007 *Sound and structural vibration : radiation, transmission and response* (Amsterdam ; Boston: Elsevier/Academic)
- [145] Choi W, Woodhouse J and Langley R S 2012 Sound radiation from point-excited structures: Comparison of plate and sphere *J Sound Vib* **331** 2156-72
- [146] Lynch C M, Woodhouse J and Langley R S 2013 Sound radiation from point-driven shell structures *J Sound Vib* **332** 7089-98
- [147] Weinreich G 1997 Directional tone color *J Acoust Soc Am* **101** 2338-46
- [148] Hutchins C M 1981 The Acoustics of Violin Plates *Sci Am* **245** 170-&

- [149] Schleske M 1996 Eigenmodes of vibration in the working process of the violin *Journal of the Catgut Acoustical Society* **3** 2-6
- [150] Woodhouse J 1993 A set of violins for player-rating experiments. In: *SMAC93*, (Stockholm pp 438-40)
- [151] Davis E B 2013 On the effective material properties of violin plates. In: *SMAC2013*, (Stockholm pp 9-15)
- [152] Dettloff J A 1985 Statistical relationships between acoustical parameters of violin tonewoods *Journal of the Catgut Acoustical Society* **43** 13-5
- [153] Playfair Q 2003 Curtate cycloid arching in golden age Cremonese violin family instruments *Journal of the Catgut Acoustical Society* **4** 48-58
- [154] Sirr S A and Waddle J R 1997 CT analysis of bowed stringed instruments *Radiology* **203** 801-5
- [155] Stoppani G 2013 Acoustic measurements in the workshop. In: *SMAC2013*, (Stockholm pp 16-23)
- [156] Barlow C Y 1997 Materials selection for musical instruments *Proceedings of the Institute of Acoustics* **19** 69-78
- [157] Ashby M F 2011 *Materials selection in mechanical design* (Burlington, MA: Butterworth-Heinemann)
- [158] Besnainou C 1995 From Wood Mechanical Measurements to Composite-Materials for Musical-Instruments - New Technology for Instrument Makers *Mrs Bull* **20** 34-6
- [159] Martin D 2007 Designing and building ultra-light instruments *J Violin Soc Am* **21** 165-83
- [160] Curtin J 2007 Building ultra-light instruments *J Violin Soc Am* **21** 156-64
- [161] Waltham C 2009 A balsa violin *Am J Phys* **77** 30-5
- [162] Yano H and Minato K 1992 Improvement of the Acoustic and Hygroscopic Properties of Wood by a Chemical Treatment and Application to the Violin Parts *J Acoust Soc Am* **92** 1222-7
- [163] Nagyvary J, DiVerdi J A, Owen N L and Tolley H D 2006 Wood used by Stradivari and Guarneri *Nature* **444** 565-
- [164] Beavitt A 1996 Taking Tone from the Air + Observations on a Process of Humidity Cycling by Which Stringed Instruments Can Reach Their Optimum Playing State *Strad* **107** 916-&
- [165] Schwarze F W M R, Spycher M and Fink S 2008 Superior wood for violins - wood decay fungi as a substitute for cold climate *New Phytol* **179** 1095-104
- [166] Roy K 2006 *The violin: Its History and Making* (Barrington NH: Karl Roy)
- [167] Rossell S E, Abbot E G M and Levy J F 1973 Bacteria and Wood - Review of Literature Relating to Presence, Action and Interaction of Bacteria in Wood *J Wood Sci* 28-35
- [168] Hill W H, Hill A F and Hill A E 1963 *Antonio Stradivari, his life and work, 1644-1737* (New York,: Dover Publications)
- [169] Bodig J and Jayne B A 1993 *Mechanics of wood and wood composites* (Malabar, Fla.: Krieger Pub.)
- [170] Kahle E and Woodhouse J 1994 The Influence of Cell Geometry on the Elasticity of Softwood *J Mater Sci* **29** 1250-9
- [171] Schelleng J C 1968 Acoustical Effects of Violin Varnish *J Acoust Soc Am* **44** 1175-&
- [172] Dunnwald H 1990 An Extended Method of Objectively Determining the Sound Quality of Violins *Acustica* **71** 269-76
- [173] Bissinger G 2008 Structural acoustics of good and bad violins *J Acoust Soc Am* **124** 1764-73

- [174] Saitis C, Giordano B L, Fritz C and Scavone G P 2012 Perceptual evaluation of violins: A quantitative analysis of preference judgments by experienced players *J Acoust Soc Am* **132** 4002-12
- [175] Askenfelt A 1986 Measurement of Bow Motion and Bow Force in Violin Playing *J Acoust Soc Am* **80** 1007-15
- [176] Askenfelt A 1989 Measurement of the Bowing Parameters in Violin Playing .2. Bow Bridge Distance, Dynamic-Range, and Limits of Bow Force *J Acoust Soc Am* **86** 503-16
- [177] Demoucron M, Askenfelt A and Causse R 2009 Measuring Bow Force in Bowed String Performance: Theory and Implementation of a Bow Force Sensor *Acta Acust United Ac* **95** 718-32
- [178] Schoonderwaldt E and Demoucron M 2009 Extraction of bowing parameters from violin performance combining motion capture and sensors *J Acoust Soc Am* **126** 2695-708
- [179] Schoonderwaldt E, Demoucron M, Altenmuller E and Leman M 2013 Auditory perception of note transitions in simulated complex bowing patterns *J Acoust Soc Am* **133** 4311-20
- [180] Woodhouse J, Manuel E K Y, Smith L A, Wheble A J C and Fritz C 2012 Perceptual Thresholds for Acoustical Guitar Models *Acta Acust United Ac* **98** 475-86
- [181] Mathews M V and Kohut J 1973 Electronic Simulation of Violin Resonances *J Acoust Soc Am* **53** 1620-6
- [182] Gorrell S 1975 A viola with electronically synthesized resonances *Catgut Acoustical Society Newsletter* **24** 11-3
- [183] Farina A, Langhoff A and Tronchin L 1998 Acoustic characterisation of "virtual" musical instruments: Using MLS technique on ancient violins *J New Music Res* **27** 359-79
- [184] Gaydecki P 2012 The foundations of digital signal processing using Signal Wizard Systems (R) *Int J Elec Eng Educ* **49** 310-20
- [185] Fritz C, Cross I, Moore B C J and Woodhouse J 2007 Perceptual thresholds for detecting modifications applied to the acoustical properties of a violin *J Acoust Soc Am* **122** 3640-50
- [186] Pollack I 1975 Auditory Informational Masking *J Acoust Soc Am* **57** S5-S
- [187] Watson C S, Kelly W J and Wroton H W 1976 Factors in Discrimination of Tonal Patterns .2. Selective Attention and Learning under Various Levels of Stimulus Uncertainty *J Acoust Soc Am* **60** 1176-86
- [188] Florentine M and Buus S 1981 An Excitation-Pattern Model for Intensity Discrimination *J Acoust Soc Am* **70** 1646-54
- [189] Macmillan N A and Creelman C D 1991 *Detection theory : a user's guide* (Cambridge England ; New York: Cambridge University Press)
- [190] Fritz C, Blackwell A F, Cross I, Woodhouse J and Moore B C J 2012 Exploring violin sound quality: Investigating English timbre descriptors and correlating resynthesized acoustical modifications with perceptual properties *J Acoust Soc Am* **131** 783-94
- [191] Fritz C, Woodhouse J, Cheng F P H, Cross I, Blackwell A F and Moore B C J 2010 Perceptual studies of violin body damping and vibrato *J Acoust Soc Am* **127** 513-24
- [192] Fletcher H and Sanders L C 1967 Quality of Violin Vibrato Tones *J Acoust Soc Am* **41** 1534-&
- [193] McIntyre M E and Woodhouse J 1974 Toward a psychoacoustically realistic violin physics *Catgut Acoustical Society Newsletter* **22** 18-9
- [194] Gough C E 2005 Measurement, modelling and synthesis of violin vibrato sounds *Acta Acust United Ac* **91** 229-40

- [195] Fritz C, Curtin J, Poitevineau J, Morrel-Samuels P and Tao F-C 2012 Player preferences among new and old violins *Proceedings of the National Academy of Sciences* **109** 760-3
- [196] Fritz C, Curtin J, Poitevineau J, Borsarello H, Wollman I, Tao F-C and Ghasarossian T 2014 Soloist evaluations of six old Italian and six new violins *Proceedings of the National Academy of Sciences*
- [197] Woodhouse J 1993 On the Playability of Violins .2. Minimum Bow Force and Transients *Acustica* **78** 137-53
- [198] Schoonderwaldt E, Guettler K and Askenfelt A 2008 An empirical investigation of bow-force limits in the Schelleng diagram *Acta Acust United Ac* **94** 604-22
- [199] Schoonderwaldt E 2009 The Violinist's Sound Palette: Spectral Centroid, Pitch Flattening and Anomalous Low Frequencies *Acta Acust United Ac* **95** 901-14
- [200] Schumacher R T 1992 Analysis of Aperiodicities in Nearly Periodic Wave-Forms *J Acoust Soc Am* **91** 438-51
- [201] Schumacher R T and Woodhouse J 1995 The Transient-Behavior of Models of Bowed-String Motion *Chaos* **5** 509-23
- [202] Guettler K 2002 On the creation of the Helmholtz motion in bowed strings *Acta Acust United Ac* **88** 970-85
- [203] Galluzzo P M 2003 On the playabiity of stringed instruments. University of Cambrige)
- [204] Galluzzo P M and Woodhouse J 2014 High-Performance Bowing Machine Tests of Bowed-String Transients *Acta Acust United Ac* **100** 139-53
- [205] Wegst U G K 2006 Wood for sound *Am J Bot* **93** 1439-48
- [206] Wegst U G K, Oberhoff S, Weller M and Ashby M F 2007 Materials for violin bows *Int J Mater Res* **98** 1230-7

Captions

Figure 1: Frequency responses of two violins: specifically, the drive-point admittance at the violin bridge, described in detail in section 3.3.1. Solid curve: anonymous violin of low value; dashed curve: violin by Giuseppe Guarneri “del Gesu”.

Figure 2: Idealised version of the “Helmholtz motion” of a bowed string: (a) sketch of the string displacement at three points in the vibration cycle (with exaggerated vertical scale); (b) waveform of string velocity at the bow-string contact point; (c) waveform of transverse force exerted on the violin bridge.

Figure 3: Sketch of Schelleng’s diagram [13], showing the region of the bow force – bow position plane within which it is possible to sustain a steady Helmholtz motion of the string.

Figure 4: Measured waveforms of string velocity at the bowed point, after Cremer [2]. Upper trace: large bow force; lower trace: smaller bow force.

Figure 5: The simplest theoretical model for the motion of a string bowed at a single point. Upper diagram: sketch; lower diagram: flowchart showing the interaction between linear and nonlinear phenomena.

Figure 6: Friction force as a function of relative sliding speed $v - v_b$ at the contact point, according to the “Stribeck” or “friction curve” model. Stars: measured values during steady sliding of an interface containing violin rosin; solid line: curve fit to these measurements, extended to show the sticking portion of the nonlinear characteristic (vertical line) and the forward-slipping portion in the lower right. Coulomb’s law is assumed here, and the friction force has been normalised by the normal force to give the coefficient of friction.

Figure 7: Friedlander’s construction [27] for determining the friction force and relative sliding speed at a given moment, given knowledge of the incident velocity $v_h(t)$, from the intersection of the friction curve with a straight line. Case I: sliding; II: sticking; III: case with ambiguity, resolved by a hysteresis loop as described in the text.

Figure 8: Simulated waveforms: (a,b) Helmholtz motion with two values of normal force; (c) Double slip motion; (d) Double flyback motion. Upper trace: bridge force (shifted vertically for clarity); lower trace: string velocity at bowed point; dashed line: zero line for velocity trace. Simulation model has $\beta = 0.11$, bow speed 0.05 m/s and nominal string frequency 147 Hz (appropriate to the open D string of a cello). The model allows some torsional motion of the string, so the velocity of the string’s centre-line, plotted here, need not be exactly constant during sticking: the string can roll on the sticking bow.

Figure 9: Finite bow width and differential slipping: (a) sketch of the kinematics leading to differential slipping, showing part of the string in two positions during a Helmholtz motion;

(b,c) measured examples of bridge force waveforms showing differential slipping, with two levels of severity.

Figure 10: Wolf simulation, using a similar model to Fig. 8 but with the addition of a single body resonance at the same frequency as the fundamental mode of the string. Upper trace: string velocity at the bowed point; lower trace: body velocity, scaled up by a factor 10 and shifted for clarity. The visible modulation of the upper trace is caused by alternation of Helmholtz motion and double-slipping. Onset of double-slipping can be seen to occur when the body motion reaches a high value, and Helmholtz motion to resume when the body motion becomes small.

Figure 11: The viscosity of a particular sample of violin rosin as a function of temperature. Measurements at lower temperatures correspond to “solid” rosin, those at higher temperatures to the right of the gap correspond to “liquid” rosin. The author is indebted to Malcolm Mackley and Simon Butler for these measurements.

Figure 12: Trajectory in the force-velocity plane for a stick-slip vibration of a simple oscillator excited using violin rosin. The hysteresis loop during sticking is traversed in the anticlockwise direction. The loops on the near-vertical sticking portion of the trajectory are a measurement artefact: see text. The dashed line shows the steady-sliding measurements from Fig. 6, which were made using the same violin rosin.

Figure 13: Scanning electron micrographs showing the tracks left in the rosin surface of a dip-coated glass rod after single uses to excite vibration of a violin E string [69]. Upper plot shows portions of three tracks. Each short vertical line shows the footprint of a single sticking event. Lower plot shows one of these sticking scars in detail. Scale bars in the lower left of the plots show 100 μm (upper plot) and 1 μm (lower plot).

Figure 14: A violin by Antonio Stradivari, labelled to identify some of the main component parts.

Figure 15: Holographic interferograms of a few of the low-frequency modes of a guitar body in which the main motion occurs in the top plate. (a): 215 Hz; (b) 268 Hz; (c) 436 Hz; (d) 553 Hz. A similar top-plate deformation to case (a) also occurs at 103 Hz in this particular guitar, because of coupling to motion of the internal air. Fringes show contour lines of equal vibration amplitude, and the wide white bands indicate nodal lines. Pictures reproduced by permission of Bernard Richardson, Cardiff University.

Figure 16: Three “signature modes” of the body of a typical violin, visualised by nodal line patterns deduced from an early example of modal testing: (a) mode “CBR”, at 436 Hz in this case; (b) Mode “B1-” at 454 Hz; (c) Mode “B1+” at 538 Hz. Each plot shows the top plate (left) and the back plate (right) as seen from the outside, with + symbols denoting motion outwards from the box and – symbols motion inwards. Blue solid lines show the approximate path of nodal lines, calculated by linear interpolation between the grid points.

Figure 17: Modes of a doubly-symmetric violin-shaped box, to serve as basis modes for building up the modes of a more realistic model (see text). Computed with FE analysis, reproduced by permission of Colin Gough.

Figure 18: Signature modes of a violin body without neck or soundpost. For each mode, the left pair shows the top and back plates as measured while the right pair shows simplified FE computations. Colour scales show motion: cold and warm colours denote opposite signs. Measurements reproduced by permission of George Stoppani, FE results by permission of Colin Gough.

Figure 19: Measured bridge admittances of (a) 5 violins and (b) 5 classical and flamenco guitars. The vertical axis is non-dimensionalised using a typical wave impedance for the lowest string of the respective instruments (0.34 Ns/m for the violin, 0.70 Ns/m for the guitar) to give the string-to-body impedance ratio, expressed in dB, and the horizontal axis is plotted on a logarithmic scale starting from the nominal lowest note of the instrument. Successive octaves of that lowest note are marked.

Figure 20: Sketches of the first two in-plane resonances of a violin bridge with clamped feet: (a) rocking motion, typically around 3 kHz; (b) bouncing motion, typically around 6 kHz.

Figure 21: Sketch of a rectangular plate being driven through a mass-spring oscillator: see text.

Figure 22: Driving-point admittances, illustrating direct and reverberant field effects. (a) Simulated results for a rectangular plate with freely hinged boundary conditions on all sides, in amplitude (upper plot) and phase (lower plot). Red curve: plate alone; black curves: plate driven through a mass-spring resonator as sketched in Fig. 21; dashed lines: computed estimate of $Y_{dir}(\omega)$. (b) Similar results for a violin, in amplitude and phase and including the computed $Y_{dir}(\omega)$.

Figure 23: Computed $Y_{dir}(\omega)$ for (a) four different violins; (b) four different guitars. Note different vertical scales. The averaging bandwidth to compute $Y_{dir}(\omega)$ was 1 kHz, so constant values are shown for frequencies up to 500 Hz.

Figure 24: Total sound power radiated from a set of plates and shells driven at a point by a sinusoidal force of unit magnitude, from Lynch et al. [146]. The three spheroids have

different eccentricities, and give results in an obvious succession as they depart progressively from the spherical shape. All structures have the same material, thickness and total surface area. The vertical dashed line marks the critical frequency for a flat plate of this material. The short vertical lines mark the frequency of the lowest mode for the structure with the corresponding line type. The chosen “typical” driving point on each structure was as follows: the baffled flat plate was driven at a point $1/\pi$ of the length and the same fraction of the width from one corner; the spheroids were driven at a point halfway around a quarter-line of longitude from pole to equator.

Figure 25: Data for Young’s modulus and density for a wide range of materials, plotted on logarithmic scales. Lines of slope 3 link materials that would lead to equally loud violins according to the simple criterion used here: some guide lines of this slope are shown. Materials leading to the loudest instruments correspond to moving the line as far left as possible. Upper plot: “all” materials; lower plot: data for woods only, and showing the intermediate region representing E_{mean} as defined in the text. Charts generated by the Cambridge Engineering Selector.

Figure 26: Plot of predicted Schelleng minimum bow force as a function of the fundamental frequency of the played note, for a particular violin. The four curves correspond to the four strings. Vertical lines mark semitones, coloured lines mark the notes G.

Figure 27: Measured Guettler diagram for the open D string of a cello, bowed at $\beta = 0.08$. Square outline near the upper centre of the plot indicates the four transients plotted in Figure 28. Plot reproduced from Galluzzo and Woodhouse [204].

Figure 28: Four particular measured bridge-force transients, corresponding to the cases marked in Figure 27 and laid out in the same spatial arrangement. Each plot begins at the moment of first slip, and the horizontal and vertical scales are the same in all cases. Plots reproduced from Galluzzo and Woodhouse [204].

Figure 29: Simulated Guettler diagrams for a model of the cello string used in Fig. 27, computed using (a) the friction-curve model; (b) the thermal friction model (see text). Plots reproduced from Galluzzo [203] by permission of the author.

Figure 30: Recorded bridge-force signal from a short musical passage on a violin G string, performed by Keir GoGwilt

Figure 31: Details of the four marked portions of the waveform in Fig. 30

Figure 32: Sonogram of the first part of the recording shown in Fig. 30. Contours are logarithmically spaced at intervals of 5 dB, showing a total range of 50 dB from the maximum value.

Figures

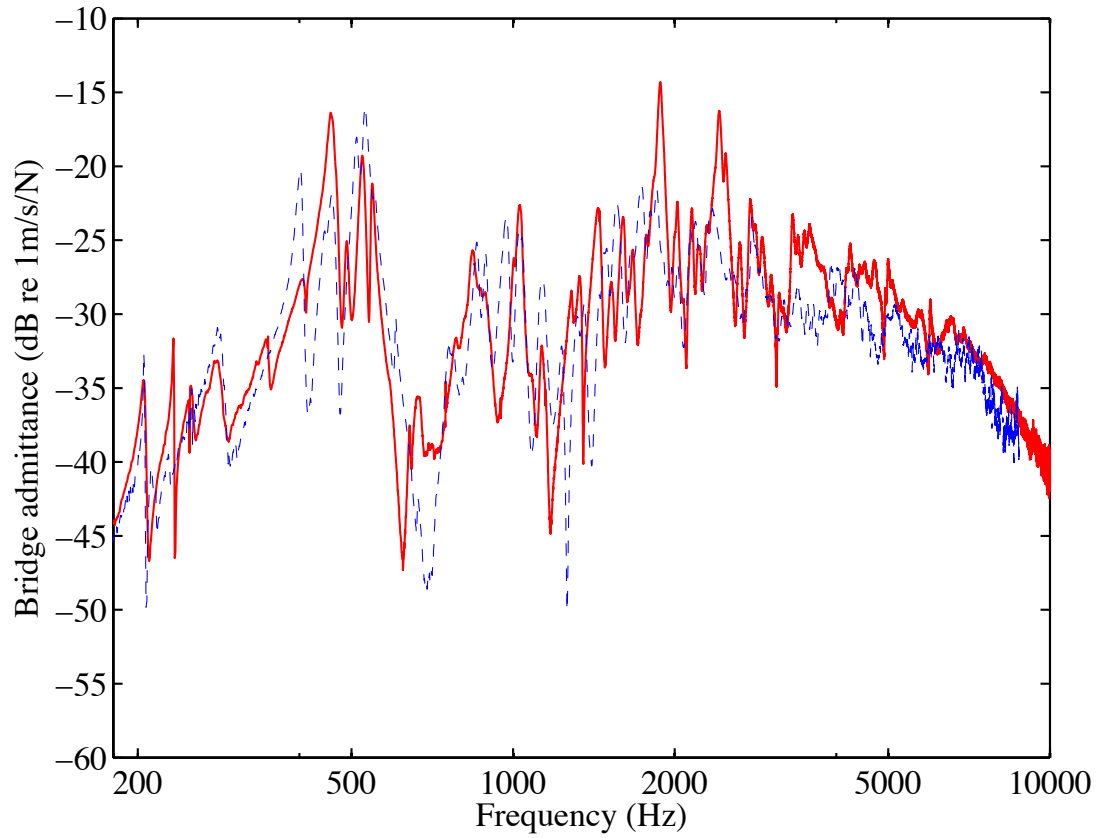


Figure 1: Frequency responses of two violins: specifically, the drive-point admittance at the violin bridge, described in detail in section 3.3.1. Solid curve: anonymous violin of low value; dashed curve: violin by Giuseppe Guarneri “del Gesu”.

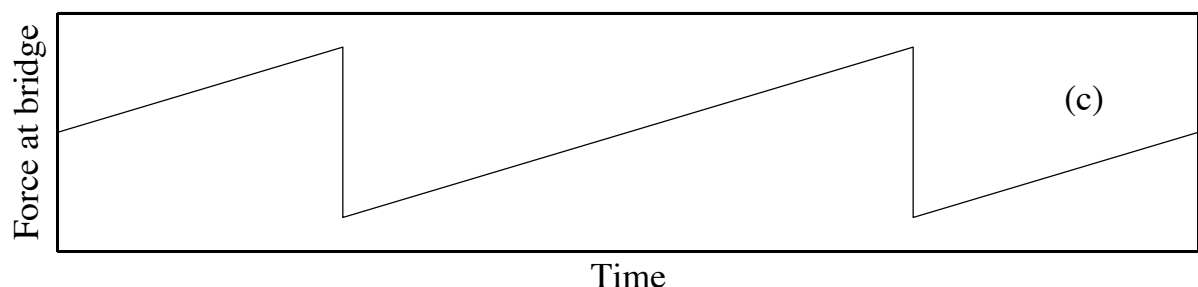
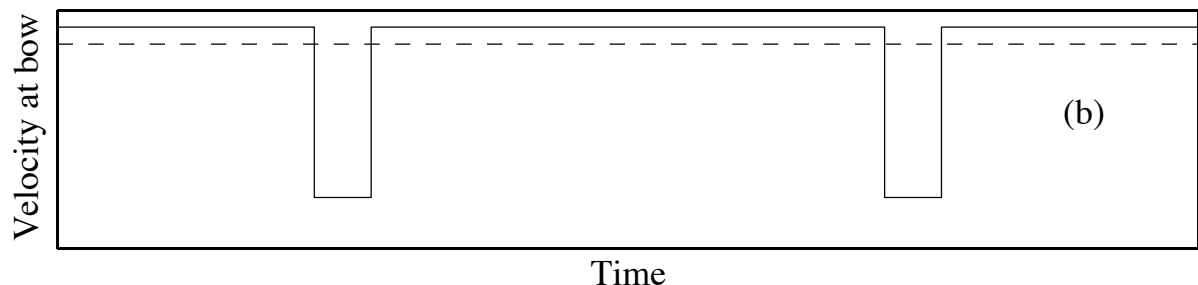
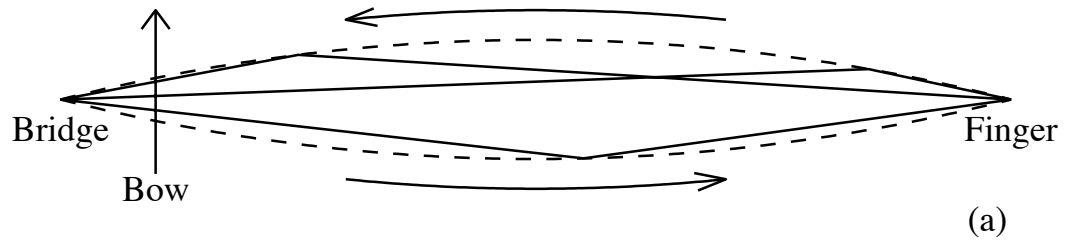


Figure 2: Idealised version of the “Helmholtz motion” of a bowed string: (a) sketch of the string displacement at three points in the vibration cycle (with exaggerated vertical scale); (b) waveform of string velocity at the bow-string contact point; (c) waveform of transverse force exerted on the violin bridge.

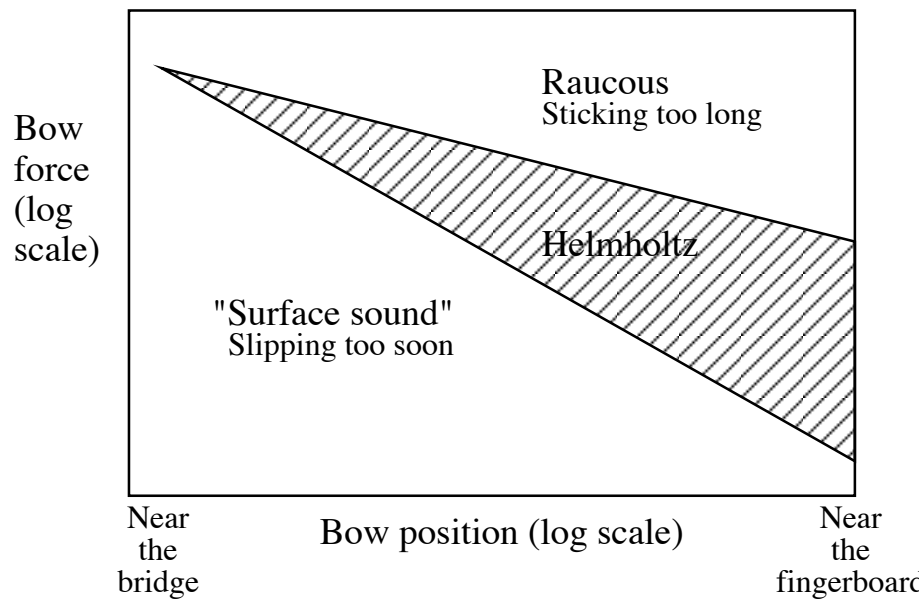


Figure 3: Sketch of Schelleng's diagram [13], showing the region of the bow force – bow position plane within which it is possible to sustain a steady Helmholtz motion of the string.

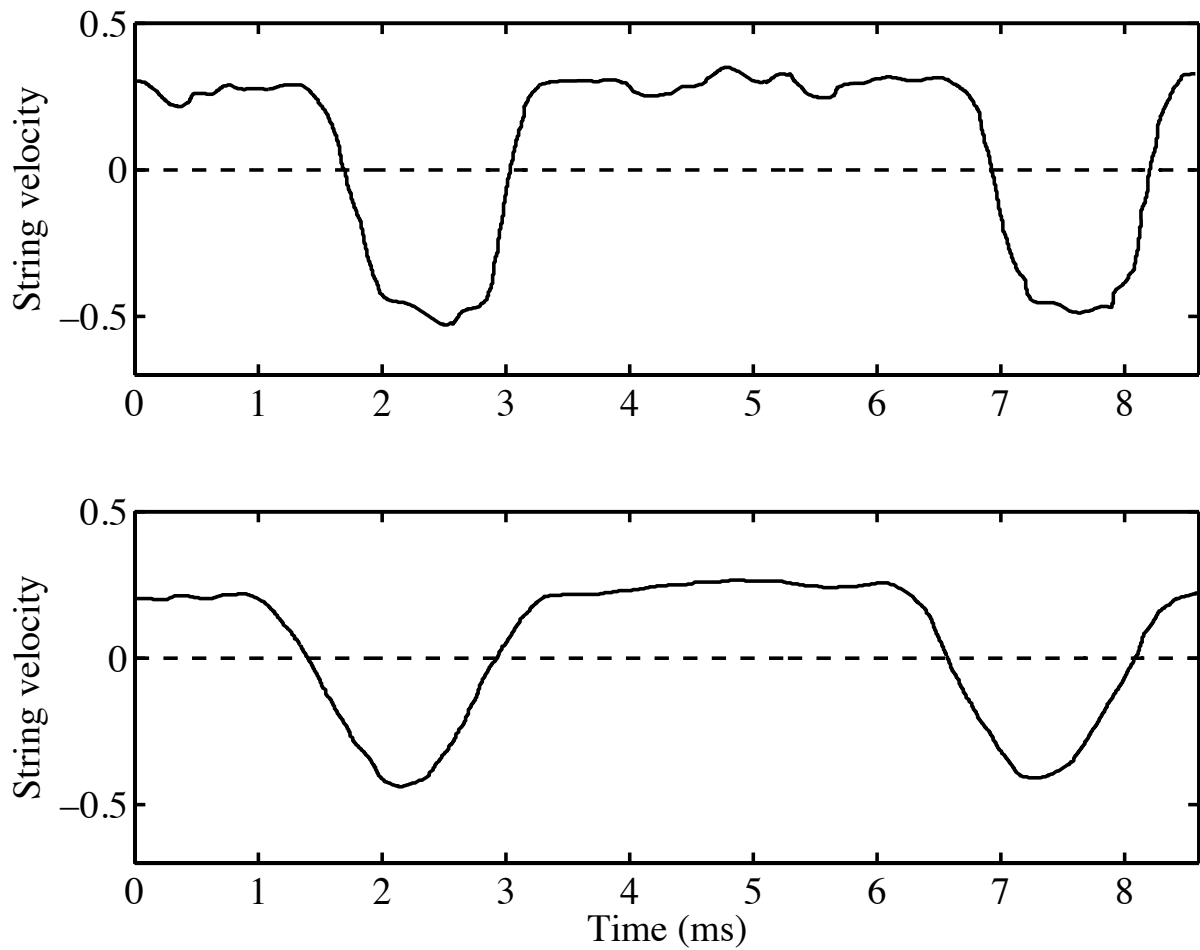


Figure 4: Measured waveforms of string velocity at the bowed point, after Cremer [2]. Upper trace: large bow force; lower trace: smaller bow force.

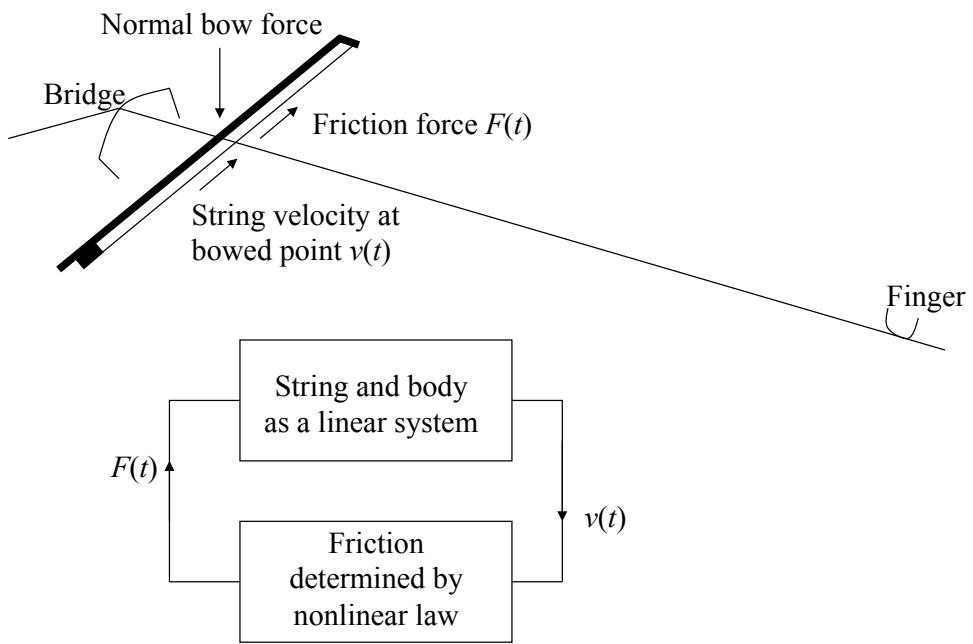


Figure 5: The simplest theoretical model for the motion of a string bowed at a single point. Upper diagram: sketch; lower diagram: flowchart showing the interaction between linear and nonlinear phenomena.

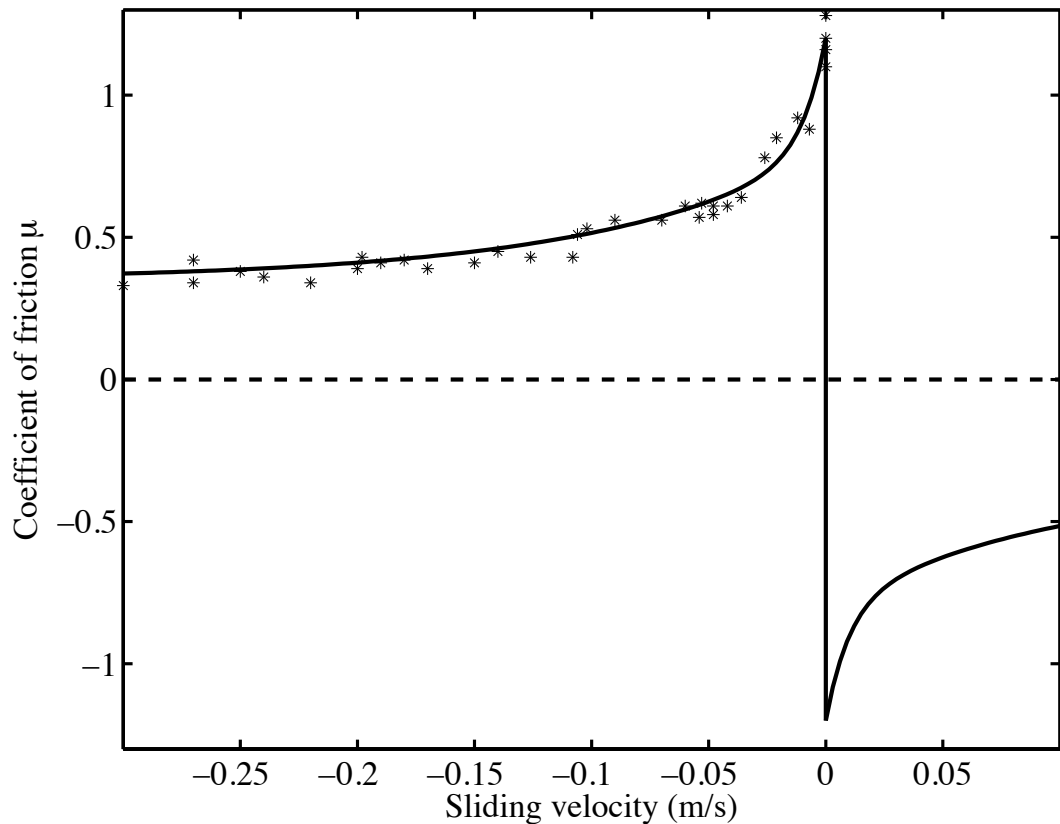


Figure 6: Friction force as a function of relative sliding speed $v - v_b$ at the contact point, according to the “Stribeck” or “friction curve” model. Stars: measured values during steady sliding of an interface containing violin rosin; solid line: curve fit to these measurements, extended to show the sticking portion of the nonlinear characteristic (vertical line) and the forward-slipping portion in the lower right. Coulomb’s law is assumed here, and the friction force has been normalised by the normal force to give the coefficient of friction.

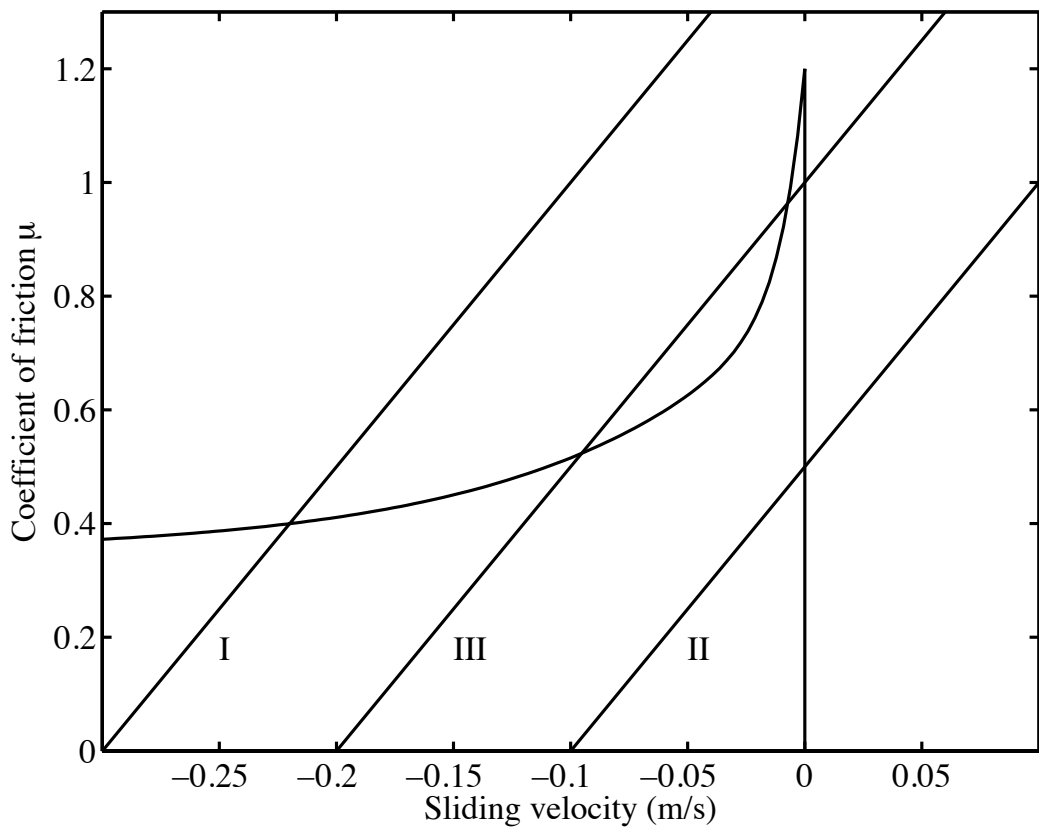


Figure 7: Friedlander's construction [27] for determining the friction force and relative sliding speed at a given moment, given knowledge of the incident velocity $v_h(t)$, from the intersection of the friction curve with a straight line. Case I: sliding; II: sticking; III: case with ambiguity, resolved by a hysteresis loop as described in the text.

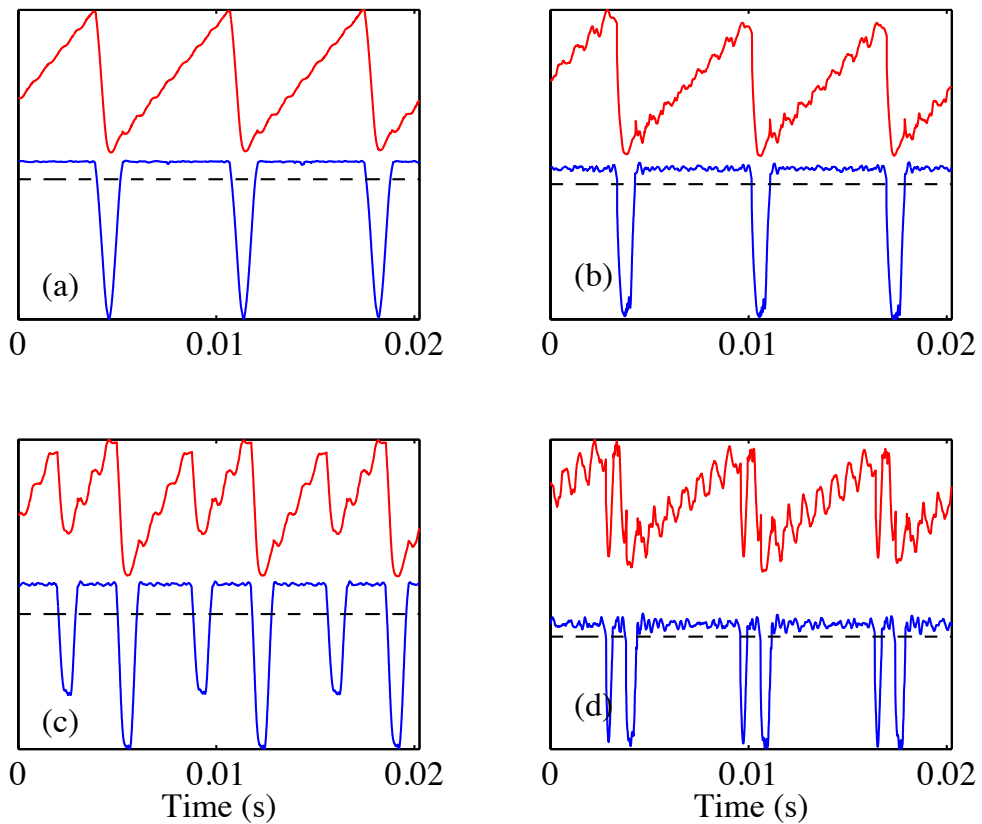


Figure 8: Simulated waveforms: (a,b) Helmholtz motion with two values of normal force; (c) Double slip motion; (d) Double flyback motion. Upper trace: bridge force (shifted vertically for clarity); lower trace: string velocity at bowed point; dashed line: zero line for velocity trace. Simulation model has $\beta = 0.11$, bow speed 0.05 m/s and nominal string frequency 147 Hz (appropriate to the open D string of a cello). The model allows some torsional motion of the string, so the velocity of the string's centre-line, plotted here, need not be exactly constant during sticking: the string can roll on the sticking bow.

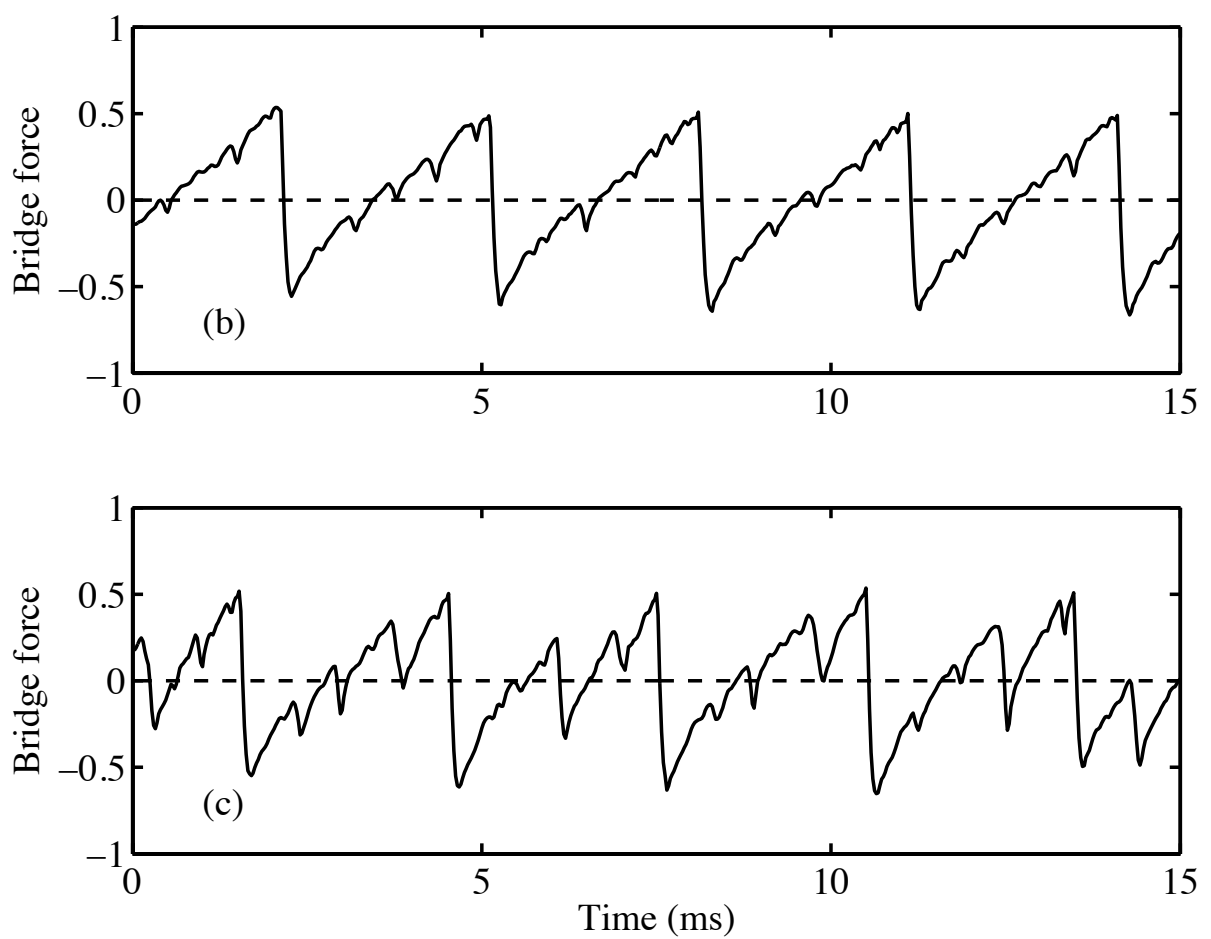
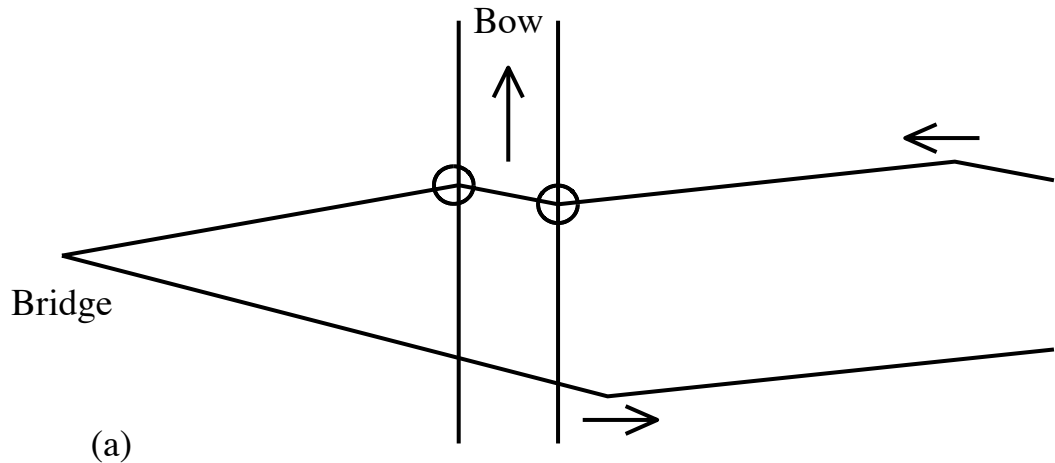


Figure 9: Finite bow width and differential slipping: (a) sketch of the kinematics leading to differential slipping, showing part of the string in two positions during a Helmholtz motion; (b,c) measured examples of bridge force waveforms showing differential slipping, with two levels of severity.

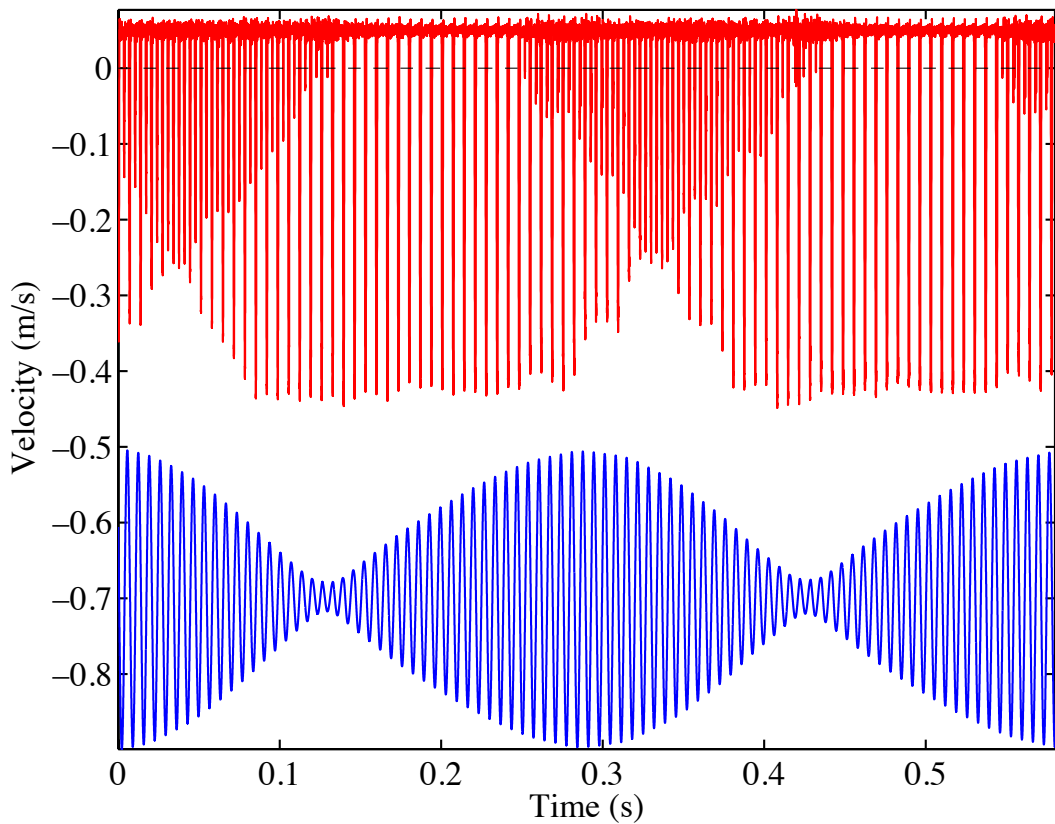


Figure 10: Wolf simulation, using a similar model to Fig. 8 but with the addition of a single body resonance at the same frequency as the fundamental mode of the string. Upper trace: string velocity at the bowed point; lower trace: body velocity, scaled up by a factor 10 and shifted for clarity. The visible modulation of the upper trace is caused by alternation of Helmholtz motion and double-slipping. Onset of double-slipping can be seen to occur when the body motion reaches a high value, and Helmholtz motion to resume when the body motion becomes small.

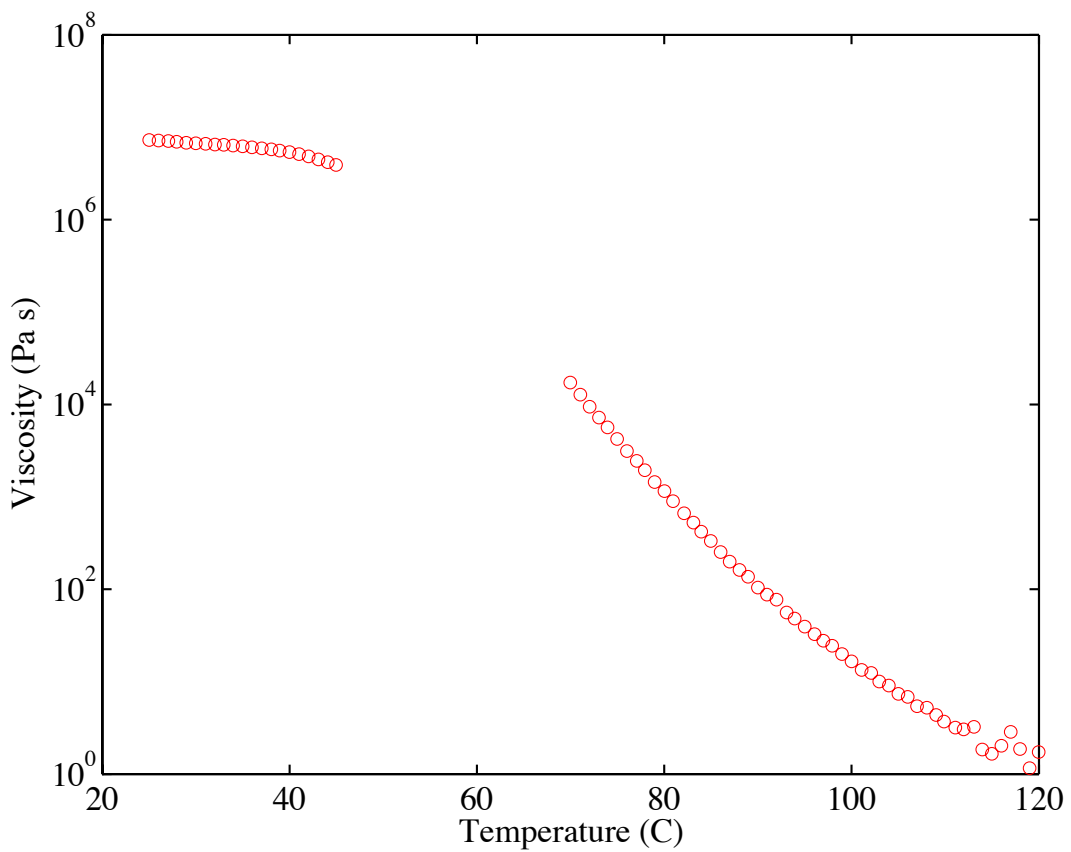


Figure 11: The viscosity of a particular sample of violin rosin as a function of temperature. Measurements at lower temperatures correspond to “solid” rosin, those at higher temperatures to the right of the gap correspond to “liquid” rosin. The author is indebted to Malcolm Mackley and Simon Butler for these measurements.

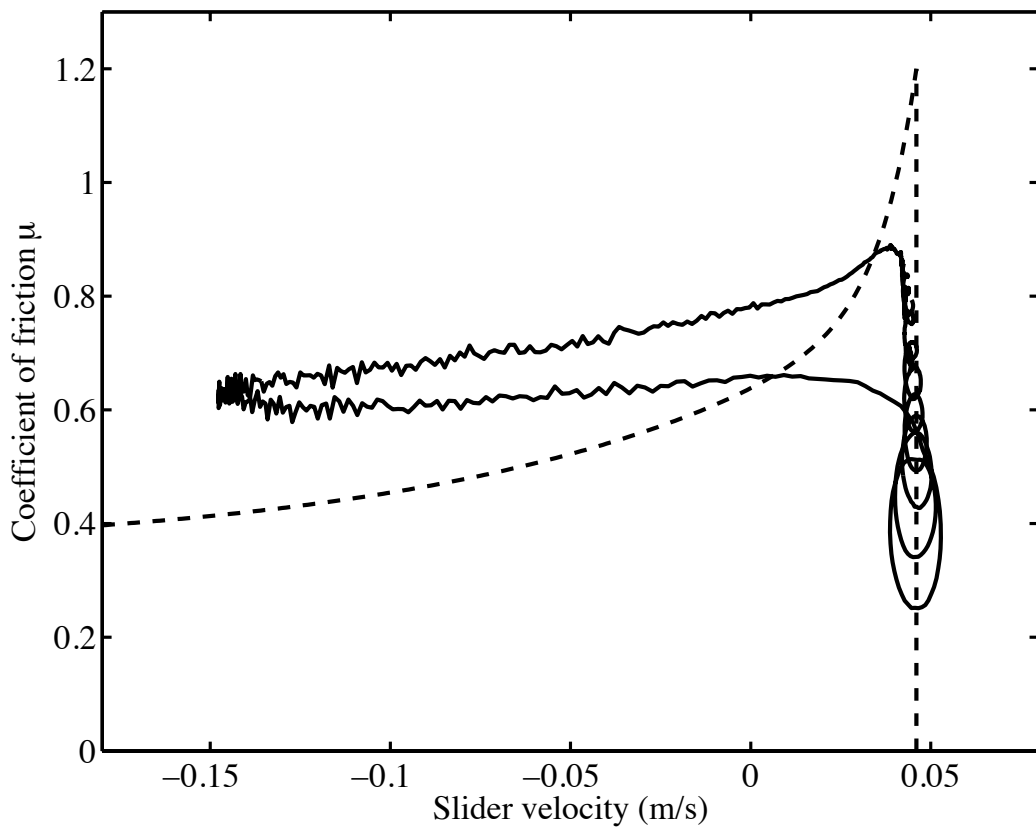
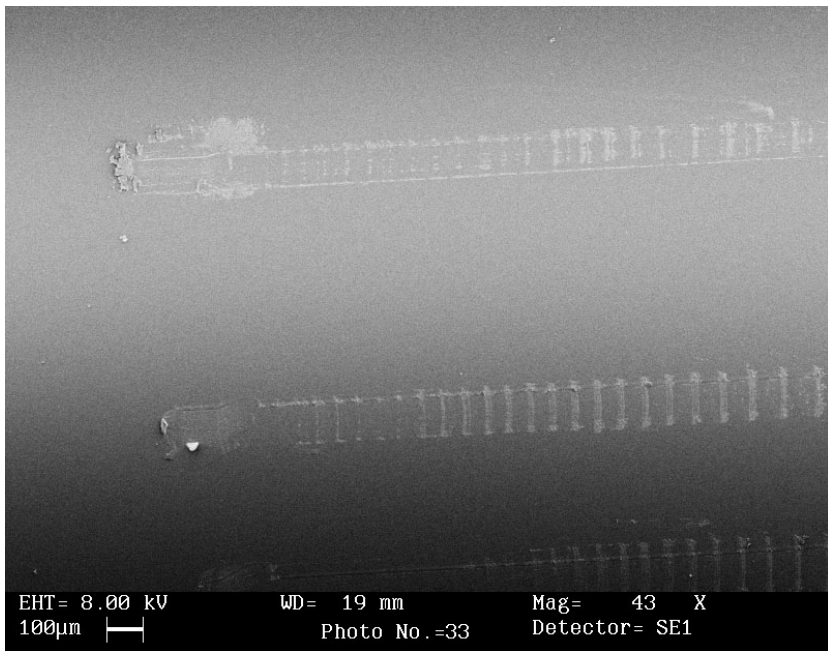
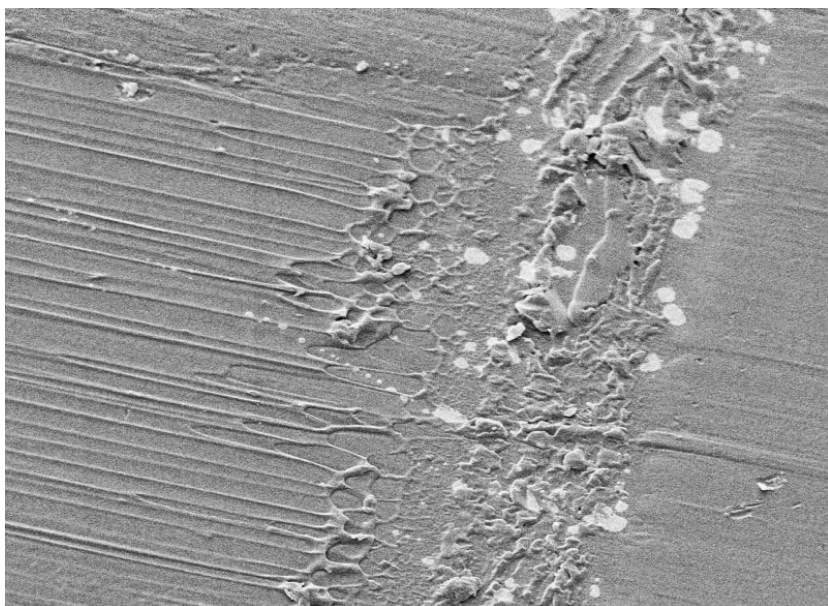


Figure 12: Trajectory in the force-velocity plane for a stick-slip vibration of a simple oscillator excited using violin rosin. The hysteresis loop during sticking is traversed in the anticlockwise direction. The loops on the near-vertical sticking portion of the trajectory are a measurement artefact: see text. The dashed line shows the steady-sliding measurements from Fig. 6, which were made using the same violin rosin.



EHT = 8.00 kV WD = 19 mm Mag = 43 X
100μm | Photo No. = 33 Detector = SE1



EHT = 8.00 kV WD = 18 mm Mag = 1.51 K X
1μm | Photo No. = 83 Detector = SE1

Figure 13: Scanning electron micrographs showing the tracks left in the rosin surface of a dip-coated glass rod after single uses to excite vibration of a violin E string [69]. Upper plot shows portions of three tracks. Each short vertical line shows the footprint of a single sticking event. Lower plot shows one of these sticking scars in detail. Scale bars in the lower left of the plots show 100 μm (upper plot) and 1 μm (lower plot).

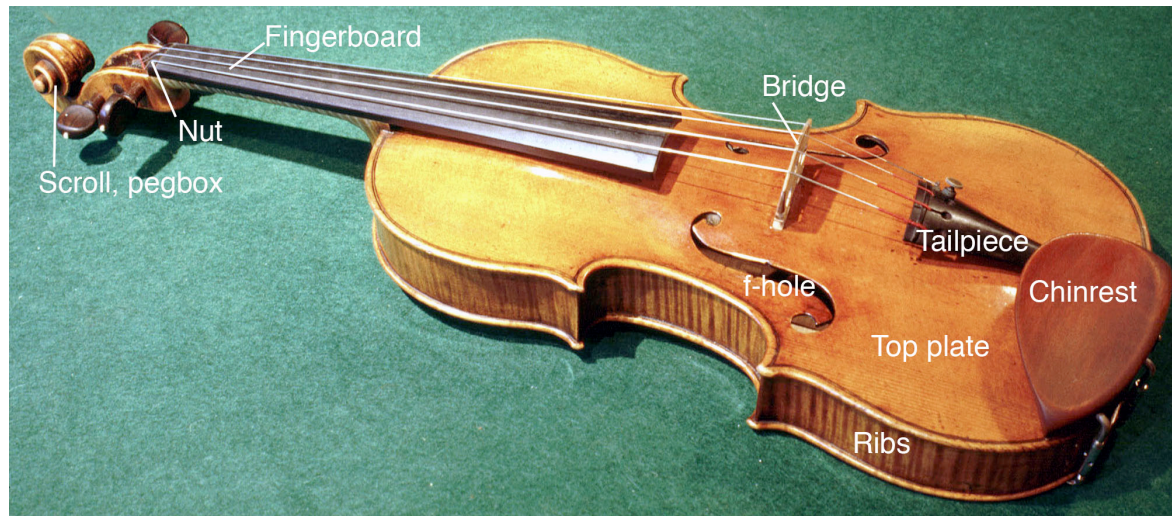


Figure 14: A violin by Antonio Stradivari, labelled to identify some of the main component parts.

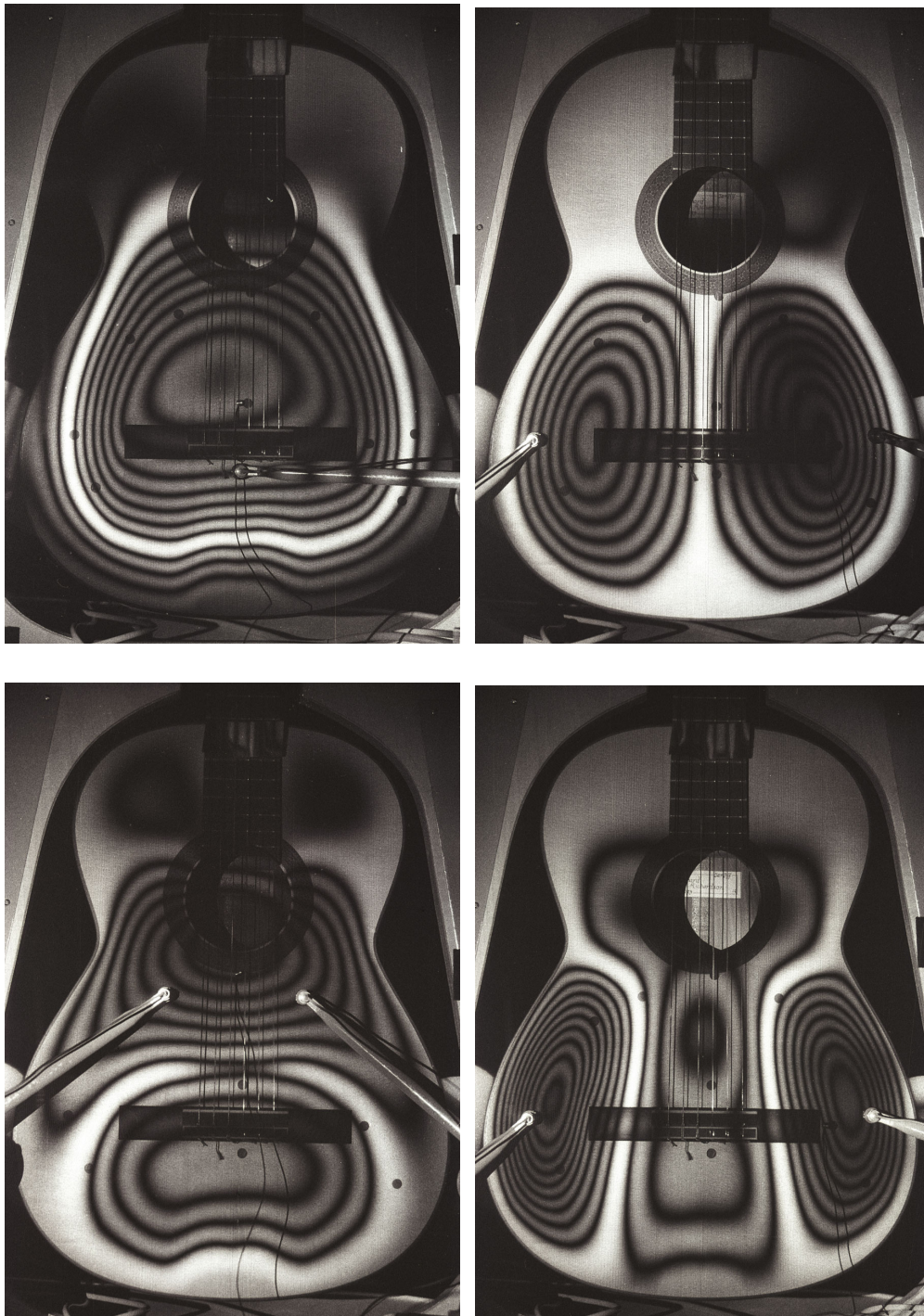


Figure 15: Holographic interferograms of a few of the low-frequency modes of a guitar body in which the main motion occurs in the top plate. (a): 215 Hz; (b) 268 Hz; (c) 436 Hz; (d) 553 Hz. A similar top-plate deformation to case (a) also occurs at 103 Hz in this particular guitar, because of coupling to motion of the internal air. Fringes show contour lines of equal vibration amplitude, and the wide white bands indicate nodal lines. Pictures reproduced by permission of Bernard Richardson, Cardiff University.

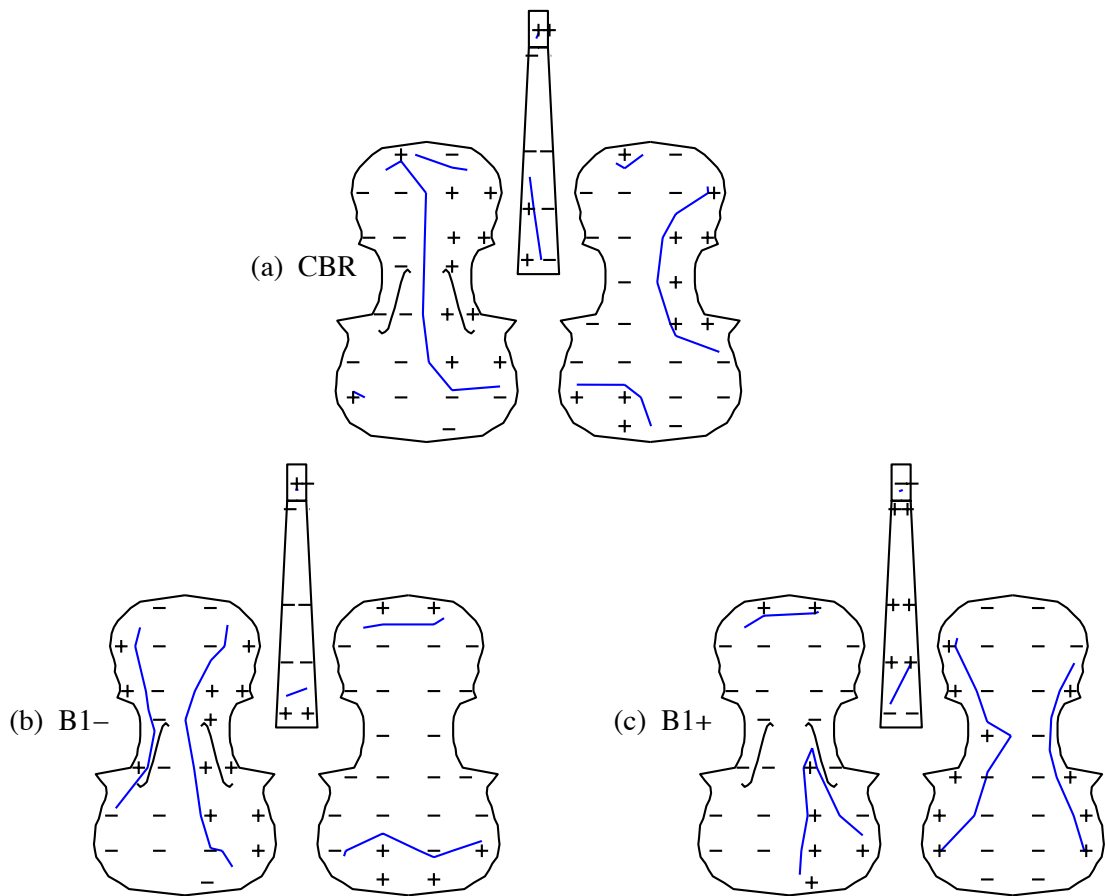


Figure 16: Three “signature modes” of the body of a typical violin, visualised by nodal line patterns deduced from an early example of modal testing: (a) mode “CBR”, at 436 Hz in this case; (b) Mode “B1-” at 454 Hz; (c) Mode “B1+” at 538 Hz. Each plot shows the top plate (left) and the back plate (right) as seen from the outside, with + symbols denoting motion outwards from the box and – symbols motion inwards. Blue solid lines show the approximate path of nodal lines, calculated by linear interpolation between the grid points.

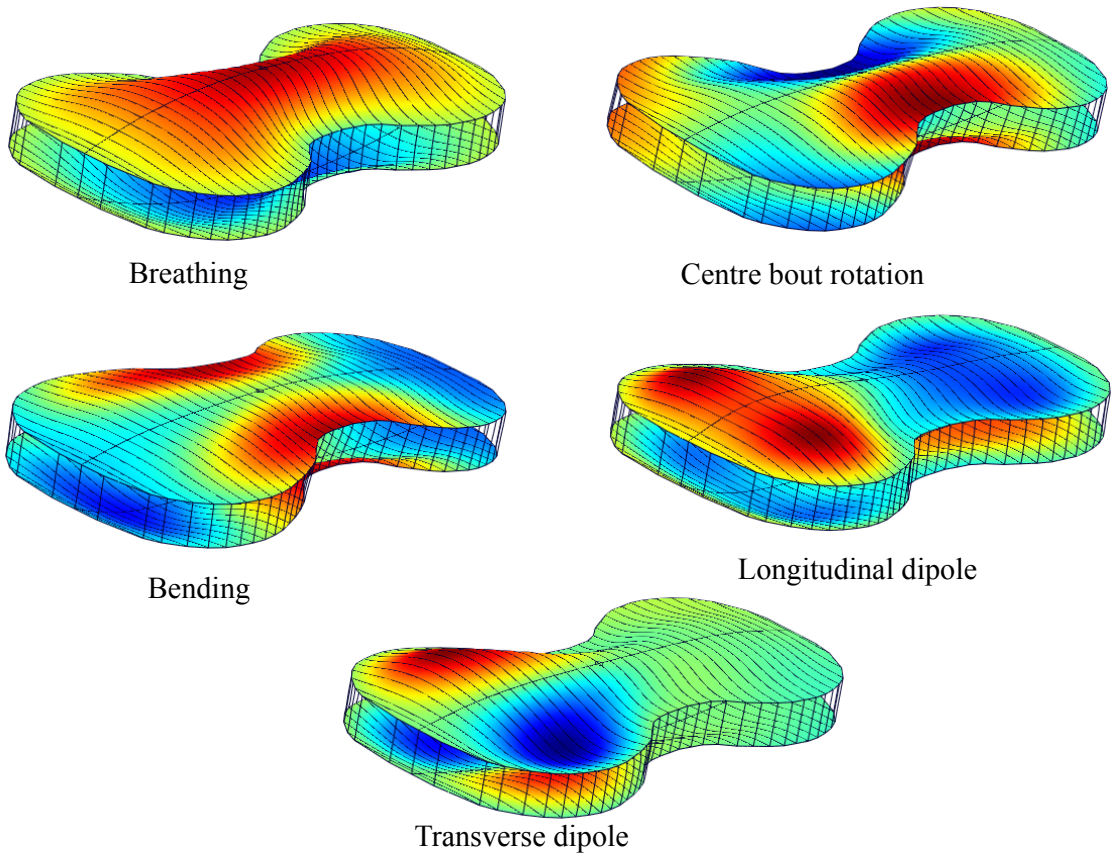


Figure 17: Modes of a doubly-symmetric violin-shaped box, to serve as basis modes for building up the modes of a more realistic model (see text). Computed with FE analysis, reproduced by permission of Colin Gough.

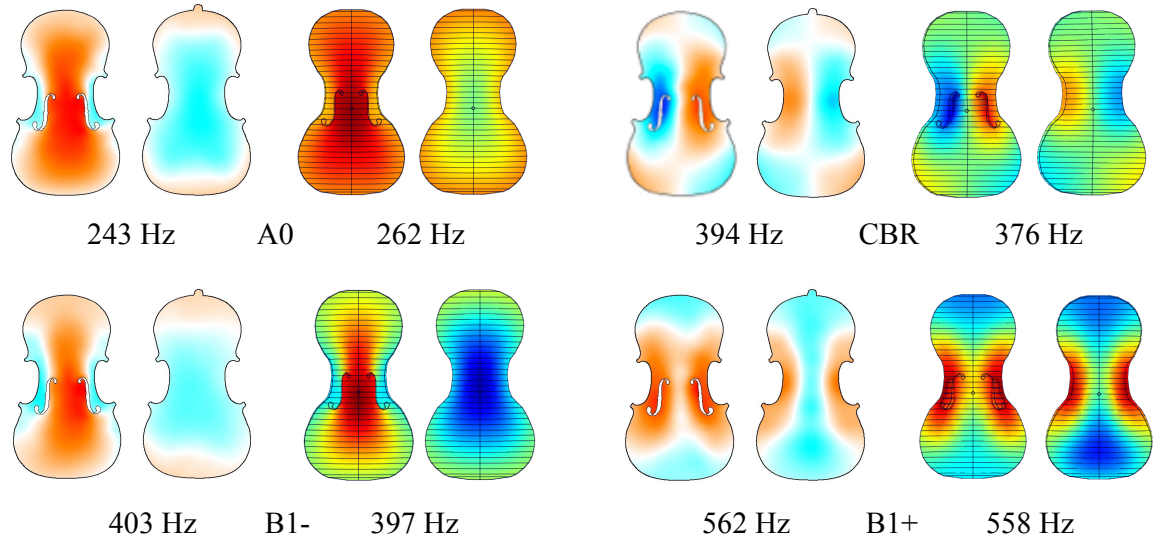


Figure 18: Signature modes of a violin body without neck or soundpost. For each mode, the left pair shows the top and back plates as measured while the right pair shows simplified FE computations. Colour scales show motion: cold and warm colours denote opposite signs. Measurements reproduced by permission of George Stoppani, FE results by permission of Colin Gough.

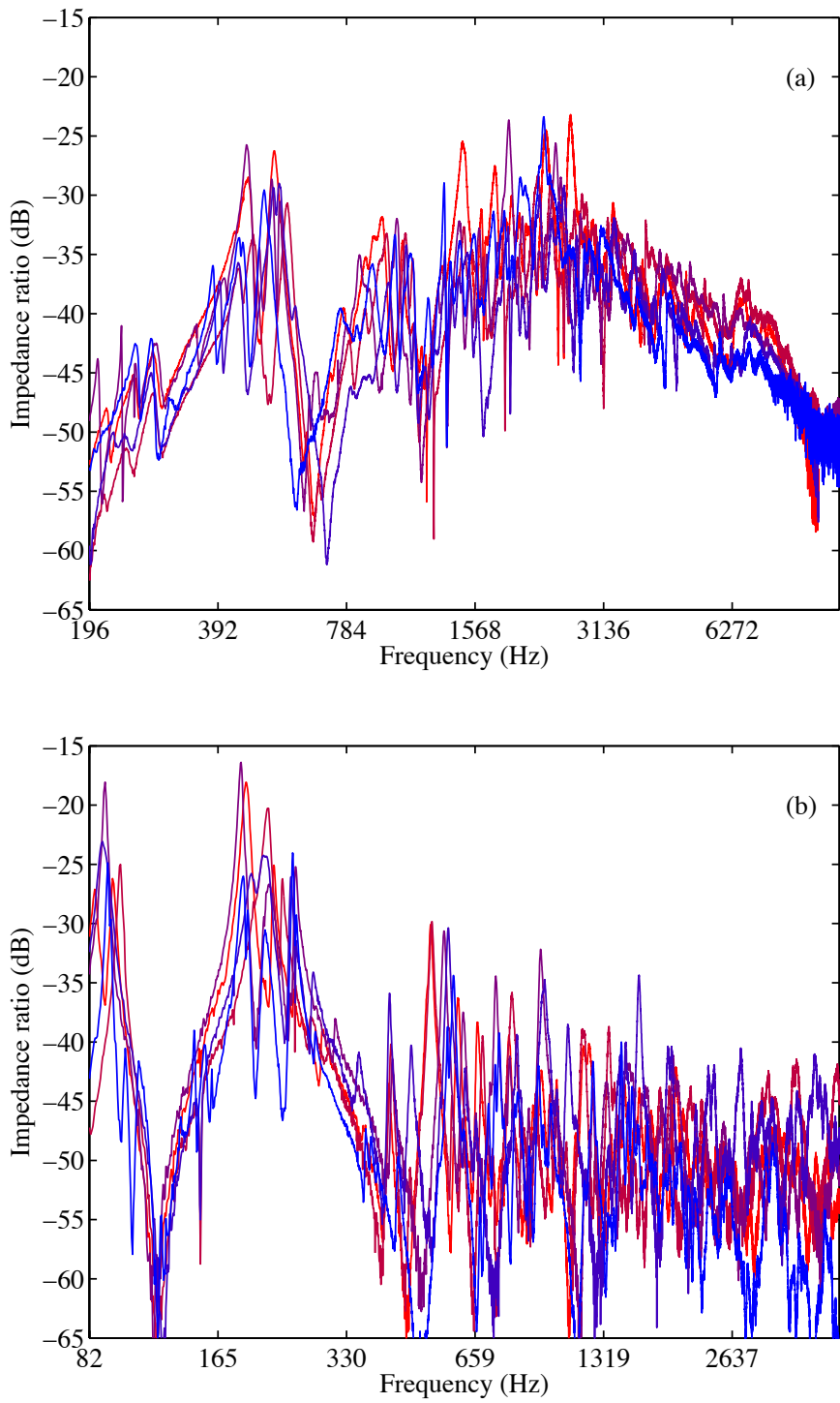


Figure 19: Measured bridge admittances of (a) 5 violins and (b) 5 classical and flamenco guitars. The vertical axis is non-dimensionalised using a typical wave impedance for the lowest string of the respective instruments (0.34 Ns/m for the violin, 0.70 Ns/m for the guitar) to give the string-to-body impedance ratio, expressed in dB, and the horizontal axis is plotted on a logarithmic scale starting from the nominal lowest note of the instrument. Successive octaves of that lowest note are marked.

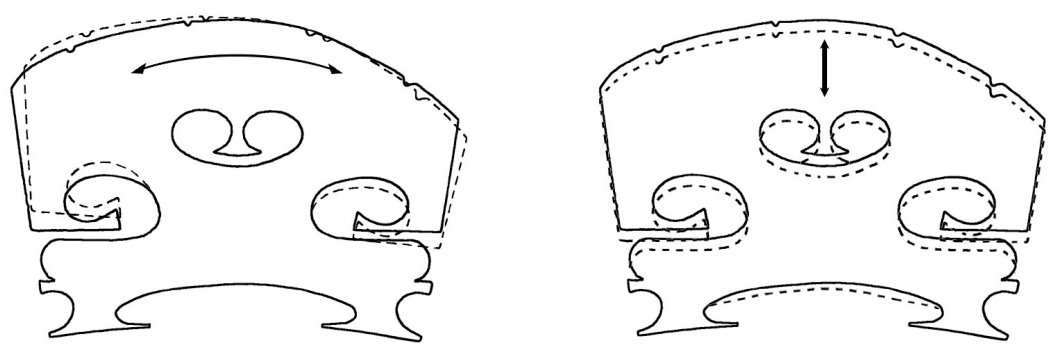


Figure 20: Sketches of the first two in-plane resonances of a violin bridge with clamped feet:
(a) rocking motion, typically around 3 kHz; (b) bouncing motion, typically around 6 kHz.

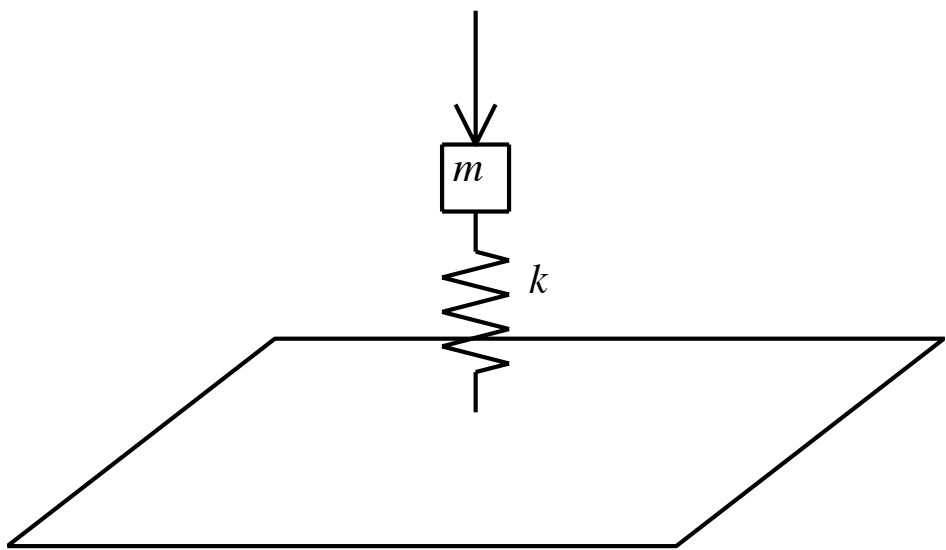


Figure 21: Sketch of a rectangular plate being driven through a mass-spring oscillator: see text.

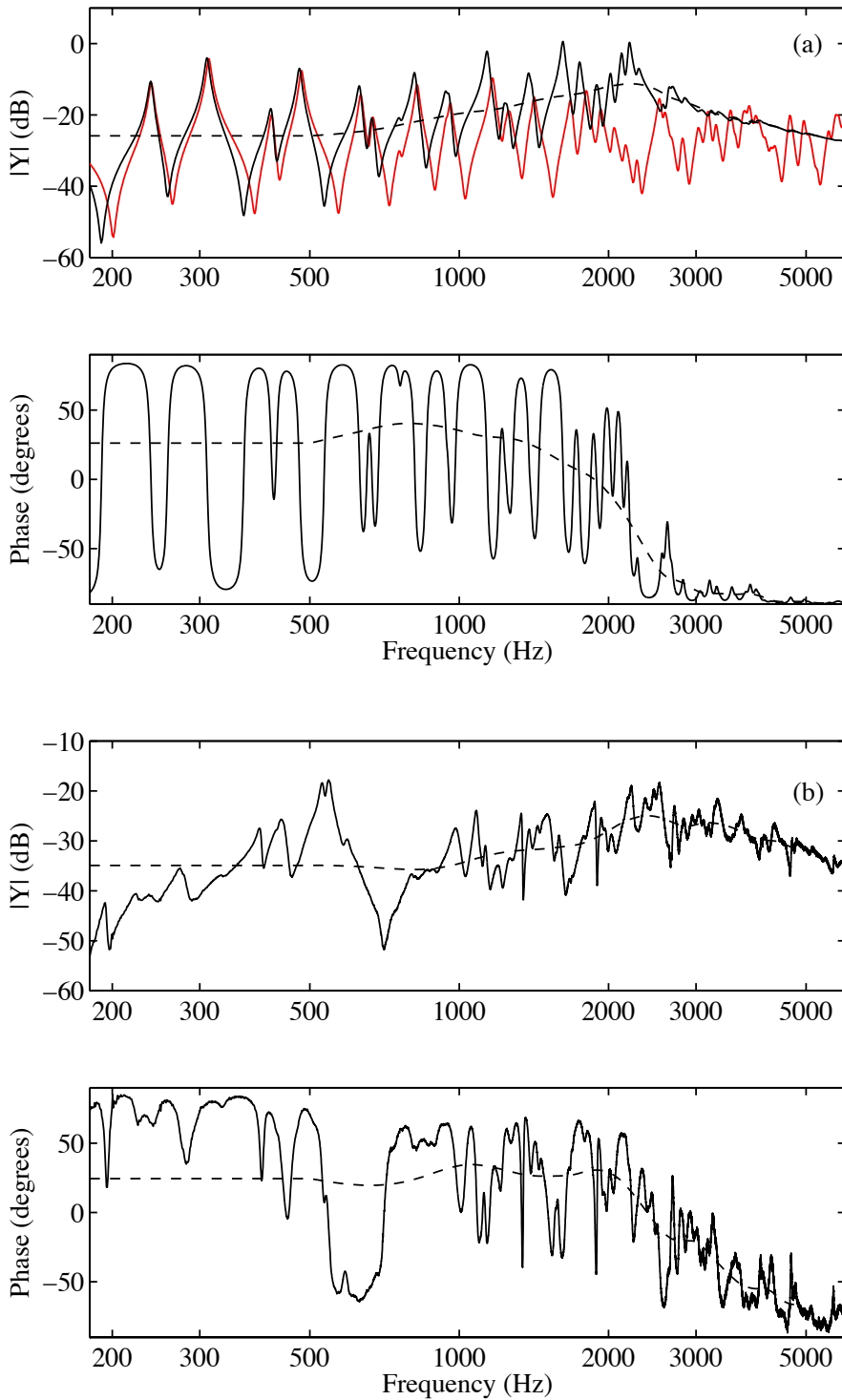


Figure 22: Driving-point admittances, illustrating direct and reverberant field effects. (a) Simulated results for a rectangular plate with freely hinged boundary conditions on all sides, in amplitude (upper plot) and phase (lower plot). Red curve: plate alone; black curves: plate driven through a mass-spring resonator as sketched in Fig. 21; dashed lines: computed estimate of $Y_{dir}(\omega)$. (b) Similar results for a violin, in amplitude and phase and including the computed $Y_{dir}(\omega)$.

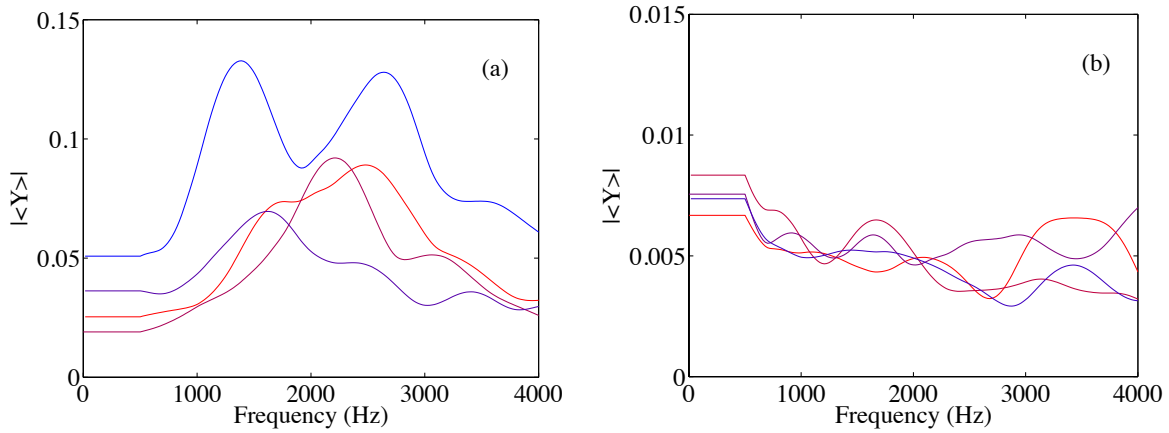


Figure 23: Computed $Y_{dir}(\omega)$ for (a) four different violins; (b) four different guitars. Note different vertical scales. The averaging bandwidth to compute $Y_{dir}(\omega)$ was 1 kHz, so constant values are shown for frequencies up to 500 Hz.

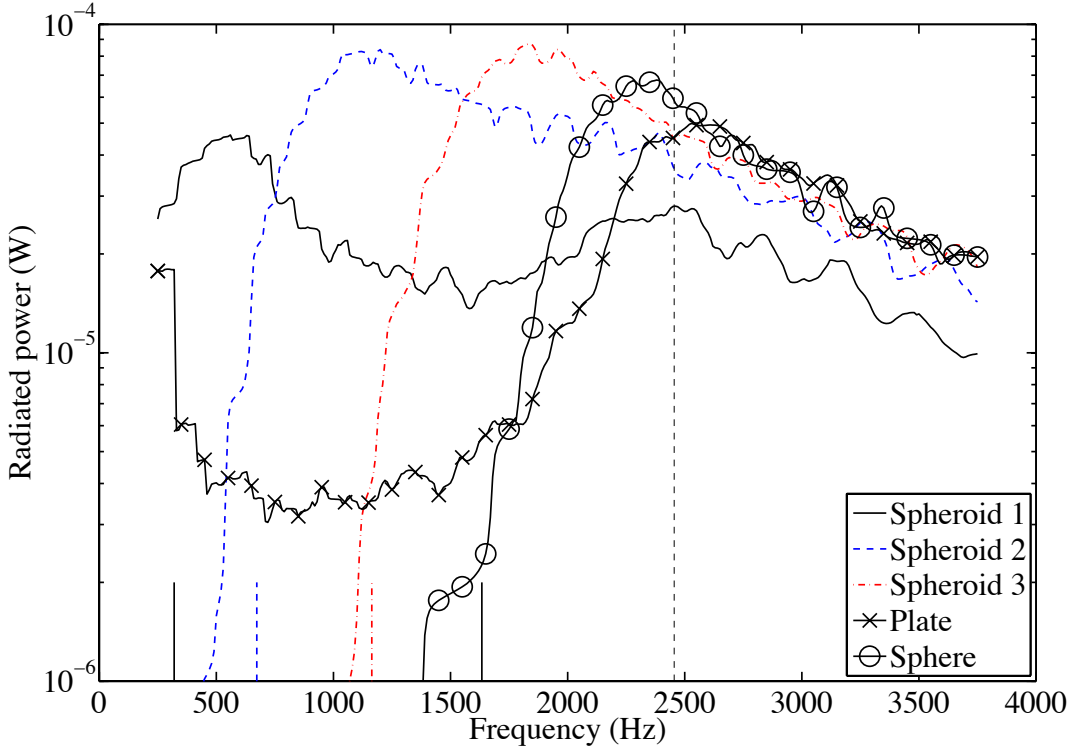


Figure 24: Total sound power radiated from a set of plates and shells driven at a point by a sinusoidal force of unit magnitude, from Lynch et al. [146]. The three spheroids have different eccentricities, and give results in an obvious succession as they depart progressively from the spherical shape. All structures have the same material, thickness and total surface area. The vertical dashed line marks the critical frequency for a flat plate of this material. The short vertical lines mark the frequency of the lowest mode for the structure with the corresponding line type. The chosen “typical” driving point on each structure was as follows: the baffled flat plate was driven at a point $1/\pi$ of the length and the same fraction of the width from one corner; the spheroids were driven at a point halfway around a quarter-line of longitude from pole to equator.

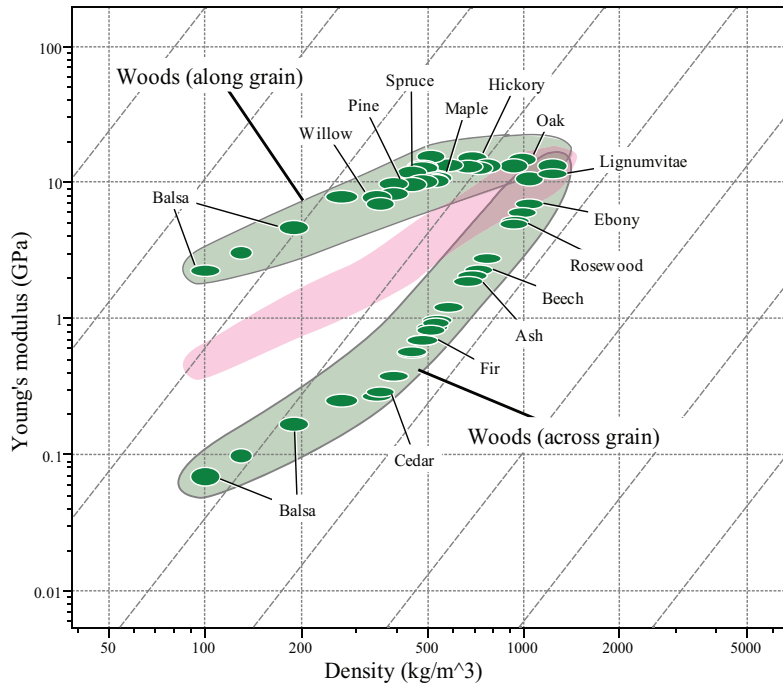
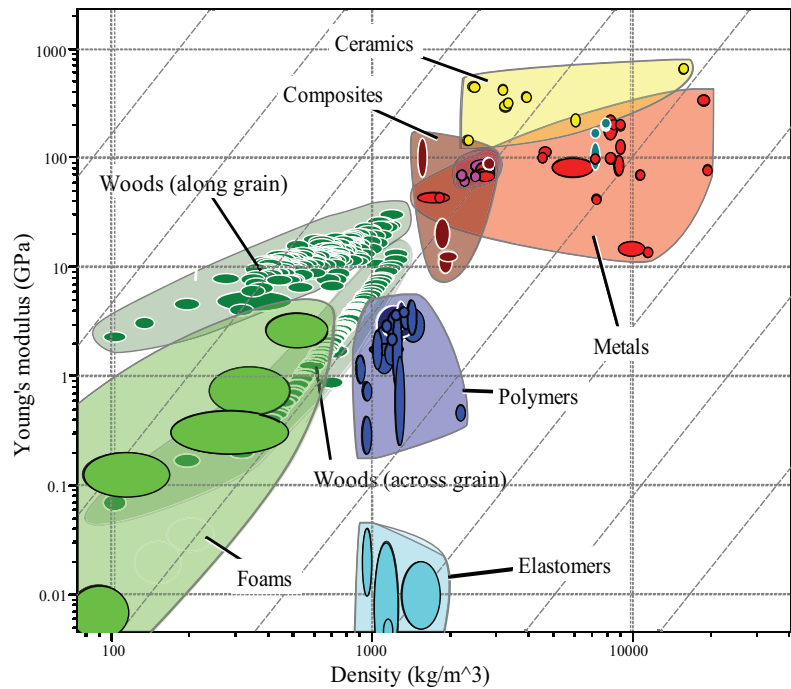


Figure 25: Data for Young's modulus and density for a wide range of materials, plotted on logarithmic scales. Lines of slope 3 link materials that would lead to equally loud violins according to the simple criterion used here: some guide lines of this slope are shown. Materials leading to the loudest instruments correspond to moving the line as far left as possible. Upper plot: “all” materials; lower plot: data for woods only, and showing the intermediate region representing E_{mean} as defined in the text. Charts generated by the Cambridge Engineering Selector.

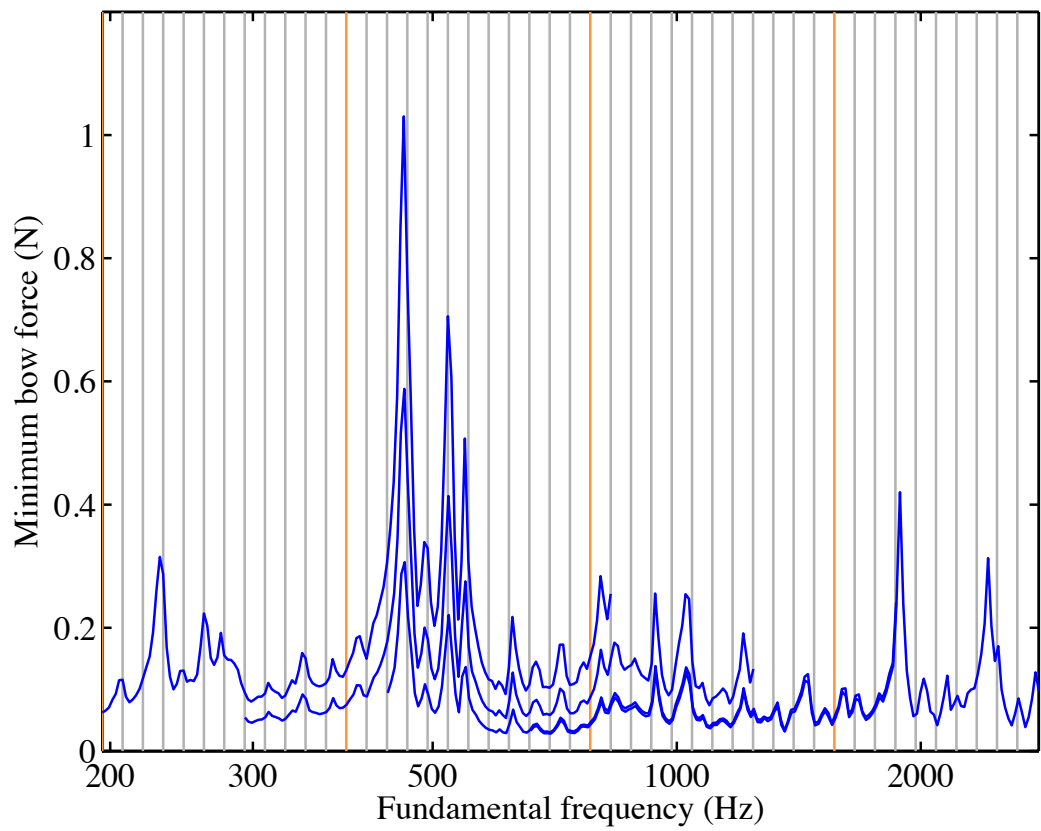


Figure 26: Plot of predicted Schelleng minimum bow force as a function of the fundamental frequency of the played note, for a particular violin. The four curves correspond to the four strings. Vertical lines mark semitones, coloured lines mark the notes G.

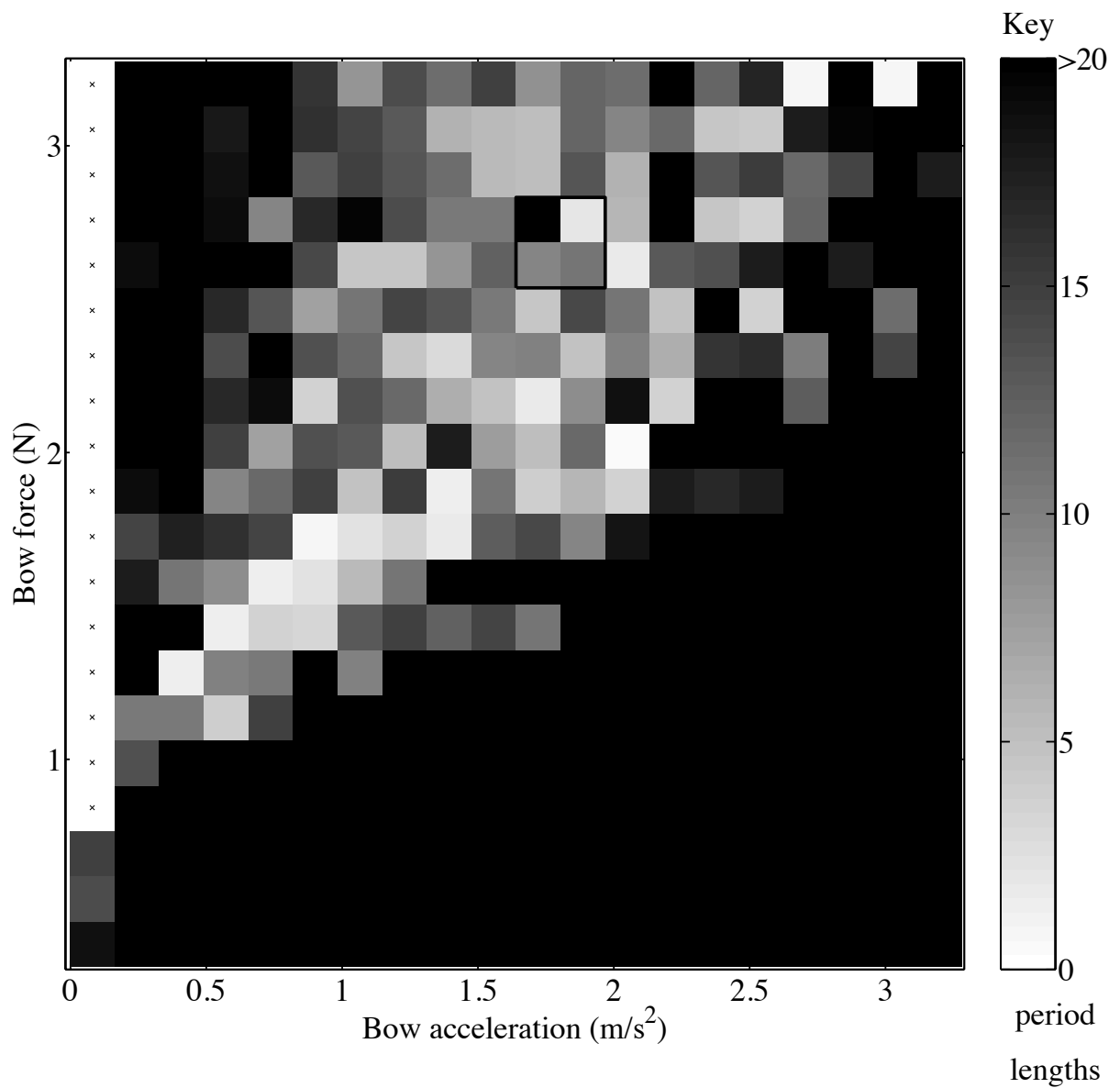


Figure 27: Measured Guettler diagram for the open D string of a cello, bowed at $\beta = 0.08$. Square outline near the upper centre of the plot indicates the four transients plotted in Figure 28. Plot reproduced from Galluzzo and Woodhouse [204].

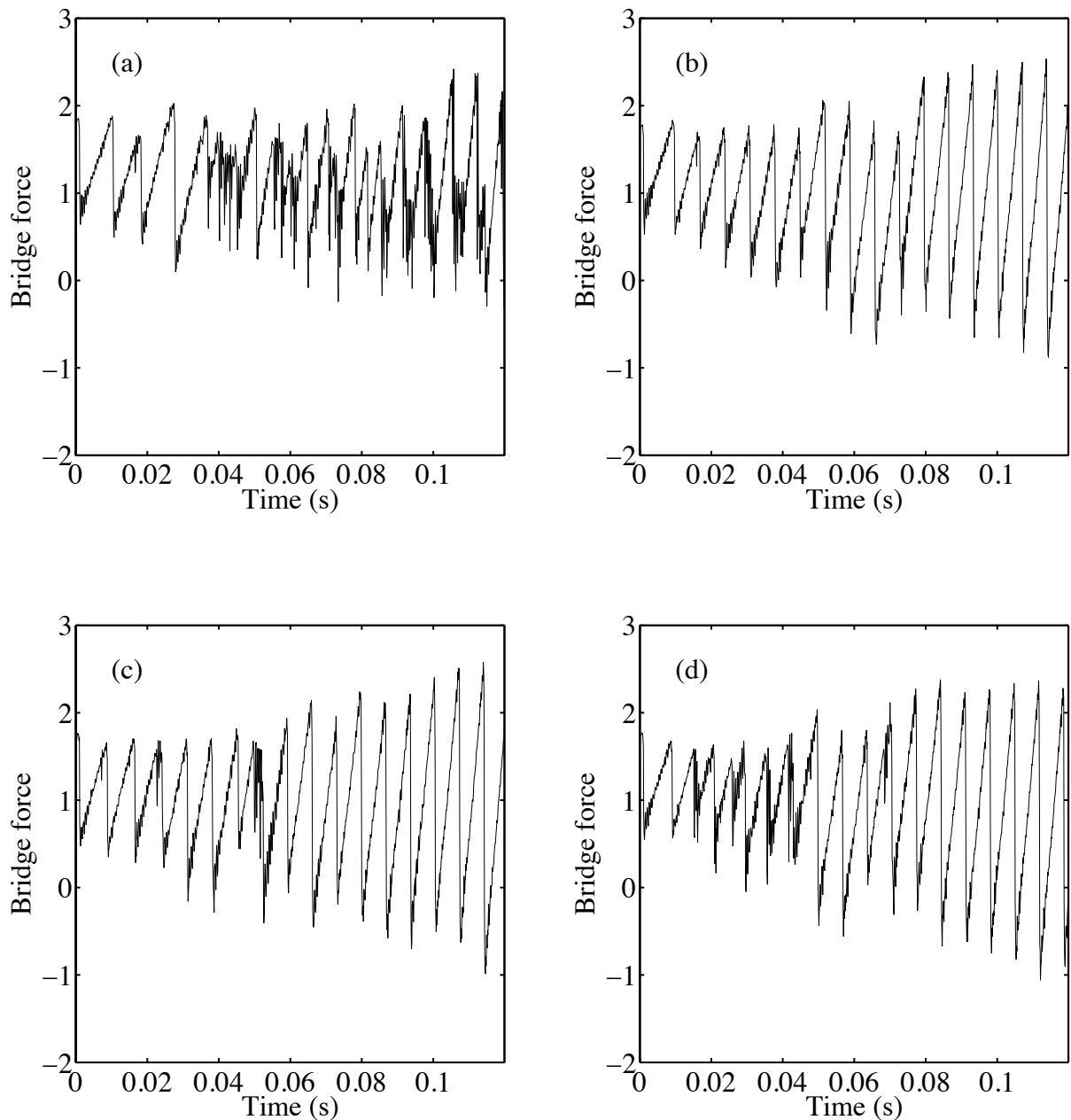


Figure 28: Four particular measured bridge-force transients, corresponding to the cases marked in Figure 27 and laid out in the same spatial arrangement. Each plot begins at the moment of first slip, and the horizontal and vertical scales are the same in all cases. Plots reproduced from Galluzzo and Woodhouse [204].

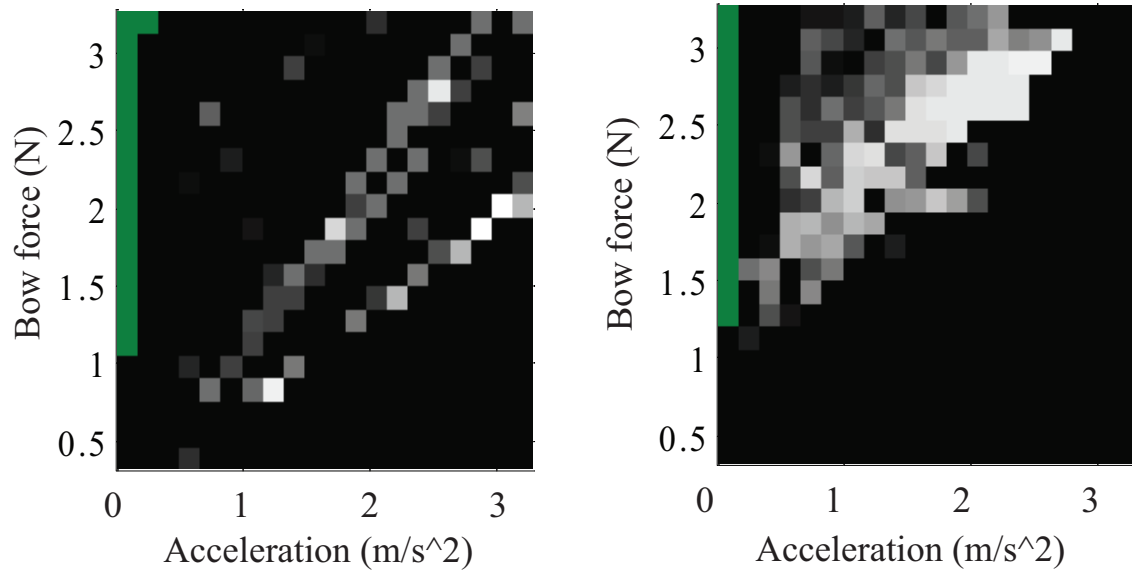


Figure 29: Simulated Guettler diagrams for a model of the cello string used in Fig. 27, computed using (a) the friction-curve model; (b) the thermal friction model (see text). Plots reproduced from Galluzzo [203] by permission of the author.

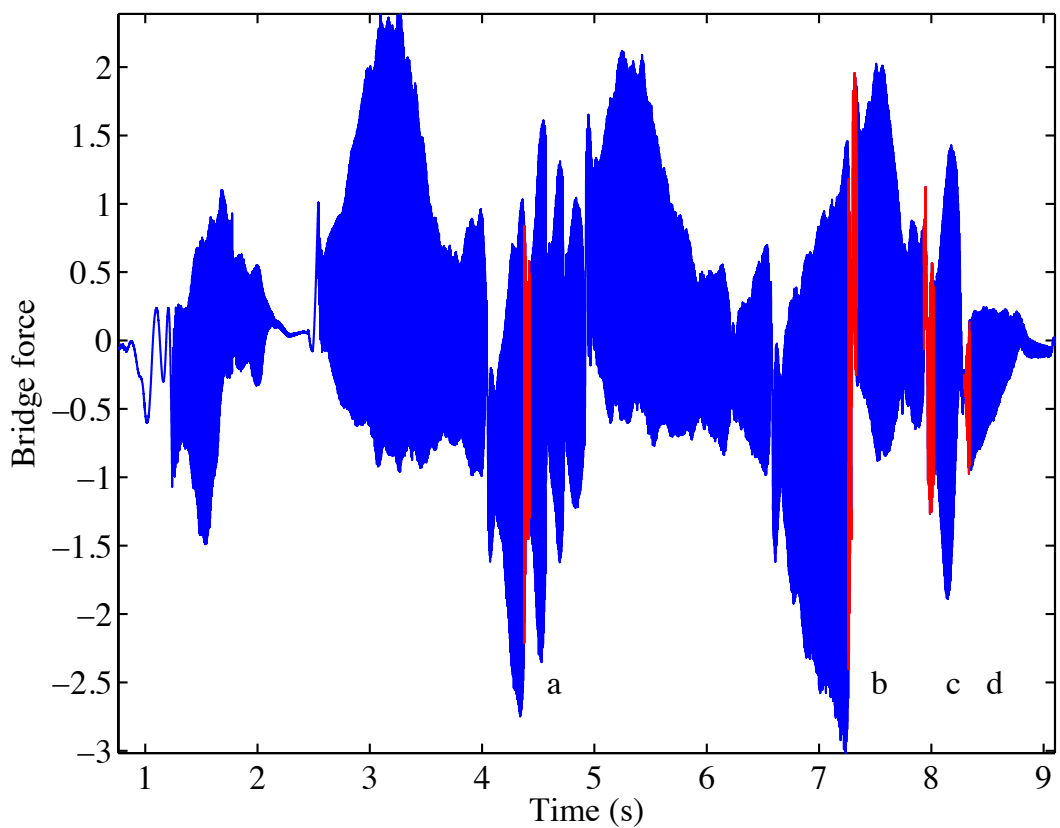


Figure 30: Recorded bridge-force signal from a short musical passage on a violin G string, performed by Keir GoGwilt

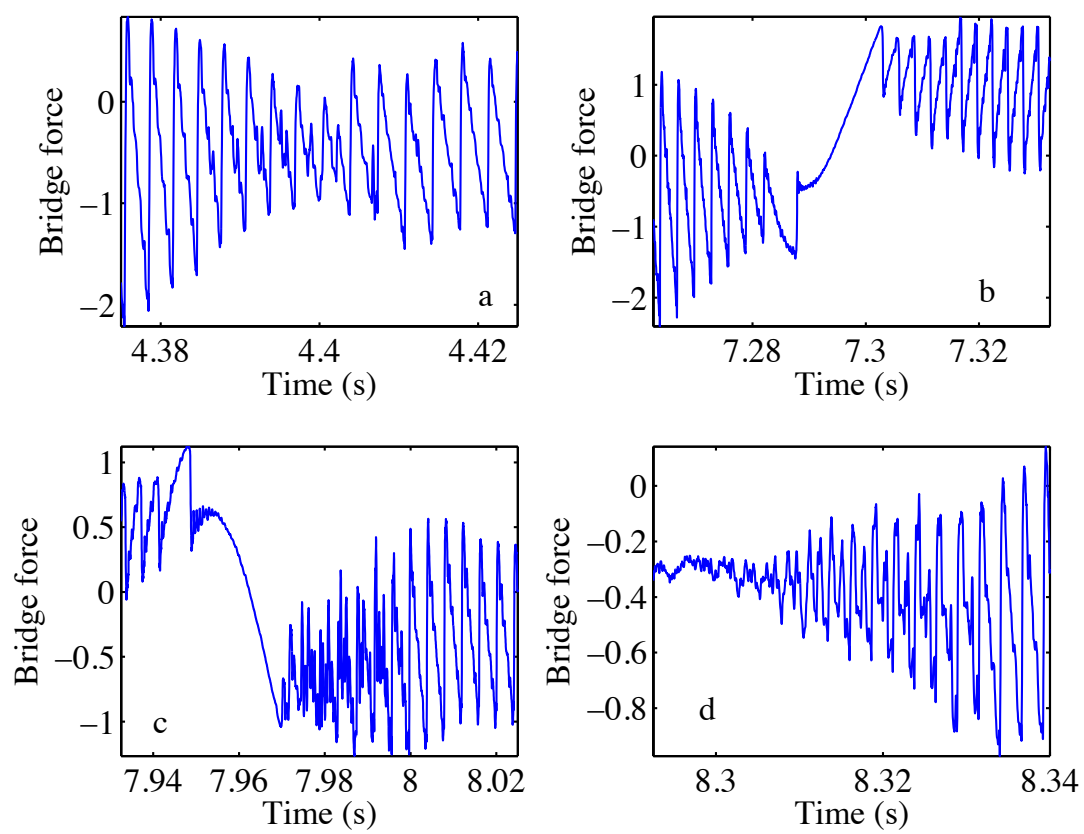


Figure 31: Details of the four marked portions of the waveform in Fig. 30

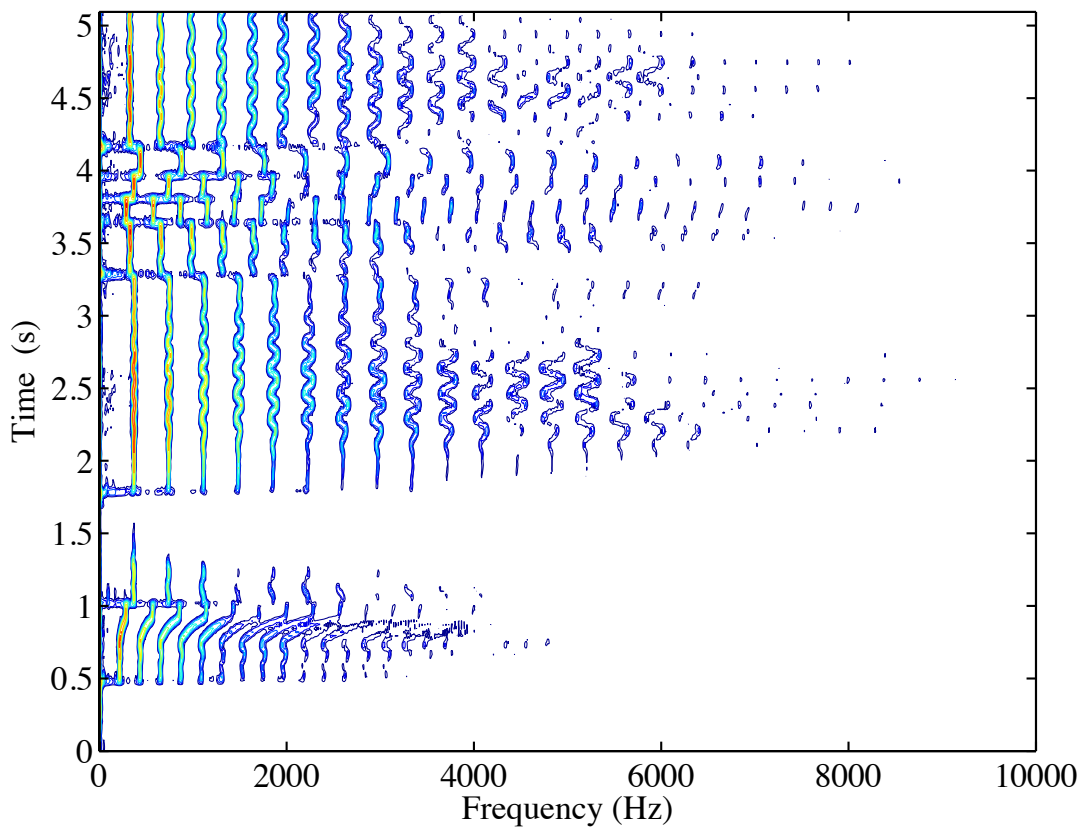


Figure 32: Sonogram of the first part of the recording shown in Fig. 30. Contours are logarithmically spaced at intervals of 5 dB, showing a total range of 50 dB from the maximum value.